

Zirconium Complexes of Cyclopentene-Bridged Diamidophosphine Ligands for Dinitrogen Activation

by

TING ZHU

B.Sc., Nankai University, 2007

A thesis submitted in partial fulfillment of
the requirements for the degree of

MASTER OF SCIENCE

in

THE FACULTY OF GRADUATE STUDIES

(CHEMISTRY)

THE UNIVERSITY OF BRITISH COLUMBIA
(Vancouver)

August 2010

© Ting Zhu, 2010

Abstract

The synthesis of two new diiminophosphine proligands, $^{CY5}[NPN]^{DMP}H_2$ (DMP = 2,6- $Me_2C_6H_3$) and $^{CY5}[NPN]^{DIPP}H_2$ (DIPP = 2,6- $iPr_2C_6H_3$), is reported. These two proligands feature a cyclopentane ring linker between the phosphine and imino donors. The precursors of the proligands were prepared from cyclopentanone and the corresponding substituted aniline. After lithiation and slow addition of $PhPCl_2$, the diiminophosphine proligands could be obtained. It is easy to vary the bulkiness of the proligands in this synthetic strategy. The synthesis of a diamidodioxo ligand based on the scaffold of calix[4]arene was also attempted.

The bis(dimethylamido)zirconium complexes of the two ligands, $^{CY5}[NPN]^{DMP}$ and $^{CY5}[NPN]^{DIPP}$, were prepared via protonolysis from the proligands and $Zr(NMe_2)_4$. The dichlorozirconium or diiodozirconium species could be obtained from the corresponding bis(dimethylamido)zirconium complex upon addition of excess Me_3SiCl or Me_3SiI . Most of the zirconium complexes are well characterized in the solid state by single crystal X-ray diffraction.

A Zr- N_2 complex, $\{^{CY5}[NPN]^{DMP}Zr(THF)\}_2(\mu-\eta^2:\eta^2-N_2)$, was synthesized from $^{CY5}[NPN]^{DMP}ZrCl_2$ and 2.2 equivalents of KC_8 in THF under 4 atm of N_2 . By single crystal X-ray analysis, N_2 has been reduced to an N_2^{4-} unit and is side-on bound to two Zr atoms. However, large number of side products was observed in the reaction. The reduction of $^{CY5}[NPN]^{DIPP}ZrCl_2$ was also attempted. From the minor product identified from single crystal X-ray diffraction, the cyclopentene ring linker was cleaved in the reduction of $^{CY5}[NPN]^{DIPP}ZrCl_2$.

Table of Contents

Abstract	ii
Table of Contents	iii
List of Tables	vi
List of Figures	vii
Abbreviations	ix
Acknowledgements	xiii
Statement of Co-authorship	xv

Chapter 1: Dinitrogen Activation and Ligand Design

1.1 Introduction	1
1.2 Activation of Molecular Nitrogen	3
1.3 Reactivity of Coordinated Dinitrogen Complexes	8
1.4 Ligand Design and Evolution in the Fryzuk Group	10
1.5 Scope of Thesis	14
1.6 References	16

Chapter 2: Ligand Design and Synthesis for Activation of Dinitrogen

2.1 Introduction	18
2.2 Results and Discussion	25
2.2.1 Synthesis of $^{CY5}[NPN]^{DMP}H_2$ and Its Analogue $^{CY5}[NPN]^{DIPP}H_2$	25
2.2.2 Attempts to Synthesize a NONO Type Proligand Based on the Scaffold of	

Calix[4]arene.....	28
2.3 Conclusions.....	31
2.4 Experimental.....	32
2.4.1 General Experimental	32
2.4.2 Starting Materials and Reagents	33
2.5 References.....	39

Chapter 3: Zirconium Complexes of the Cyclopentenyl-linked

Diamidophosphine ligands and Attempts to Activate Dinitrogen

3.1 Introduction.....	41
3.2 Results and Discussion	46
3.2.1 Synthesis of Zirconium Complexes of ^{CY5} [NPN] ^{DMP} H ₂	46
3.2.2 Synthesis of Zirconium Complexes of ^{CY5} [NPN] ^{DIPP} H ₂	51
3.2.3 Synthesis of Zirconium Dinitrogen Complexes.....	56
3.3 Conclusions.....	63
3.4 Experimental.....	65
3.4.1 General Experimental	65
3.4.2 Starting Materials and Reagents	65
3.5 References.....	72

Chapter 4: Thesis Summary and Future Work

4.1 Thesis Summary.....	74
4.2 Future Work	75

4.3 References.....	80
---------------------	----

Appendix: X-ray Crystal Structure Data and Analysis

A.1 X-ray Crystal Structure Data.....	81
A.2 X-ray Crystal Structure Analysis	85
A.3 References	86

List of Tables

Table 1.1	Bonding modes of dinitrogen complexes and the corresponding activation level	4
Table A.1	Crystal Data and Structure Refinement for 2.5 and $^{CY5}[NPN]^{DMP}Zr(NMe_2)_2$ (3.1)	81
Table A.2	Crystal Data and Structure Refinement for $^{CY5}[NPN]^{DMP}ZrCl_2$ (3.2) and $^{CY5}[NPN]^{DMP}ZrI_2$ (3.3).	82
Table A.3	Crystal Data and Structure Refinement for $^{CY5}[NPN]^{DIPP}Zr(NMe_2)_2$ (3.4) and $^{CY5}[NPN]^{DIPP}ZrCl_2$ (3.5)	83
Table A.4	Crystal Data and Structure Refinement for $\{^{CY5}[NPN]^{DMP}Zr(THF)\}_2(\mu-\eta^2:\eta^2-N_2)$ (3.7)	84

List of Figures

Figure 1.1	Nitrogenase enzymes and the Haber-Bosch process to fix nitrogen (Pi = inorganic phosphate)	2
Figure 1.2	a) The first transition metal dinitrogen compound; b) Dinitrogen bound in an end-on mode by two metal centres	4
Figure 1.3	Dewar-Chatt-Duncanson synergistic bonding model (alternatively, d_z^2 can form a σ -bond with the σ -orbital of N_2)	5
Figure 1.4	Orbital interactions between two metal centres and the side-on bound N_2	6
Figure 2.1	Three multidentate ligand systems studied in the Fryzuk group	20
Figure 2.2	New designs of diamidophosphine ligand	21
Figure 2.3	A tridentate methylene-linked aryloxide ligand	23
Figure 2.4	Two examples of calix[4]arene-ligated complexes that activate dinitrogen.	24
Figure 2.5	The possible isomers of the diiminophosphine proligand, $CY^5[NPN]^{DMP}H_2$	27
Figure 2.6	Solid-state molecular structure of 1,3-dimethoxy-2-monotriflated calix[4]arene, 2.5 (<i>t</i> -butyl groups are represented by single carbon atoms for simplicity).....	30
Figure 3.1	N_2 activated from late transition metal complexes	42
Figure 3.2	Activation of N_2 through reduction of metal halide (silyl methyl substituents of $[P_2N_2]$ omitted)	43
Figure 3.3	Activation of N_2 by early transition metal halides.....	44
Figure 3.4	Activation of N_2 through elimination of hydrocarbon.....	44

Figure 3.5	Activation of N ₂ with low-valent metal complexes	45
Figure 3.6	ORTEP drawing of the solid-state molecular structure of ^{CY5} [NPN] ^{DMP} Zr(NMe ₂) ₂ , 3.1	47
Figure 3.7	ORTEP drawing of the solid-state molecular structure of ^{CY5} [NPN] ^{DMP} ZrCl ₂ , 3.2	49
Figure 3.8	ORTEP drawing of the solid-state molecular structure of ^{CY5} [NPN] ^{DMP} ZrI ₂ , 3.3	50
Figure 3.9	ORTEP drawing of the solid-state molecular structure of ^{CY5} [NPN] ^{DIPP} Zr(NMe ₂) ₂ , 3.4	53
Figure 3.10	ORTEP drawing of the solid-state molecular structure of ^{CY5} [NPN] ^{DIPP} ZrCl ₂ , 3.5	55
Figure 3.11	ORTEP drawing of the solid-state molecular structure of { ^{CY5} [NPN] ^{DMP} Zr(THF)} ₂ (μ-η ² :η ² -N ₂), 3.7	58
Figure 3.12	The side view of the stereochemistry around Zr in 3.7	59
Figure 3.13	ORTEP drawing of the solid-state molecular structure of 3.8	62
Figure 3.14	The minor byproduct observed in the preparation of ([P ₂ N ₂]Zr) ₂ (μ-η ² :η ² -N ₂) (silyl methyl substituents of [P ₂ N ₂] omitted)	65

Abbreviations

Anal.	analysis
Ar	aryl group or argon
atm	atmosphere
BINAP	2,2'-bis(diphenylphosphino)-1,1'-binaphthyl
Bn	benzyl
b.p.	boiling point
bs	broad singlet
ⁿ Bu	normal butyl group (-CH ₂ CH ₂ CH ₂ CH ₃)
°C	degrees Celsius
ca.	approximately
Calcd.	calculated
Cp [*]	pentamethylcyclopentadienyl group ([C ₅ Me ₅])
cryst	crystal
d	doublet
dba	dibenzylideneacetone
deg (°)	degree
D	deuterium
EA	elemental analysis
EI-MS	electron impact mass spectrometry
Et	ethyl group (-CH ₂ CH ₃)
Et ₂ O	diethyl ether

FW	formula weight
g	gram(s)
GC-MS	gas chromatography-mass spectrometry
gof	goodness of fit
hr	hour(s)
^1H	proton
$\{^1\text{H}\}$	proton decoupled
HOMO	highest occupied molecular orbital
Hz	hertz
K	kelvin
kJ	kilojoules
L	neutral two-electron donor
LDA	lithium diisopropylamide
LUMO	lowest unoccupied molecular orbital
LutH	2,6-lutidinium
m	multiplet
<i>m</i> -	<i>meta</i> position of aryl ring
M	metal (or molar if referring to concentration)
M^+	parent ion
Me	methyl group ($-\text{CH}_3$)
m/z	mass/charge (mass spectrometry unit)
Mes or mesityl	2,4,6-trimethylphenyl
MHz	megahertz

mol	mole(s)
MW	molecular weight
NMR	nuclear magnetic resonance
[NPN]	$[\text{PhP}(\text{CH}_2\text{SiMe}_2\text{NPh})_2]^{2-}$ unless referring to the family of NPN ligands
$[\text{NPN}]^*$	$[\{N-(2,4,6\text{-Me}_3\text{C}_6\text{H}_2)(2\text{-N-5-MeC}_6\text{H}_3)\}_2\text{PPh}]^{2-}$
$[\text{NPN}]^S$	$[\{N-(2,4,6\text{-Me}_3\text{C}_6\text{H}_2)(3\text{-N-SC}_4\text{H}_2)\}_2\text{PPh}]^{2-}$
<i>o</i> -	<i>ortho</i> position of aryl ring
OBu	butoxide
ORTEP	oakridge thermal ellipsoid plotting program
R	alkyl or aryl group
<i>p</i> -	<i>para</i> position of aryl ring
Ph	phenyl ring ($-\text{C}_6\text{H}_5$)
pH	negative logarithm of the proton concentration ($-\log [\text{H}^+]$)
pK _a	negative logarithm of the acidity constant ($-\log K_a$)
[PNP]	$[\text{N}(\text{SiMe}_2\text{CH}_2\text{P}^i\text{Pr}_2)_2]^-$
$[\text{P}_2\text{N}_2]$	$[\text{PhP}(\text{CH}_2\text{SiMe}_2\text{NSiMe}_2\text{CH}_2)_2\text{PPh}]^{2-}$
ppm	parts per million
^{<i>i</i>} Pr	isopropyl group ($-\text{CH}(\text{CH}_3)_2$)
Py	pyridine
R	alkyl or aryl group
reflns	reflections
R _f	retention factor
rt	room temperature

s	singlet
sept	septet
sys	system
t	triplet
T	temperature
THF	tetrahydrofuran
TLC	thin layer chromatography
TMS	trimethylsilyl group (-Si(CH ₃) ₃)
tol	tolyl group (-C ₆ H ₄ CH ₃)
V	unit cell volume
X	halide substituent, unless specified otherwise
Z	number of formula units in the unit cell
Å	angstrom
δ	chemical shift in ppm
Δ	heat
η^n	hapticity of order n
μ	bridging
ρ_{calc}	calculated density

Acknowledgements

I would like to thank Professor Michael Fryzuk for all of his continuous support, guidance and patience in my research. It has been a delight to work in his laboratory to study the dinitrogen chemistry. I have learned so much during my studies, not only in chemistry, but also as a life experience.

I am highly grateful to past and present members of the Fryzuk group for creating such a pleasant and supportive environment to work in, and for all the great help showing me techniques and giving suggestions. I would like to thank Dr. Maria João Ferreira and Fiona Hess. I could not have started my research without their guidance and help. Special thanks to Nathan Halcovitch and Dr. Howie Jong for the numerous hours spent on my crystals. Thanks to Rui F. Munhá and Dr. Joachim Ballmann for the productive discussions about chemistry and crystallography. Thanks very much to Fiona Hess, Dr. Joachim Ballmann, Truman Wambach, Kyle Parker, Rui F. Munhá and Dr Patricia Horrillo-Martinez for reading my thesis and giving excellent suggestions. Many thanks to past and present members Bryan Shaw, Lee Wence, Dr. Owen Summerscales, and Dr. Jörg Schachner.

Many thanks are due to the excellent support staff at the Chemistry Department at U.B.C. Great thanks to Dr. Brian Patrick for his patient instruction and help solving my X-ray structures. Thanks to Ken Love and the mechanical shop for their excellent help fixing and maintaining different facilities. I am very grateful to the NMR team Dr. Neal, Dr. Maria Ezhova and Zorana Danilovic for their friendly help with the instruments. I also appreciate very much the great help from Marshall Lapawa (MS), David Wong (EA) and Brian Ditchburn (glassblower). I would

also like to thank Dr. Subramanian Iyer for being a great supervisor for the inorganic undergraduate labs.

Finally, I would like to thank my parents as well as my brother Qiming for always being there to support me. I would like to thank my good friend Veeru for his friendship and encouragement, which carried me through the most difficult time of my research.

Statement of Co-authorship

This thesis was written by Ting Zhu under the supervision of Professor Michael D. Fryzuk, who assisted with the development of related work. All research was performed by Ting Zhu. The X-ray crystal structures were processed by Nathan Halcovitch and Dr. Howie Jong. The X-ray data were solved in the assistance of Rui Munha, Nathan Halcovitch and Dr. Brian O. Patrick.

Chapter 1

Dinitrogen Activation and Ligand Design

1.1 Introduction

Nitrogen is an essential component of the building blocks for life. Although the majority of the air we breathe is dinitrogen, this material is unavailable for direct use by most organisms. It must first be converted into a chemically available form such as ammonia.¹ Only certain bacteria, known as diazotrophs, are capable of this transformation (Figure 1.1), in which the nitrogenase enzyme is capable of overcoming the high activation barrier required to produce ammonia from dinitrogen.²

The nitrogenase enzyme consists of two proteins: the Fe protein, which uses ATP to supply the electrons necessary for the reduction of dinitrogen, and the MoFe protein, which contains the active site for dinitrogen binding and reduction, known as the FeMo cofactor. The latter's cofactor consists of a MoFe_7S_9 cluster, where a histidine and a cysteine ligand on Mo and Fe, respectively, anchor the cofactor to the protein.³ The site for N_2 coordination and activation within the MoFe_7S_9 cluster is uncertain.⁴ The presence of eight transition metals in the FeMo cofactor is a clear indication that metal atoms play a significant role in the catalytic fixation of dinitrogen. This has inspired research into iron and molybdenum complexes, in addition to other transition metal complexes, as synthetic models of nitrogenase.⁵

Since the industrial revolution, the production of nitrogen-containing chemicals from N_2 has increased significantly. The Haber-Bosch process produces millions of tons of ammonia annually (Figure 1.1), which is used in agriculture as fertilizer and in other industries as a starting

material for the synthesis of nitrogenous products. The fertilizers made from ammonia are estimated to be responsible for sustaining roughly 40% of the world's population.¹ The Haber-Bosch process employs heterogeneous iron or ruthenium catalysts to combine H_2 and N_2 under high temperatures ($400 - 600\text{ }^\circ\text{C}$) and pressures ($400 - 500\text{ atm}$).¹ It is highly energy-intensive and is estimated to consume about 1% of the world's annual energy supply.⁶ At the same time, the combustion of natural gas to supply the intensive energy demand generates large amounts of the greenhouse gas CO_2 .

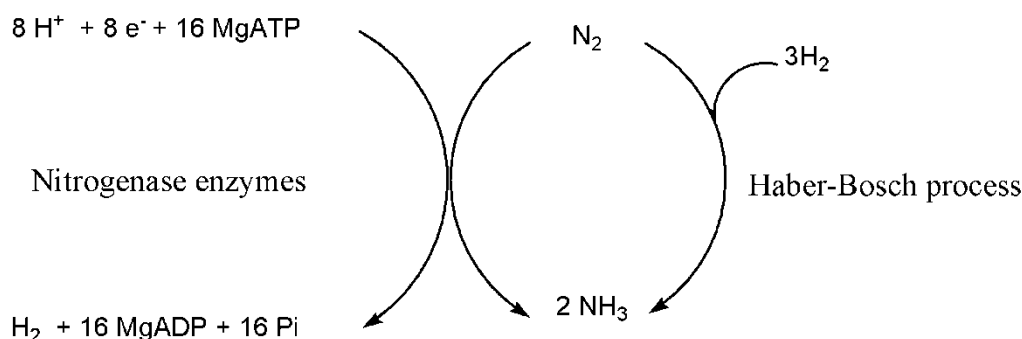


Figure 1.1. Nitrogenase enzymes and the Haber-Bosch process to fix nitrogen (Pi = inorganic phosphate).

The great concern regarding pollution of the environment, depletion of global energy resources and the ever growing world population requires a better solution for dinitrogen fixation. Organometallic chemistry has facilitated industrial and synthetic production of many desired organic compounds. Nitrogenase enzymes and the Haber-Bosch process require the presence of metal compounds. Therefore, scientists are devoting great effort to explore the role that transition metals can play in the fixation of dinitrogen.

1.2 Activation of Molecular Nitrogen

In principle, dinitrogen can offer its lone pairs or its π electrons for bonding to a metal, but in practice it is both a poor σ -donor and a poorer π -acceptor. Several factors contribute to its inert nature: the molecule has a strong triple bond and lacks a dipole moment; the energy gap between the highest occupied molecular orbital (-15.6 eV) and the lowest unoccupied molecular orbital (7.3 eV) in N_2 is large.⁷ Therefore, the chemistry of dinitrogen activation is not simple.

The extent of activation can be quantified by infrared or Raman spectroscopy. Upon coordination, an activated dinitrogen unit has a lower energy stretching frequency than free molecular nitrogen. X-ray or neutron diffraction is the most straightforward way to tell the N-N bond length which correlates to the bond order. Generally, the greater the bond is lengthened from free dinitrogen (1.0975 Å), the greater the degree of activation. A metal-bound dinitrogen unit with a bond length approximating that of hydrazine (1.449 Å) is considered strongly activated and referred to as a hydrazido or N_2^{4-} ligand. Similarly, a metal-bound dinitrogen unit with a double bond displays properties that resemble diazo compounds and is referred to as a diazenido or N_2^{2-} ligand.

The dinitrogen ligand can bridge two or more metal centres and the bonding modes can be end-on and side-on. The end-on fashion is by far most prevalent, especially in late metal chemistry. However, dinitrogen bound in this way is not extensively activated. Greater activation can be achieved via reaction with low valent early transition metal complexes, where a variety of bonding modes are observed. The bonding modes of coordinated dinitrogen complexes and the corresponding level of activation are illustrated in Table 1.1.

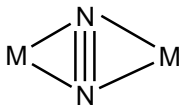
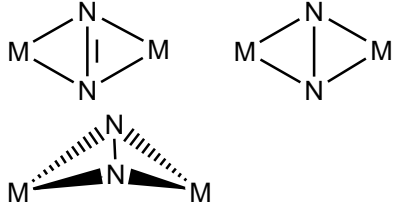
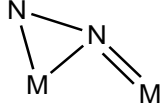
Weak Activation	Strong Activation	Bonding Mode
$M-N\equiv N$		End-on Mononuclear
$M-N\equiv N-M$	$M=N-N=M$	End-on Dinuclear
		Side-on Dinuclear
		Side-on End-on Dinuclear

Table 1.1. Bonding modes of dinitrogen complexes and the corresponding activation level.

The first dinitrogen complex, $[\text{Ru}(\text{NH}_3)_5\text{N}_2]^{2+}$, was reported by Bert Allen and Caesar Senoff in 1965 (Figure 1.2a),⁸ in which N_2 is coordinated end-on to a mononuclear ruthenium centre. This landmark discovery showed that dinitrogen can coordinate to a metal centre as a ligand. Since then, further research into the chemistry of N_2 complexes started to emerge.

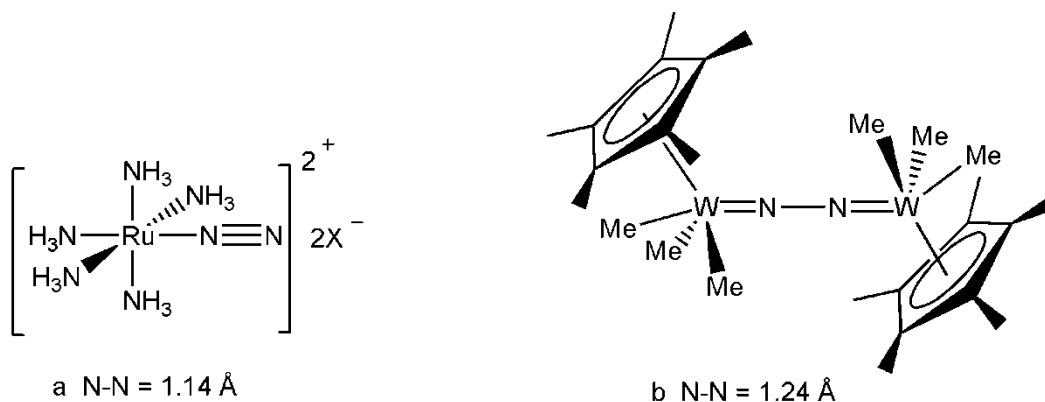


Figure 1.2. a) The first transition metal dinitrogen compound; b) Dinitrogen bound in an end-on mode by two metal centres.⁹

The Dewar-Chatt-Duncanson synergistic bonding model can explain the activation of N_2 in the end-on bonding mode (Figure 1.3).¹⁰ The filled N_2 σ orbital forms a dative bond with an

empty metal orbital (d_z^2 or $d_{x^2-y^2}$). Back donation of electron density from the filled d_{xz} , d_{yz} or d_{xy} orbitals of the metal into empty π^* orbitals of the N_2 moiety can weaken the N-N bond and activate the ligand for further reactivity. As mentioned above, this terminal bonding mode is by far the most common in the late transition metal chemistry. Dinitrogen coordinated in this way is not particularly activated as typically the N-N bond length is similar to that found in free dinitrogen. In the same end-on mode, greater activation of dinitrogen can be achieved by coordinating to two metal centres as shown in Figure 1.2b.⁹

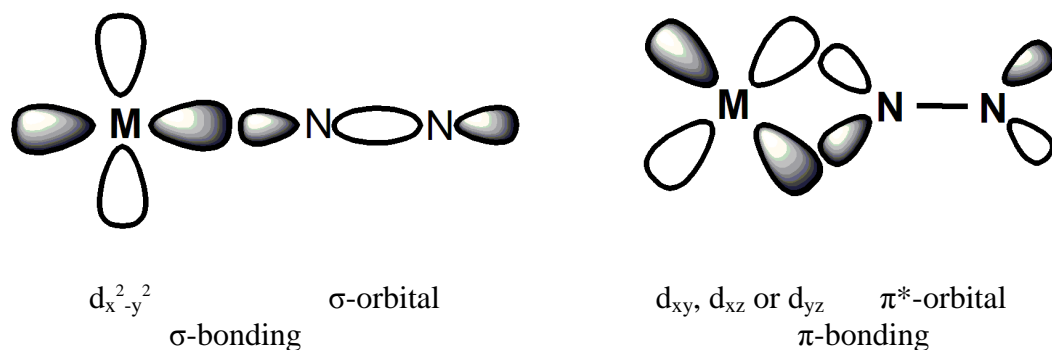
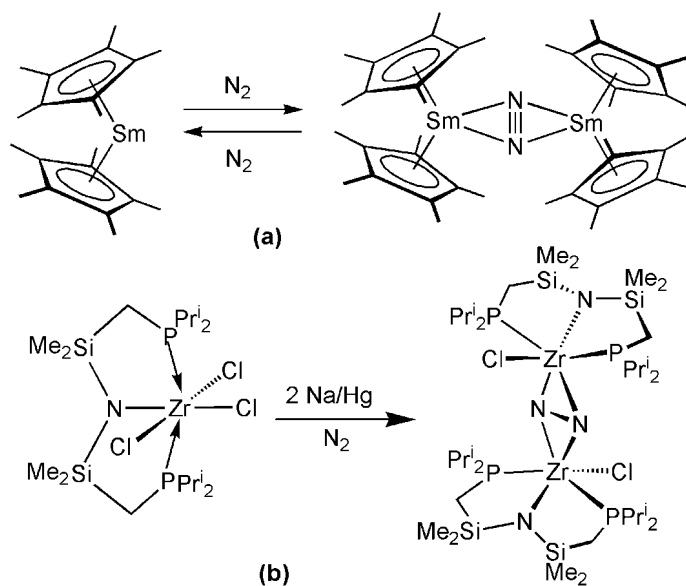


Figure 1.3. Dewar-Chatt-Duncanson synergistic bonding model (alternatively, d_z^2 can form a σ -bond with the σ -orbital of N_2).

In 1988, $[(C_5Me_5)_2Sm]_2(\mu-\eta^2:\eta^2-N_2)$ was prepared for the first time and a new bonding mode for dinitrogen was discovered. The N_2 core is bound side-on to two metal centers in a planar and symmetrical array (Scheme 1.1a). The N-N bond length is 1.088(12) Å, shorter than free N_2 (1.0975 Å). Therefore, the N_2 unit in this complex is very weakly activated.¹¹ Two years later, the first strongly activated side-on bound N_2 complex was first reported by the Fryzuk group. The Zr- N_2 complex was prepared by reduction of $[N(SiMe_2CH_2P^iPr_2)_2]ZrCl_3$ by two equivalents Na(Hg) amalgam under 4 atmospheres of N_2 in toluene (Scheme 1.1b). The N-N bond length is 1.548(7) Å, which is even longer than the single bond in hydrazine. The Zr centres are each assigned +4 oxidation state with the N_2 moiety designated a hydrazido unit.¹²



Scheme 1.1

For an N_2 unit that is bound side-on, the filled π -orbital of N_2 and a vacant d_z^2 or $d_{x^2-y^2}$ orbital on the metal have the proper symmetry for the formation of σ -bonds. Back donation of the available d -orbital of a metal to the π^* -orbitals of N_2 forms molecular orbitals with π - and δ -symmetry, which further weaken the N-N bond (Figure 1.4).¹³ Since the discovery of these two dinitrogen complexes, many other transition metals with side-on bound N_2 have been found.¹⁴

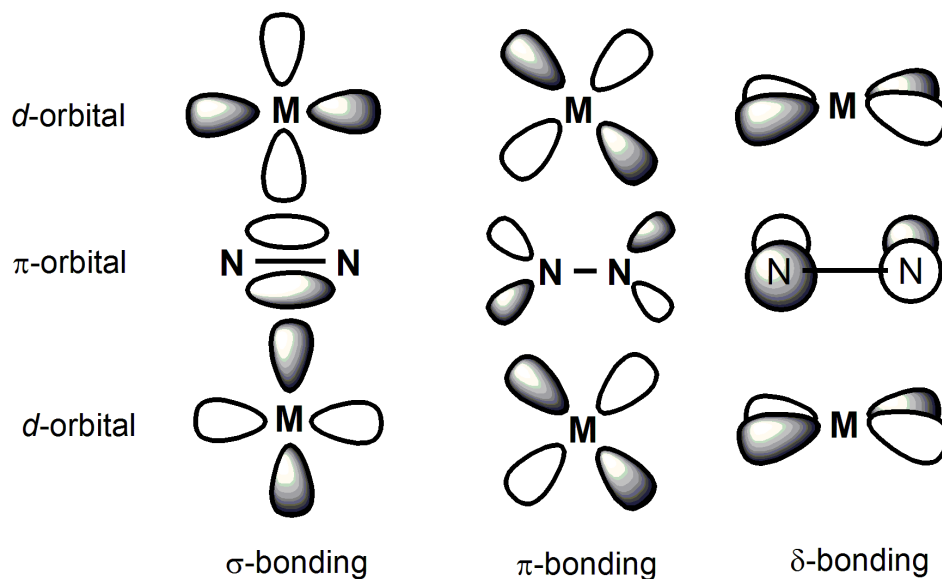
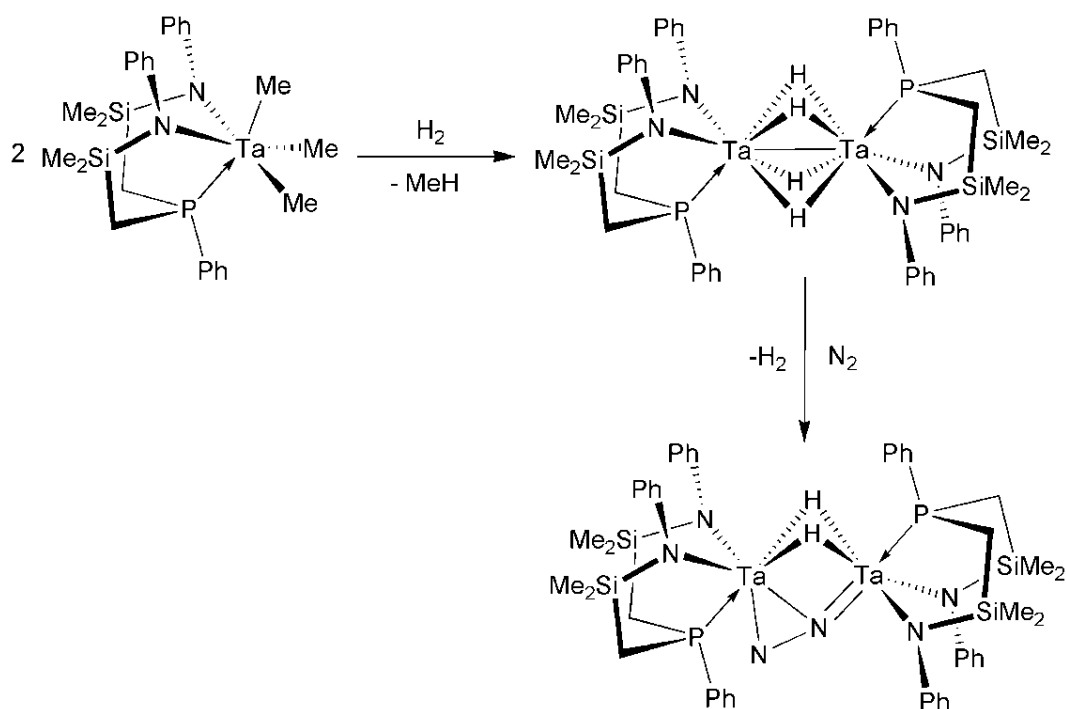


Figure 1.4. Orbital interactions between two metal centres and the side-on bound N_2 .

In 1998, another new bonding mode of dinitrogen complex was discovered, in which the dinitrogen unit is side-on end-on bound to two tantalum centres. As shown in scheme 1.2, hydrogenation of $[\text{NPN}]\text{TaMe}_3$ (where $[\text{NPN}] = \text{PhP}(\text{CH}_2\text{SiMe}_2\text{NPh})_2$) produced the dinuclear tetrahydride $([\text{NPN}]\text{Ta})_2(\mu\text{-H})_4$. In the presence of N_2 , this tetrahydride derivative reacts with N_2 to give $([\text{NPN}]\text{Ta})_2(\mu\text{-H})_2(\mu\text{-}\eta^1:\eta^2\text{-N}_2)$, with the loss of H_2 . The N-N bond length was shown to be 1.319(4) Å, indicating that the N_2 unit was activated to a hydrazido unit.¹⁵ This reaction is intriguing for two reasons, namely no harsh reducing agents were required to generate this N_2 complex and that bimetallic tetrahydrides could serve as precursors for dinitrogen activation.



Scheme 1.2

1.3 Reactivity of Coordinated Dinitrogen Complexes

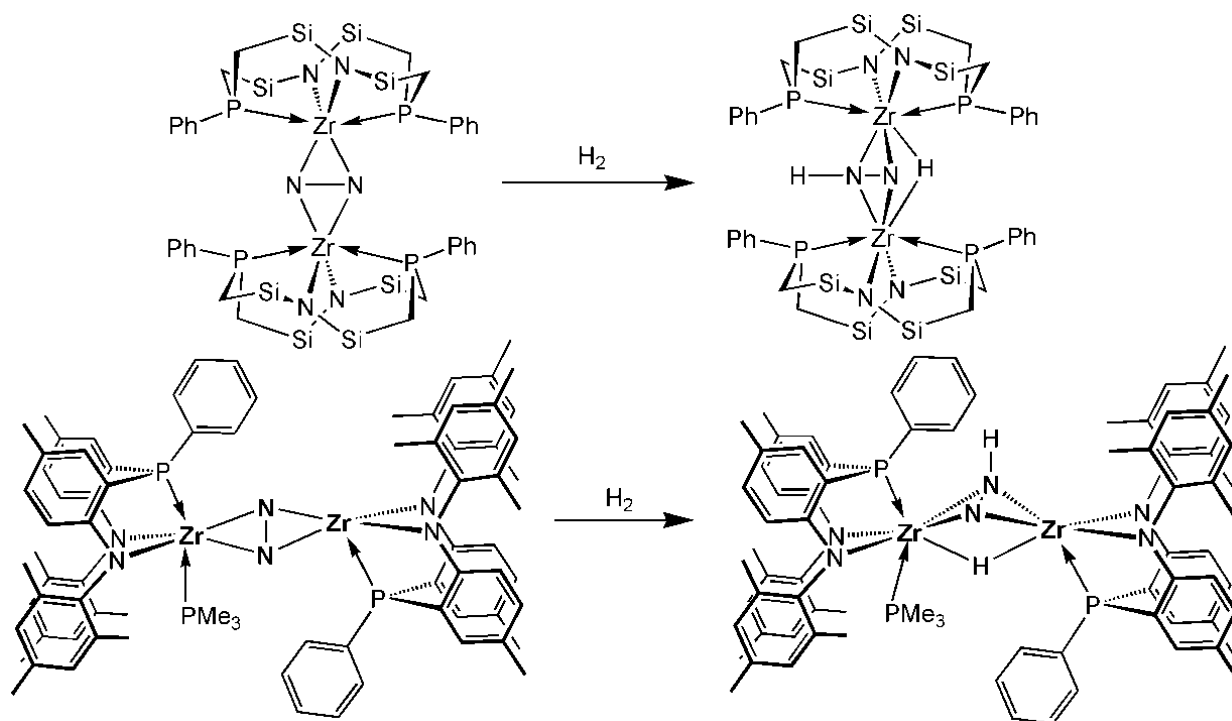
Coordinated dinitrogen complexes can react with electrophiles to form new bonds between nitrogen and other elements. Previously, functionalization of N_2 complexes generally involved addition of acids to form hydrazine, ammonia or a hydrazido metal complex stoichiometrically. In 1975, Chatt and co-workers quantitatively converted one N_2 ligand in *cis*- $[W(N_2)_2(PMe_2Ph)_4]$ into NH_3 by treatment with sulfuric acid in MeOH at room temperature.¹⁶ Related systems of this type, $[M(N_2)_2(P)_4]$ ($M = W, Mo$; $P =$ tertiary phosphine), showed similar reactivity in N_2 activation and produced NH_3 through protonolysis.¹⁷

A few catalytic processes for the formation of nitrogenous compounds have been discovered. The Hidai group have been able to produce silyl amines catalytically with molybdenum and tungsten nitrogen complexes (*cis*- $Mo(N_2)_2(PMe_2Ph)_4$ or *cis*- $W(N_2)_2(PMe_2Ph)_4$) using sodium amalgam as the reductant and Me_3SiCl as the electrophile. This reaction produces $N(SiMe_3)_3$ with 24 turnovers, but a side reaction occurs between the reducing agent and the electrophile Me_3SiCl to generate $Me_3SiSiMe_3$,¹⁸ limiting further silylamine production.

The Schrock group has reported a triamidoamine molybdenum catalyst that is able to generate NH_3 from N_2 , although the catalytic activity is limited to 4-7 turnover cycles. This system makes use of the different solubilities of the reducing reagent ($[Cr(\eta^2-C_5Me_5)_2]$) and the proton source $\{LutH\}\{BAr_4\}$ ($LutH = 2,6$ -lutidinium, $Ar = 3,5-(CF_3)_2C_6H_3$) to prevent competitive side reaction, and promotes protonation of the coordinated N_2 to produce ammonia.¹⁹

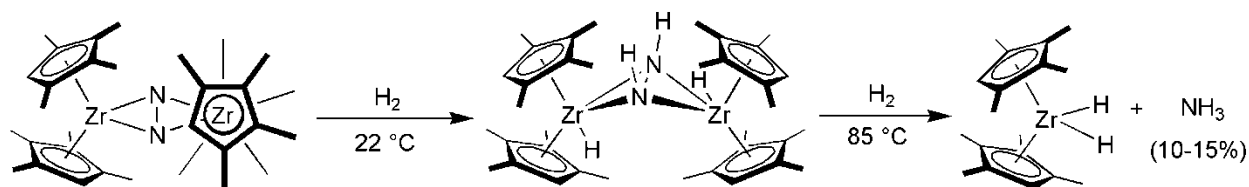
Since the discovery of the first side-on bound N_2 complex $[(C_5Me_5)_2Sm]_2(\mu-\eta^2:\eta^2-N_2)$,¹¹ the reactivity of side-on bound N_2 complexes has been studied extensively. The first functionalization of a side-on N_2 moiety was discovered by Fryzuk and co-workers in 1997. The

N_2 complex $([\text{P}_2\text{N}_2]\text{Zr})_2(\mu\text{-}\eta^2\text{:}\eta^2\text{-N}_2)$ can add one equivalent of H_2 to form an N-H bond and a bridging hydride. Such a direct hydrogenation of an activated N_2 unit was previously unprecedented in the literature (Scheme 1.3).²⁰ Another side-on bound Zr- N_2 complex, $([\text{NPN}]\text{*Zr})_2(\mu\text{-}\eta^2\text{:}\eta^2\text{-N}_2)$, explored in recent years by the Fryzuk group shows similar reactivity towards dihydrogen. H_2 reacts with $([\text{NPN}]\text{*Zr}(\text{PMe}_3))(\mu\text{-}\eta^2\text{:}\eta^2\text{-N}_2)(\text{Zr}[\text{NPN}]\text{*})$ to yield an N-H bond and a bridging hydride akin to the $[\text{P}_2\text{N}_2]$ system (Scheme 1.3).²¹



Scheme 1.3

Direct formation of NH_3 from H_2 and N_2 was reported by Chirik and co-workers in 2003. In the presence of 1 atm of H_2 , the side-on bound N_2 species $([\eta^5\text{-C}_5\text{Me}_4\text{H})_2\text{Zr}]_2(\mu\text{-}\eta^2\text{:}\eta^2\text{-N}_2)$ in pentane formed $([\eta^5\text{-C}_5\text{Me}_4\text{H})_2\text{ZrH}]_2(\mu\text{-}\eta^2\text{:}\eta^2\text{-N}_2\text{H}_2)$ as a white precipitate at ambient temperature. Gentle warming of this compound in heptane resulted in the formation of ammonia in low yield along with the dihydride $(\eta^5\text{-C}_5\text{Me}_4\text{H})_2\text{ZrH}_2$ and other zirconium(IV) compounds (Scheme 1.4). This example features the direct formation of NH_3 from N_2 and H_2 .²²



Scheme 1.4

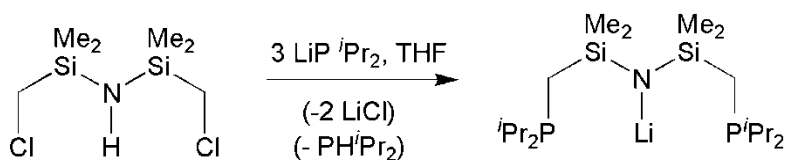
Functionalization of the side-on end-on bound N_2 complex $([NPN]Ta)_2(\mu-H)_2(\mu-\eta^1:\eta^2-N_2)$ was extensively studied in the Fryzuk group. Reactions with boranes, silanes, or alanes were shown to completely cleave the N-N bond.²³ However, the rearrangement and decomposition of the [NPN] ligand sometimes accompanied these transformations. In several cases, after successful functionalization of the coordinated dinitrogen *via* formation of new N-E (E = H, Si, Al, B, C) bond, the new N-E containing unit usually could not be released from the bimetallic complexes, which presents a significant barrier to developing catalytic processes that form nitrogenous compounds.

1.4 Ligand Design and Evolution in the Fryzuk Group

Research in the Fryzuk laboratory is focused on hybrid ligands that combine hard amide donors and soft phosphine donors to stabilize a variety of metals with different oxidation states and degree of coordinative unsaturation.²⁴⁻³¹ These multidentate amidophosphine ligands allow simultaneous coordination of amide donors, which stabilize high-valent, electron-poor metal complexes, and phosphine donors, which stabilize low-valent, electron-rich metal complexes. In the presence of strong reducing reagents, these ligands allow for dinitrogen activation by early transition metals.

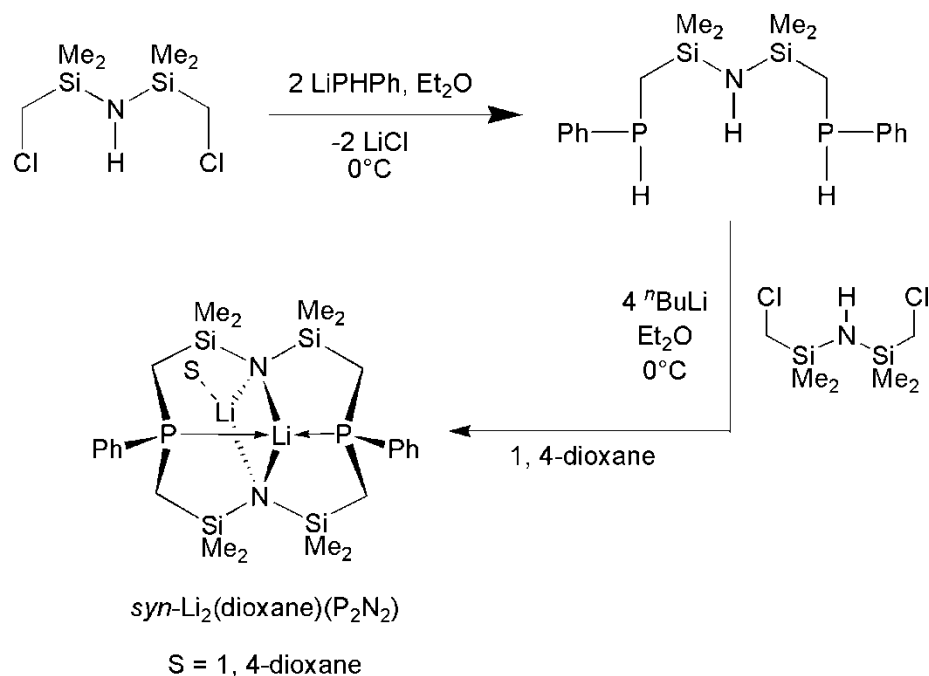
The [PNP] ligand ($[PNP] = [N(SiMe_2CH_2PR_2)_2]^-$, $R = ^iPr$) was the first to be studied, utilizing a central amido donor and two flanking phosphine groups. The preparation of this

ligand is shown in Scheme 1.5, and involves the addition of three equivalents of LiP^iPr_2 to the commercially available disilazane derivative $\text{HN}(\text{SiMe}_2\text{CH}_2\text{Cl})_2$ to generate the lithiated [PNP] ligand.²⁴ Starting from the lithium salt, the dinitrogen complex $([\text{PNP}]\text{ZrCl})_2(\mu\text{-}\eta^2\text{:}\eta^2\text{-N}_2)$ can be synthesized in two steps, which features a bridging N_2 unit in a side-on bonding mode, the N-N bond in this complex (1.548(7) Å) is elongated beyond that of hydrazine (Scheme 1.1b).¹² One drawback in using this [PNP] ligand for early metal complexes is the propensity for phosphine's dissociation. In several early metal complexes, one arm of the tripodal ligand dissociates, giving a bidentate ligand with a pendant phosphine donor arm.²⁵



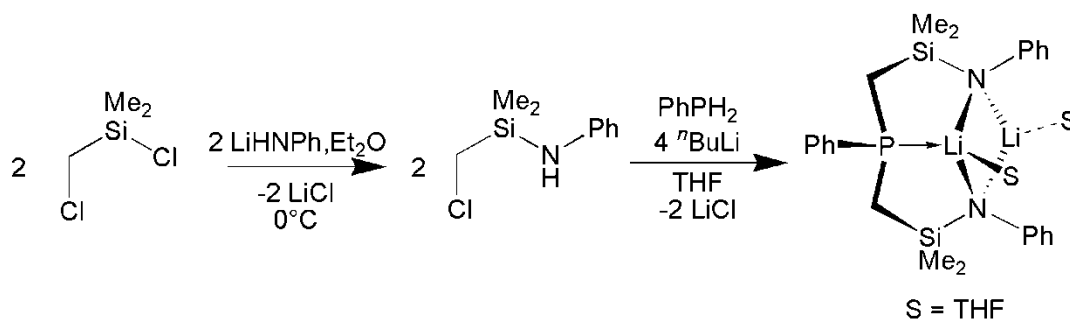
Scheme 1.5

A strategy for preventing this phosphine dissociation led to the design and synthesis of the $[\text{P}_2\text{N}_2]$ macrocyclic ligand ($[\text{P}_2\text{N}_2] = \text{PhP}(\text{CH}_2\text{SiMe}_2\text{NSiMe}_2\text{CH}_2)_2\text{PPh})^{2-}$), as shown in Scheme 1.6.²⁶ The synthesis of $[\text{P}_2\text{N}_2]$ involved linking the two phosphine donors with two disilazane moieties. The lithium salt of the ligand was isolated as a 1,4-dioxane adduct. Because of the stereochemistry at the phosphorus atoms, two isomers are possible. The *syn*-isomers can be prepared exclusively using diethyl ether as the solvent while carefully regulating temperature. Salt metathesis with $\text{ZrCl}_4(\text{THF})_2$ led to the isolation of $[\text{P}_2\text{N}_2]\text{ZrCl}_2$, which was reduced to generate the side-on bound dinitrogen complex.²⁰ However, $[\text{P}_2\text{N}_2]$ -ligated complexes of group 5 revealed a drawback of this tetradentate macrocycle ligand; the $[\text{P}_2\text{N}_2]\text{Nb}$ derivative formed less reactive end-on dinuclear complexes,²⁷ while certain $[\text{P}_2\text{N}_2]$ complexes of tantalum exhibited a lack of reactivity.²⁸ These findings were attributed to coordinative and electronic saturation of the metal centres.



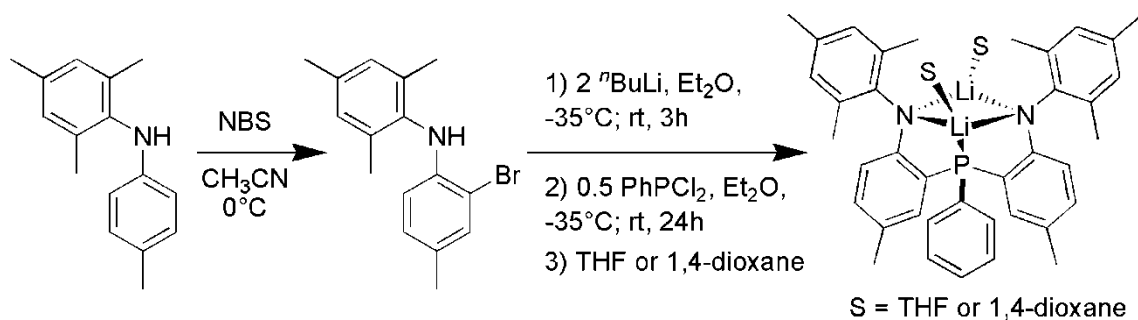
Scheme 1.6

To circumvent this problem, the dianionic diamidophosphine ligand [NPN] ($[(\text{PhNSiMe}_2\text{CH}_2)_2\text{PPh}]^{2-}$) was developed. This design solved the problems encountered with the reactivity of $[\text{P}_2\text{N}_2]$ and still maintained the dianionic nature of the ligand. The synthesis of the $\text{Li}_2[\text{NPN}]$ ligand involved the addition of four equivalents of *n*-BuLi to a mixture of one equivalent of PhPH_2 and two equivalents of $\text{PhNSiMe}_2\text{CH}_2\text{Cl}$ (Scheme 1.7).¹⁴ Through a salt metathesis reaction with ZrCl_4 , $[\text{NPN}]\text{ZrCl}_2$ was readily synthesized. This complex could be reduced in the presence of N_2 to form the side-on bound dinitrogen complex.²⁹ The end-on side-on bound N_2 -derivative $([\text{NPN}]\text{Ta})_2(\mu\text{-H})_2(\mu\text{-}\eta^1:\eta^2\text{-N}_2)$ was discovered upon exposure of $([\text{NPN}]\text{Ta})_2(\mu\text{-H})_4$ to an atmosphere of N_2 as shown in Scheme 1.2.¹⁴ As mentioned in section 1.3, rearrangement and decomposition of the NPN moiety was a major barrier to developing catalytic processes with this ligand system. Therefore, the synthesis of a more robust tridentate diamidophosphine ligand was proposed.



Scheme 1.7

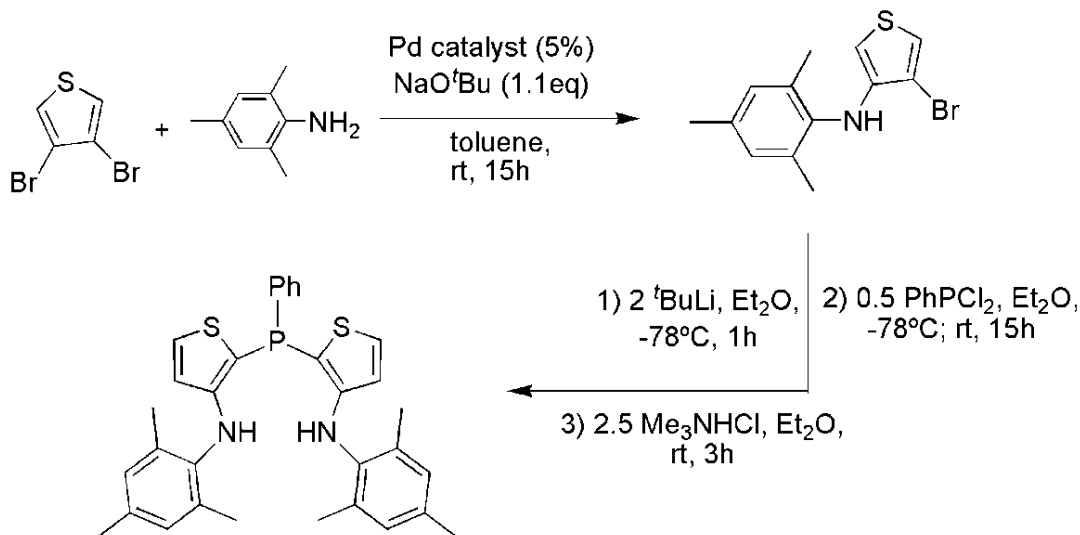
An arene-bridged ligand $[\text{NPN}]^*$ ($[\text{NPN}]^* = \{[N-(2,4,6\text{-Me}_3\text{C}_6\text{H}_2)(2\text{-}N\text{-}5\text{-MeC}_6\text{H}_3)]_2\text{PPh}\}^{2-}$) was synthesized in two steps (Scheme 1.8). After the bromination of mesityltolylamine, the brominated diarylamine was treated with two equivalents of $n\text{-BuLi}$. 0.5 equivalent of diluted dichlorophenylphosphine was then added dropwise to the lithiated amine.³⁰ The resulting arene-bridged diamidophosphine ligand with N-aryl and P-aryl substituents mimics the electronic and steric properties of the original $[\text{NPN}]$ ligand, but lacks the reactive and extremely moisture-sensitive N-Si bonds. The reduction of the corresponding $[\text{NPN}]^*\text{ZrCl}_2$ complex with KC_8 under 4 atmospheres of N_2 yielded the side-on bridged dinitrogen complex.²⁰



Scheme 1.8

A thiophene-bridged diamidophosphine ligand $[\text{NPN}]^{\text{SH}_2}$ ($[\text{NPN}]^{\text{SH}_2} = \{N-(2,4,6\text{-Me}_3\text{C}_6\text{H}_2)(3\text{-NH-SC}_4\text{H}_2)\}_2\text{PPh}$) was also synthesized and its coordination chemistry with early transition metals was explored.³¹ The synthetic route to this ligand is shown in Scheme 1.9.

However, no conclusive evidence indicated the formation of a $\text{Zr}_2\text{-N}_2$ complex from the reduction of $[\text{NPN}]^{\text{S}}\text{ZrCl}_2$ or $[\text{NPN}]^{\text{S}}\text{ZrI}_2$.



Scheme 1.9

1.5 Scope of Thesis

This thesis focuses on the synthesis of new diamidophosphine ligands and their Zr-complexes, designed to activate N_2 . In chapter two, the synthesis of two cyclopentyl linked diiminophosphine proligands is presented, which are denoted as $^{\text{CY5}}[\text{NPN}]^{\text{DMP}}\text{H}_2$ ($\text{DMP} = 2,6\text{-Me}_2\text{C}_6\text{H}_3$) and $^{\text{CY5}}[\text{NPN}]^{\text{DIPP}}\text{H}_2$ ($\text{DIPP} = 2,6\text{-}^i\text{Pr}_2\text{C}_6\text{H}_3$), respectively. They can be considered as analogues of the $[\text{NPN}]^*$ ligand previously reported by the Fryzuk group. These new proligands are very straightforward to synthesize and their intrinsic steric bulk around the amide can be fine-tuned quite readily. Attempts to prepare a diamidodioxo ligand based on calix[4]arene are also described. In chapter three, the synthesis and characterization of Zr(IV) complexes of both cyclopentenyl-linked diamidophosphine ligands are discussed. The synthesis of $\{^{\text{CY5}}[\text{NPN}]^{\text{DMP}}\text{Zr}(\text{THF})\}_2(\mu\text{-}\eta^2\text{:}\eta^2\text{-N}_2)$ from $^{\text{CY5}}[\text{NPN}]^{\text{DMP}}\text{ZrCl}_2$, KC_8 and N_2 in THF is introduced.

In chapter four, conclusions from this thesis are drawn and future work that can be undertaken with these two ligands is discussed.

1.6 References

-
- ¹ Smil, V. *Enriching the Earth*; The MIT Press: Cambridge, **2001**.
- ² Howard, J. B.; Rees, D. C. *Chem. Rev.* **1996**, 96, 2965.
- ³ a) Kim, J.; Rees, D. C. *Nature* **1992**, 360, 553. b) Einsle, O.; Tezcan, F. A.; Andrade, S. L. A.; Schmid, B.; Yoshida, M.; Howard, J. B.; Rees, D. C. *Science* **2002**, 297, 1696.
- ⁴ a) Howard, J. B.; Rees, D. C. *Chem. Rev.* **1996**, 96, 2965. b) Barrière, F. *Coord. Chem. Rev.* **2003**, 236, 71.
- ⁵ a) Holland, P. L. *Can. J. Chem.* **2005**, 83, 296. b) Hidai, M.; Mizobe, Y. *Can. J. Chem.* **2005**, 83, 358.
- ⁶ Smith, B. E. *Science* **2002**, 297, 1654.
- ⁷ Yamabe, I.; Hori, K.; Minato, T.; Fukui, K. *Inorg. Chem.* **1980**, 19, 2154.
- ⁸ Allen, A. D.; Senoff, C. V. *Chem. Commun.* **1965**, 621.
- ⁹ Rocklage, S. M.; Turner, H. W.; Fellmann, J. D.; Schrock, R. R. *Organometallics* **1982**, 1, 703.
- ¹⁰ a) Yamabe, T.; Hori, K.; Minato, T.; Fukui, K. *Inorg. Chem.* **1980**, 19, 2154. b) Blomberg, M. R. A.; Siegbahn, P. E. M. *J. Am. Chem. Soc.* **1993**, 115, 6908.
- ¹¹ Evans, W. J.; Ulbarri, T. A.; Ziller, J. W. *J. Am. Chem. Soc.* **1988**, 110, 6877.
- ¹² Fryzuk, M. D.; Haddad, T. S.; Rettig, S. J. *J. Am. Chem. Soc.* **1990**, 112, 8185.
- ¹³ Fryzuk, M. D.; Haddad, T. S.; Mylvaganam, M.; McConville, D. H.; Rettig, S. J. *J. Am. Chem. Soc.* **1993**, 115, 2782.
- ¹⁴ MacLachlan, E. A.; Fryzuk, M. D.; *Organometallics* **2006**, 25, 1530.
- ¹⁵ Fryzuk, M. D.; Johnson, S. A.; Rettig, S. J. *J. Am. Chem. Soc.* **1998**, 120, 11024.
- ¹⁶ Chatt, J.; Pearman, A. J.; Richards, R. L. *Nature* **1975**, 253, 39.
- ¹⁷ Albertin, G.; Bordignon, E.; Tonel, F. *J. Organomet. Chem.* **2002**, 660, 55.

-
- ¹⁸ Komori, K.; Oshita, H.; Mizobe, Y.; Hidai, M. *J. Am. Chem. Soc.* **1989**, *111*, 1939.
- ¹⁹ Yandulov, D. V.; Schrock, R. R. *Science* **2003**, *301*, 76.
- ²⁰ Morello, L.; Ferreira, M. J.; Patrick, B. O.; Fryzuk, M. D. *Inorg. Chem.* **2008**, *47*, 1319.
- ²¹ MacLachlan, E. A.; Hess, F. M.; Patrick, B. O.; Fryzuk, M. D. *J. Am. Chem. Soc.* **2007**, *129*, 10895.
- ²² Pool, J. A.; Lobkovsky, E.; Chirik, P. J. *Nature* **2004**, *427*, 527.
- ²³ a) Fryzuk, M. D.; MacKay, B. A.; Johnson, S. A.; Patrick, B. O. *Angew. Chem. Int. Ed.* **2002**, *41*, 3709. b) Fryzuk, M. D.; MacKay, B. A.; Patrick, B. O. *J. Am. Chem. Soc.* **2003**, *125*, 3234. c) MacKay, B. A.; Patrick, B. O.; Fryzuk, M. D. *Organometallics* **2005**, *24*, 3836.
- ²⁴ Fryzuk, M. D.; MacNeil, P. A.; Rettig, S. J.; Secco, A. S.; Trotter, J. *Organometallics* **1982**, *1*, 918.
- ²⁵ Fryzuk, m. D.; Love, J. B.; Rettig, S. J. *Organometallics* **1992**, *11*, 469.
- ²⁶ Fryzuk, M. D.; Love, J. B.; Rettig, S. J. *Chem. Commun.* **1996**, 2783.
- ²⁷ Fryzuk, M. D.; Kozak, C. M.; Bowdridge, M. R.; Patrick, B. O.; Rettig, S. J. *J. Am. Chem. Soc.* **2002**, *124*, 8389.
- ²⁸ Fryzuk, M. D.; Johnson, S. A.; Rettig, S. J. *Organometallics* **2000**, *19*, 3931.
- ²⁹ Morello, L.; Yu, P.; Carmichael, C. D.; Patrick, B. O.; Fryzuk, M. D.; *J. Am. Chem. Soc.* **2005**, *127*, 12796.
- ³⁰ MacLachlan, E. A.; Fryzuk, M. D. *Organometallics* **2005**, *24*, 1112.
- ³¹ Menard, G.; Fryzuk, M. D. *Organometallics* **2009**, *28*, 5253.

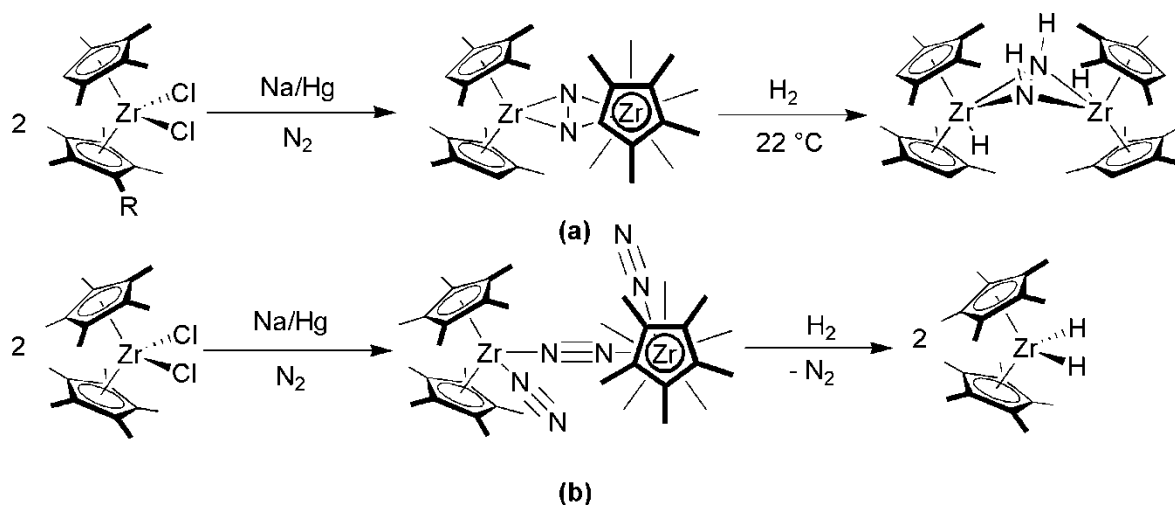
Chapter 2

Ligand Design and Synthesis for Activation of Dinitrogen

2.1 Introduction

Ancillary ligand structure is an important factor in determining the reactivity of a metal complex. A dramatic example of the effect of small changes in ligand structure is the reduction of $(\eta^5\text{-C}_5\text{Me}_4\text{H})_2\text{ZrCl}_2$ versus Cp^*ZrCl_2 ($\text{Cp}^* = \eta^5\text{-C}_5\text{Me}_5$) under N_2 as shown in Scheme 2.1. Treatment of the former complex with Na amalgam yields $[(\eta^5\text{-C}_5\text{Me}_4\text{H})_2\text{Zr}]_2(\mu\text{-}\eta^2\text{:}\eta^2\text{-N}_2)$, in which N_2 bridges two Zr atoms in a side-on mode. Subsequent hydrogenation of this N_2 complex generates $[(\eta^5\text{-C}_5\text{Me}_4\text{H})_2\text{ZrH}]_2(\mu\text{-}\eta^2\text{:}\eta^2\text{-N}_2\text{H}_2)$ with two new N-H bonds (Scheme 2.1a).¹ However, the analogous reduction of Cp^*ZrCl_2 ($\text{Cp}^* = \eta^5\text{-C}_5\text{Me}_5$) produces an end-on dinuclear complex, $[\text{Cp}^*\text{Zr}(\eta^1\text{-N}_2)]_2(\mu\text{-}\eta^1\text{:}\eta^1\text{-N}_2)$, which gives $\text{Cp}^*_2\text{ZrH}_2$ upon addition of H_2 (Scheme 2.1b).² The only difference between the two aforementioned ancillary ligands is the presence of an extra methyl on the Cp^* unit as opposed to $\text{C}_5\text{Me}_4\text{H}$. However, the extent of activation of N_2 , the bonding mode to Zr, and the reactivity of N_2 complexes are totally changed. The above example shows how important the role of ancillary ligands can be in the reactivity of metal complexes.

*A version of this chapter will be submitted for publication. Co-authors: Ting Zhu, Michael D. Fryzuk, Nathan Halcovitch.



Scheme 2.1

Ligand design and modification also play a fundamental role in dinitrogen activation research in the Fryzuk group. This work has focused on multidentate ligands combining amide and phosphine donors as discussed in chapter 1.4. Zirconium complexes, bearing [PNP], [P₂N₂], and [NPN] ligands (Figure 2.1), can form highly activated side-on bound dinitrogen complexes.³ The [NPN]-coordinated tantalum complex ([NPN]Ta)₂(μ-H)₂(μ-η¹:η²-N₂) is another fascinating example, as it comprises a unique end-on side-on bound N₂-unit.⁴ In this remarkable case, the dinitrogen is highly activated even though no harsh reducing agents were used during its synthesis. However, ligand rearrangement has been observed in some attempts to functionalize the coordinated N₂ unit.⁵

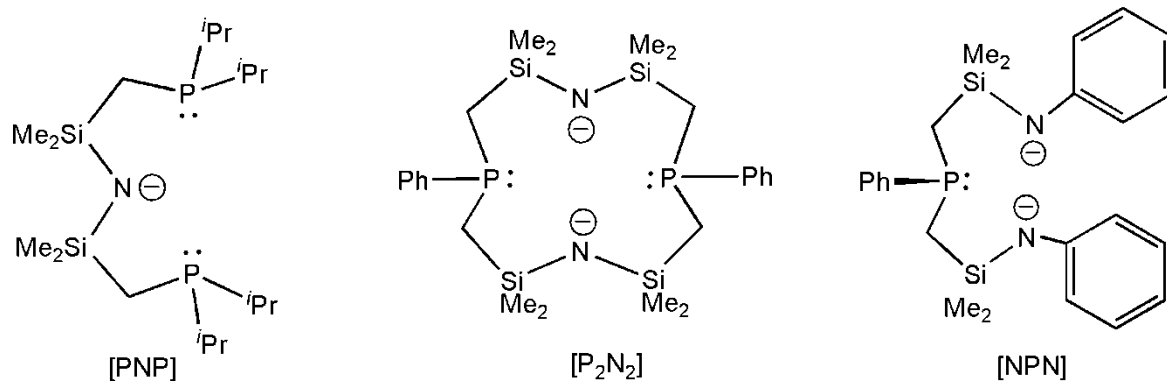


Figure 2.1. Three multidentate ligand systems studied in the Fryzuk group.

In order to prevent these undesired side reactions of the [NPN] ligand, studies were undertaken to substitute the labile $-\text{CH}_2\text{-SiMe}_2-$ backbone for a $-\text{CH}_2\text{-CH}_2-$ linker. Although a trimethyl tantalum complex was synthesized employing this modified ligand, preparation of the corresponding tantalum tetrahydride failed.⁶

[NPN]^{*} and [NPN]^s are two newer modifications of diamidophosphine ligands (Figure 2.2).⁷ The [NPN]^{*} ligand forms early transition metal complexes that can be used to activate and functionalize N_2 .⁸ This arene-bridged diamidophosphine ligand has been designed to prevent the side reactions encountered with the original [NPN] ligand. Secondary alkylamines are generally stronger bases than secondary silyl-substituted amines, while diphenylamine has similar basicity to secondary silyl-substituted amines. Therefore, compared to the more electron-donating alkylamide substituents on the $-\text{CH}_2\text{-CH}_2-$ linked diamidophosphine ligand, the phenylamide of [NPN]^{*} better mimics the electronic property of the slightly electron-withdrawing silylamide substituents of [NPN].

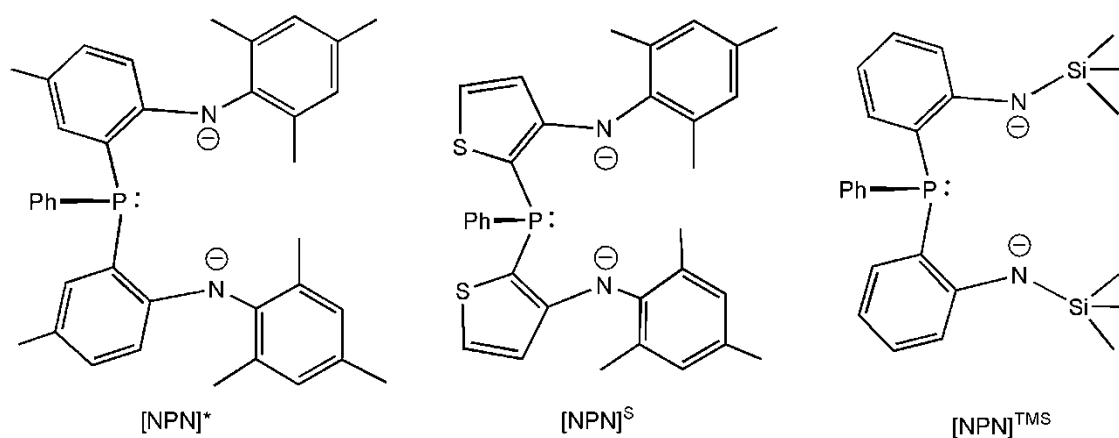
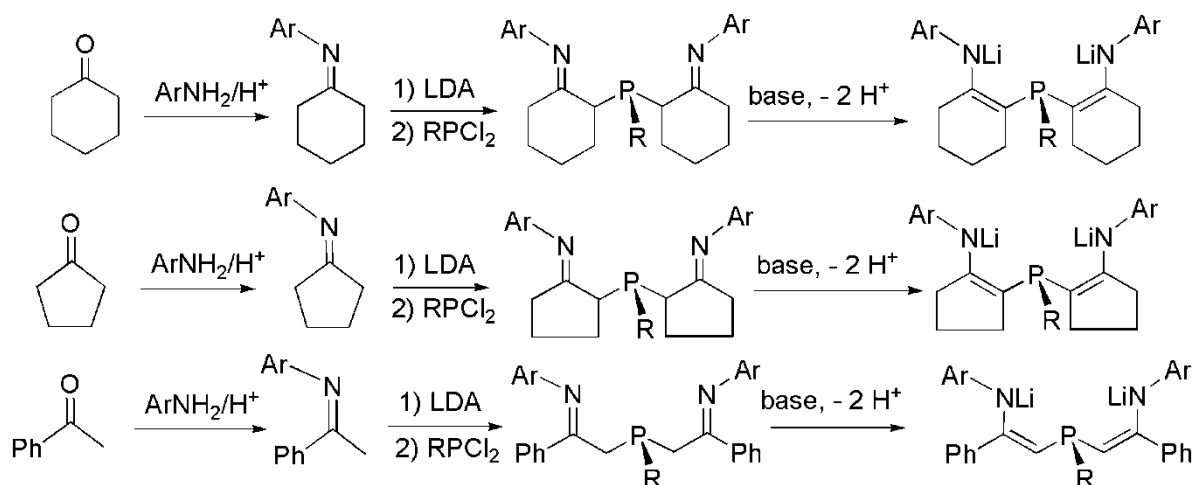


Figure 2.2. New designs of diamidophosphine ligand.

As even minor changes can introduce an unexpected effect on the reactivities of metal complexes, ligand modification studies are of significant importance. In our group, diamidophosphine ligands are further modified at the aryl groups on the amido donors or at the substituent on the phosphine in order to vary the steric and electronic effects. $[\text{NPN}]^{\text{TMS}}$, which bears silyl substituents on the amido donors, was synthesized to test its reactivity with early transition metals in activating N_2 as well (Figure 2.2).⁹ However, excluding $[\text{NPN}]^{\text{S}}$, changes at the arene bridges that connect the amido and phosphine donors have not been investigated.

To this end, three diamidophosphine ligands bearing suitable alternatives for the arene bridge were proposed based on a cyclohexene, a cyclopentene or an alkene bridge, and their syntheses were planned as shown in Scheme 2.2. In each case, only two steps can give the protonated proligand. The double bond linker could be introduced upon deprotonation of the proligands, and would mimic the aromatic double bond in $[\text{NPN}]^*$ and $[\text{NPN}]^{\text{S}}$. These synthetic strategies are much simpler than the one for $[\text{NPN}]^*$. The required starting materials are cheap and readily available as well. More importantly, the steric bulk at the aryl group can be varied easily. Even in the presence of bulky substituents at the *ortho* position of aniline, the

condensation reaction of cyclopentanone and substituted anilines can generate the corresponding precursor arylamines in high yields. In the end, the cyclopentenyl linked ligand was chosen as the target molecule, as compared to the rest two systems a five-membered ring linker would widen the area around the metal centre. A phenyl group was selected as the substituent on the phosphine, and the aryl groups on the amido donors are 2,6-dimethylphenyl and 2,6-diisopropylphenyl, respectively. These two proligands are denoted as $^{CY5}[NPN]^{DMP}H_2$, **2.2** (DMP = 2,6-Me₂C₆H₃) and $^{CY5}[NPN]^{DIPP}H_2$, **2.4** (DIPP = 2,6-*i*Pr₂C₆H₃).



Scheme 2.2

Recently, multidentate methylene-bridged aryloxide ligands have been studied in the Fryzuk group as shown in Figure 2.3.¹⁰ These studies were inspired by an aryloxide ligand system reported by Kawaguchi and co-workers.¹¹ The *ortho*-substituted bulky adamantyl group of the phenol can be easily installed, and the resulting dianionic ligand was designed for group 4 and 5 metal complexes to activate N₂. However, attempts to form early transition metal complexes (Ti, Zr, Ta) based on this ligand were not successful.¹²

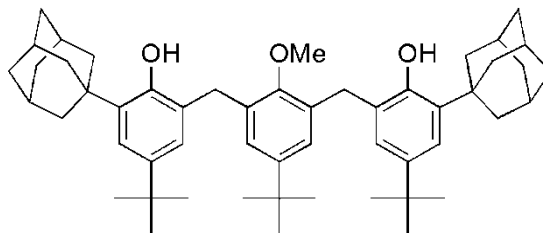


Figure 2.3. A tridentate methylene-linked aryloxide ligand.

As an extension of the study of this aryloxide coordination chemistry, part of this research project focused on the synthesis of a tetradentate sterically bulky ligand based on calix[4]arene. Calix[4]arene is a macrocycle with four oxygen donors, and can be synthesized by condensation of substituted phenols and formaldehyde.¹³ Floriani and coworkers successfully prepared early transition metal dinitrogen complexes using this oxygen-rich ligand in a variety of anionic forms. A notable example is a niobium complex which binds N_2 in an end-on fashion and displays an N-N bond length of 1.390(17) Å. This supports the presence of a formally N_2^{4-} unit (Figure 2.4a).¹⁴ Another example is a μ^3 - η^2 : η^2 : η^2 -hydrazido tetraanion bound to three Sm^{III} centers with an overall butterfly-type arrangement (Figure 2.4b).¹⁵ The N-N bond distance is elongated to 1.611(16) Å which is one of the longest N-N bond in the cases of four-electron-reduced dinitrogen complexes. Because of the outstanding properties of calix[4]arene we intended to further explore this ligand by changing two of its four phenol donors to amine donors, and to examine the resulting N_2 chemistry after coordination of this proposed ligand to early transition metals.

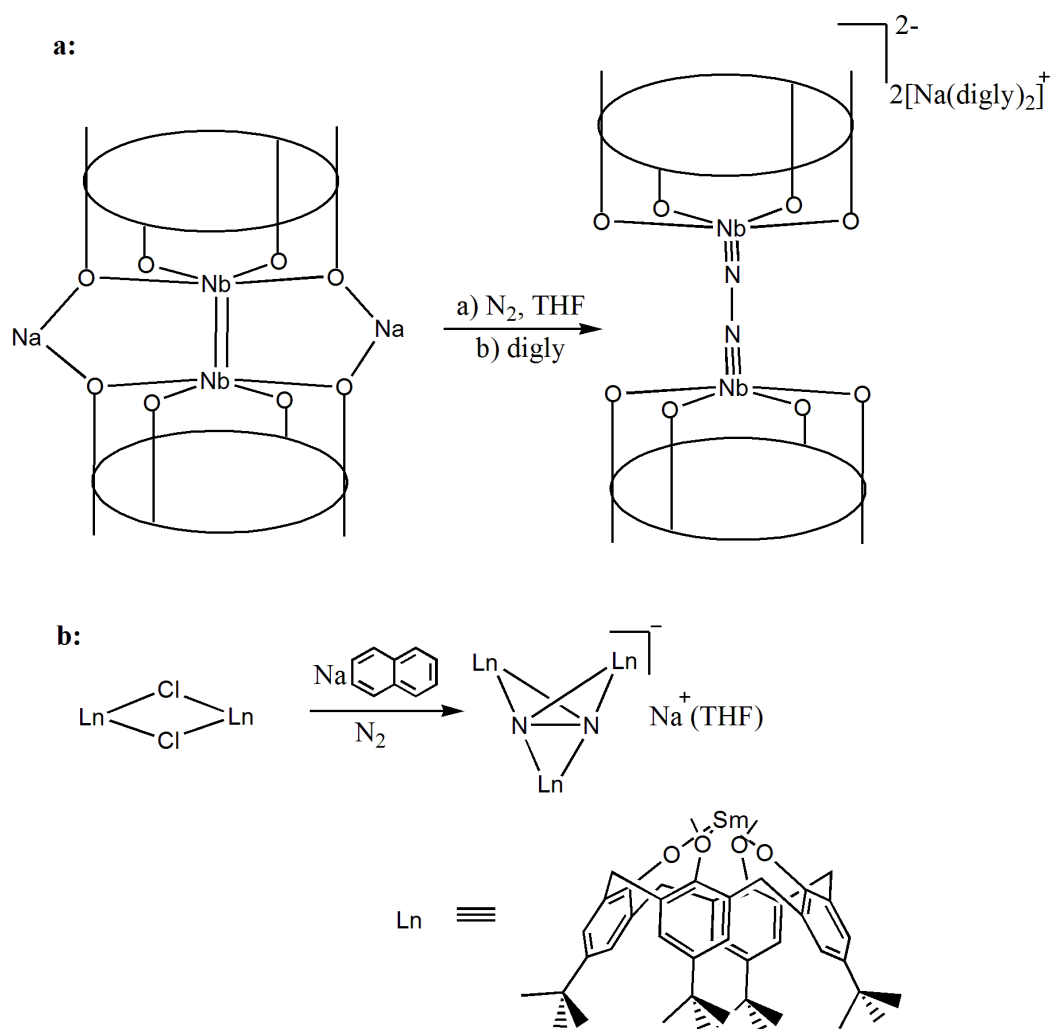


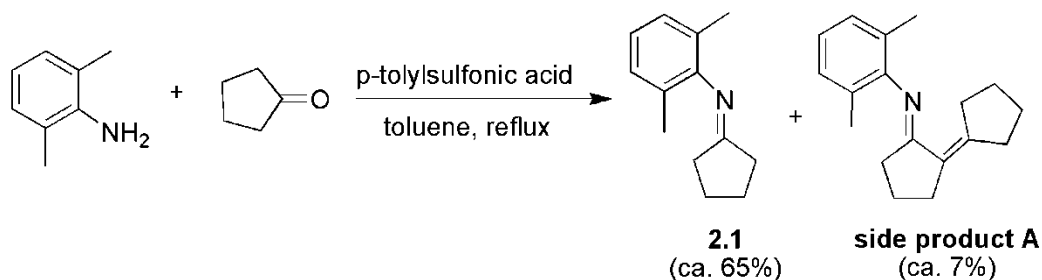
Figure 2.4. Two examples of calix[4]arene-ligated complexes that activate dinitrogen.

In this chapter, the synthesis of two tridentate diiminophosphine proligands, **2.2** and **2.4**, is introduced. The attempted synthesis of a NONO type ligand based on calix[4]arene is also discussed.

2.2 Results and Discussion

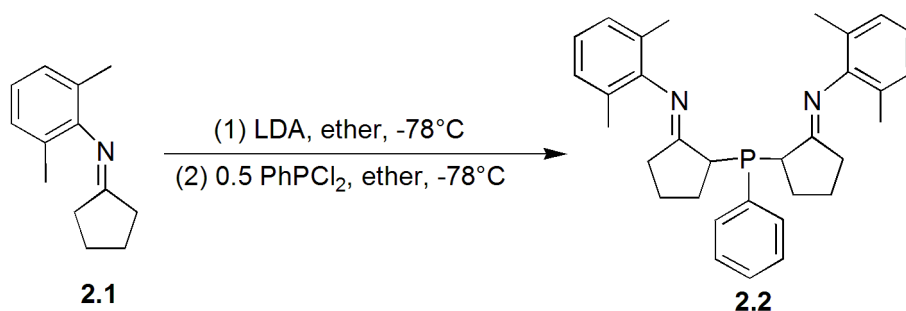
2.2.1 Synthesis of $^{CY5}[NPN]^{DMP}H_2$ and Its Analogue $^{CY5}[NPN]^{DIPP}H_2$

The precursor cyclopentylidene aniline **2.1** can be prepared from 2,6-dimethylaniline and cyclopentanone in the presence of catalytic amounts of *p*-tolylsulfonic acid under reflux in toluene for 6 hours.¹⁶ As the starting materials disappear and the product accumulates, the aldol condensation product **A** is also formed. Mass spectroscopy and 1H NMR analysis confirms the formation of **A** in addition to the desired product **2.1** (Equation 2.1). Pure **2.1** is separated through distillation under vacuum. The unreacted 2,6-dimethylaniline can also be separated by distillation and recycled. The product is characterized by 1H NMR spectroscopy as well as electron impact mass spectrometry (EI-MS).



Equation 2.1

To form the diiminophosphine proligand $^{CY5}[NPN]^{DMP}H_2$, the non-nucleophilic base LDA is made *in situ* to deprotonate **2.1**; afterwards, 0.5 equivalents of a dilute solution of $PhPCl_2$ is added slowly at low temperature (Equation 2.2). Upon work up, an oily yellow compound is obtained containing a mixture of six different species, with $^{31}P\{^1H\}$ NMR signals at δ -5.6, -6.0, -8.5, -12.1, -32.1, and -36.7. The species at δ - 8.5 ppm can be isolated through precipitation from a pentane solution of the mixture. $^1H\{^{31}P\}$ NMR, electron impact mass spectrometry (EI-MS) and elemental analysis (EA) study showed that the solid obtained was the desired diiminophosphine complex **2.2**.



Equation 2.2

It is difficult to purify and characterize the remaining five species. Based on the fact that enamine can be formed from the tautomerization of cyclopentylidene aniline, there are at least three different isomers for proligand $^{CY5}[NPN]^{DMP}H_2$ (Figure 2.5a). In addition, stereoisomers of $^{CY5}[NPN]^{DMP}H_2$ also contribute to the number of the $^{31}P\{^1H\}$ signals. Also, the carbon of the cyclopentane ring adjacent to the phosphorus atom can be in *R* or *S* configuration (Figure 2.5b), and the aryl group on the amido donor and phosphorus atom can be in a *cis* or *trans* positions of the C=N double bond (Figure 2.5c). Combining all these facts, it is possible that the other five $^{31}P\{^1H\}$ peaks could be attributed to the different isomers of proligand $^{CY5}[NPN]^{DMP}H_2$. This interpretation is supported by the fact that the reaction of the mixture of these six species with $Zr(NMe_2)_4$ forms the same metal complex, $\{^{CY5}[NPN]^{DMP}\}Zr(NMe_2)_2$ (**3.1**), as that of compound **2.2**. While stable for months in the solid state, benzene solution of pure **2.2** will eventually tautomerize into a mixture of all six isomers over the course of several weeks.

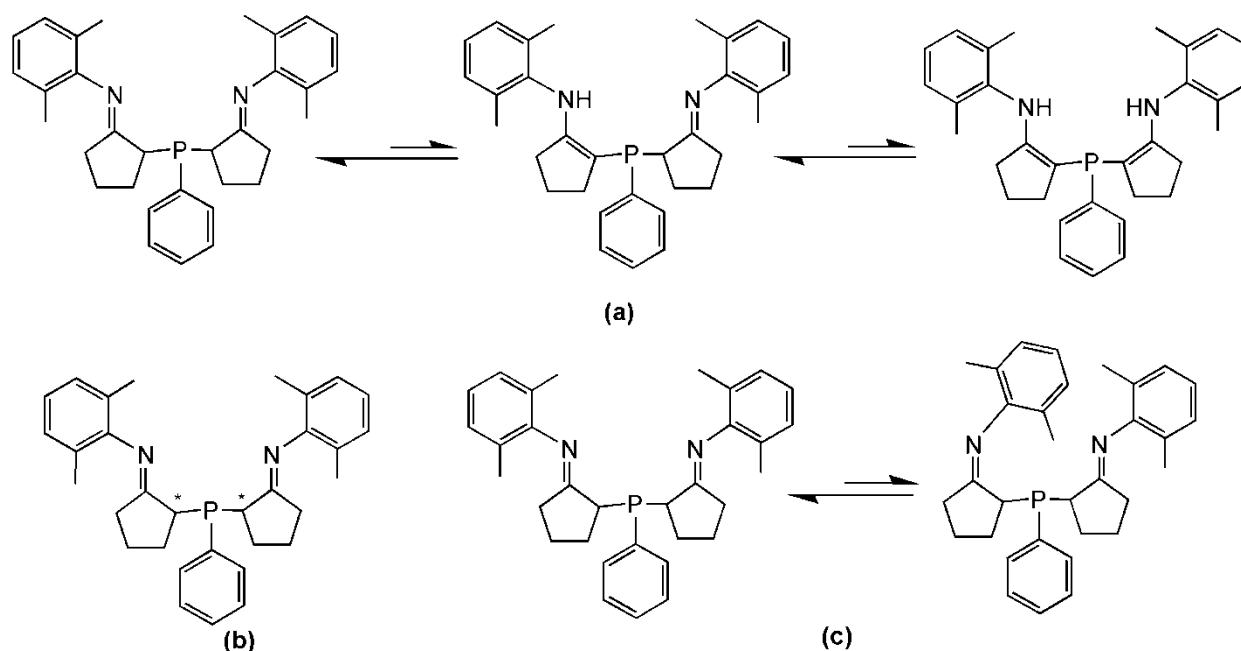
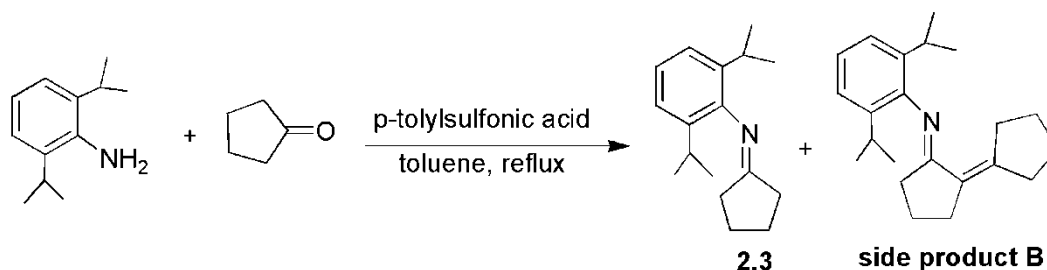


Figure 2.5. The possible isomers of the diiminophosphine proligand, $\text{CY}^5[\text{NPN}]^{\text{DMP}}\text{H}_2$.

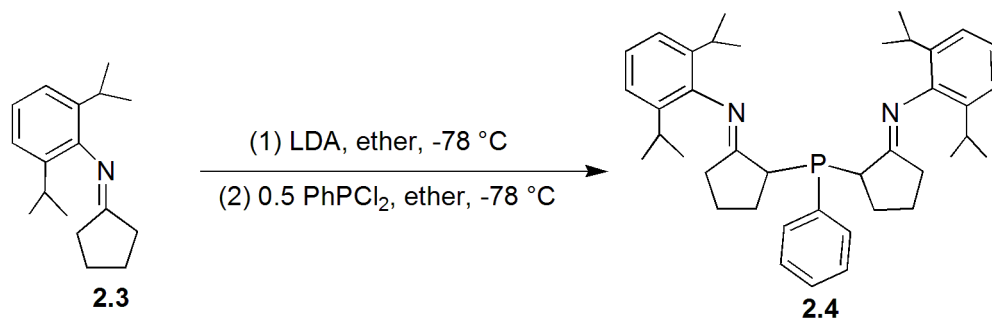
The more sterically congested analogue of **2.1**, *N*-cyclopentylidene-2,6-diisopropylaniline, **2.3**, was synthesized in the same way (Equation 2.3). Purification via distillation afforded large amounts of pure product. The formation of the aldol condensation product **B** was observed in this case as well.



Equation 2.3

The details for the synthesis of the new $\text{CY}^5[\text{NPN}]^{\text{DIPP}}\text{H}_2$ (DIPP = 2,6- $\text{Pr}_2^i\text{C}_6\text{H}_3$) proligand, **2.4**, are shown in the Equation 2.4. All steps are done *in situ* beginning with the lithiation via LDA, followed by the slow addition of PhPCl_2 . Upon work up, the $^{31}\text{P}\{^1\text{H}\}$ NMR spectrum of

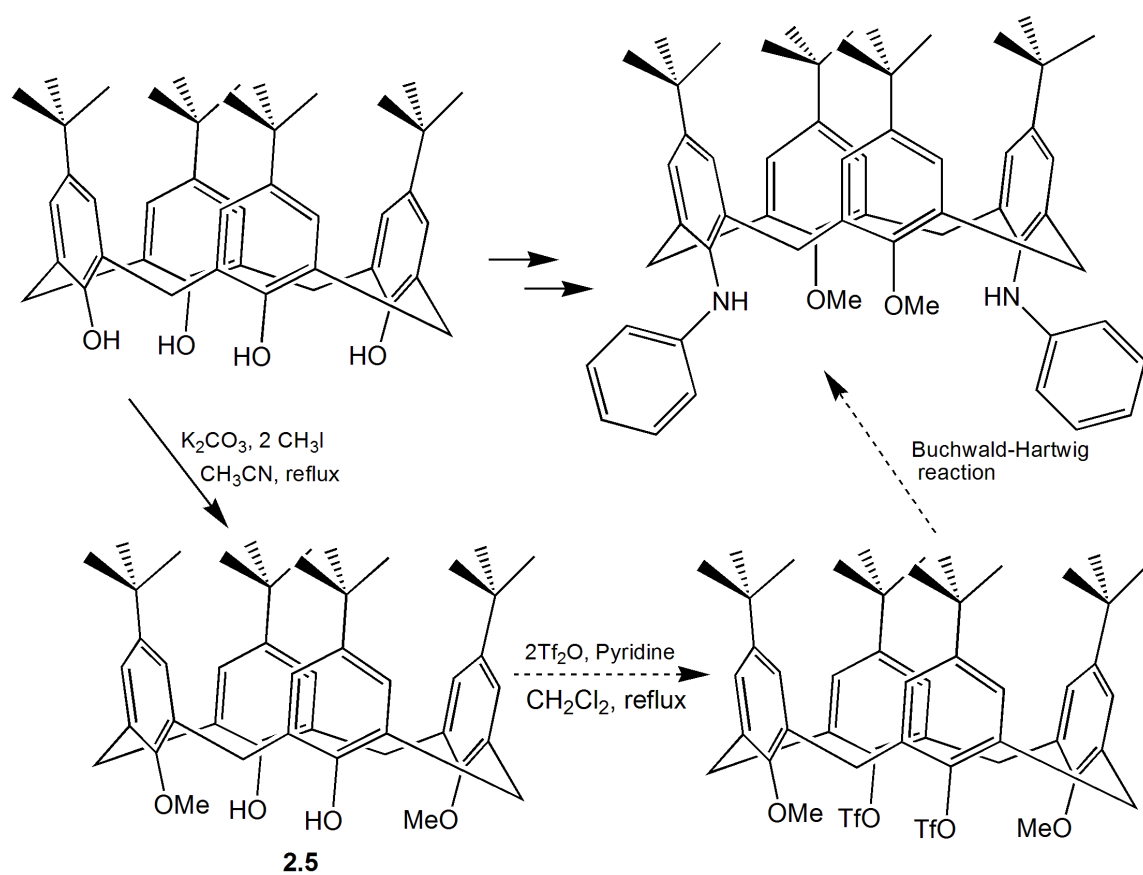
the oily yellow residue shows similar result as that of $^{CY5}[NPN]^{DMP}H_2$: five different phosphorus signals are seen at δ -2.9, -3.8, -8.8, -28.5, and -37.2. Only the species at δ -8.8 can be separated in a manner similar to that of **2.2**. 1H NMR spectrum, electron impact mass spectrometry (EI-MS) and elemental analysis (EA) were used to confirm that the desired proligand **2.4** was formed. Again, the reaction of the mixture of these five species with $Zr(NMe_2)_4$ formed the same metal complex $\{^{CY5}[NPN]^{DIPP}\}Zr(NMe_2)_2$, **3.4**, as that of compound **2.4**.



Equation 2.4

2.2.2 Attempts to Synthesize a NONO Type Proligand Based on the Scaffold of Calix[4]arene

The initial idea for the calix[4]arene project was to change two opposing oxygen donors to amido donors while protecting the other two oxygen donors by methylation. It is known that the two triflated phenols can be converted into amine groups under Buchwald-Hartwig reaction conditions.¹⁷ Therefore, we proposed a strategy to protect two phenol groups via methylation, then convert the two remaining phenols into triflates by reaction with trifluoromethanesulfonic anhydride, and finally complete the coupling reaction to obtain the NONO type proligand (Scheme 2.3).



Scheme 2.3

Unexpectedly, after successful methylation, only one phenol can be triflated even after refluxing at high temperatures in either xylene or DMF. Structure elucidation (Figure 2.6) via X-ray diffraction of the product indicates that the triflated phenol has rotated. The sterically demanding *t*-butyl group of the rotated phenol moiety assumingly protects the other phenol group to prevent it from being triflated.

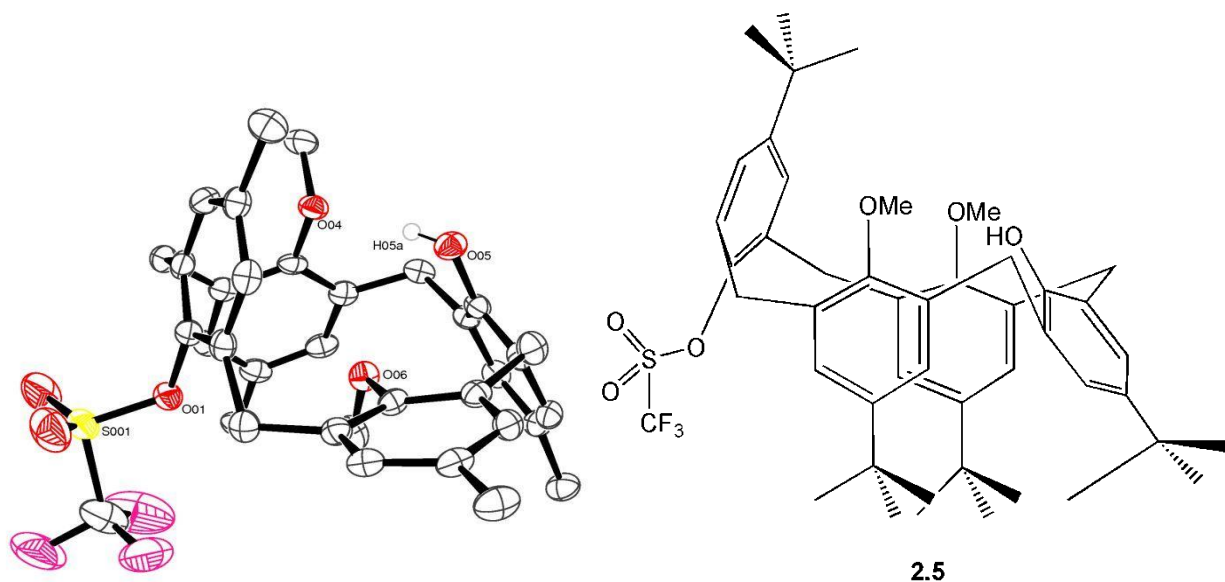
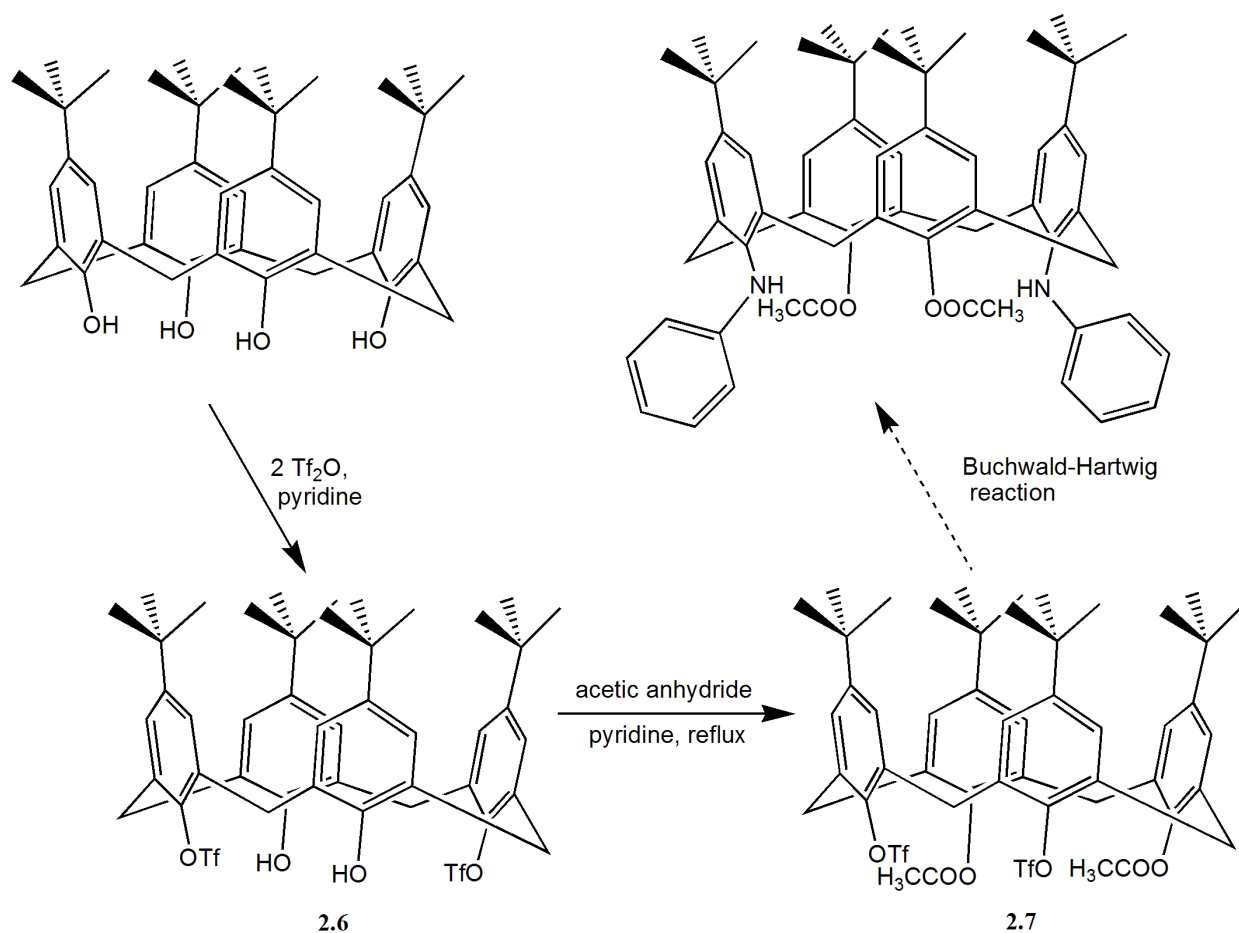


Figure 2.6. Solid-state molecular structure of 1,3-dimethoxy-2-monotriflatocalix[4]arene, **2.5** (*t*-butyl groups are represented by single carbon atoms for simplicity).

In order to solve this problem, a second synthetic route was examined. As shown in scheme 2.4, two phenols in the opposite position were first triflated by trifluoromethanesulfonic anhydride. Then acetic acid was utilized to protect the two remaining phenol groups. Compound **2.7** was successfully synthesized in this way, and conversion of the triflated phenol group into an amine was then attempted via a Pd-catalyzed Buchwald-Hartwig amination. With Pd₂(dba)₃/BINAP as the catalyst and NaO^tBu as the base, *N*-arylation of aniline by the triflated phenol was attempted in toluene by heating to 80°C. According to GC-MS and ¹H NMR analysis, amination to substitute the triflated phenol barely took place. Bitriflated calix[4]arene or calix[4]arene was the major product. It seems that the intrinsic bulkiness of the ligand makes it very difficult to add any large substituent, such as aniline. Apparently, acetylated and triflated phenols are prone to cleavage of the C-O and S-O bonds under the employed reaction conditions.

Even with weak bases such as Cs_2CO_3 or K_3PO_4 , the starting materials calix[4]arene or the bitriflated species were always recovered.



Scheme 2.4

2.3 Conclusions

In this chapter, the synthesis of two new diiminophosphine proligands has been discussed. Compared to the previously reported diamidophosphine ligands, these two ligands, $^{\text{CY5}}[\text{NPN}]^{\text{DMP}}$ (DMP = 2,6- $\text{Me}_2\text{C}_6\text{H}_3$) and $^{\text{CY5}}[\text{NPN}]^{\text{DIPP}}$ (DIPP = 2,6- $i\text{Pr}_2\text{C}_6\text{H}_3$), feature a cyclopentene ring instead of the *o*-thiophene or *o*-phenylene linker. The precursors of the proligands were synthesized by condensation of cyclopentanone and the corresponding *diortho*-substituted

aniline. The diiminophosphine proligands were generated readily from the corresponding lithiated cyclopentylideneaniline (*in situ*) and 0.5 equivalent of PhPCl_2 .

As an extension of the study of aryloxide coordination chemistry, the synthesis of an diamidodioxo ligand based on the scaffold of calix[4]arene was attempted. Due to the bulkiness created by the four *t*-butyl groups on the aryl rings, modifications on the phenol donors were unsuccessful via the chosen synthetic routes.

2.4 Experimental

2.4.1 General Experimental

Unless otherwise stated, all manipulations were performed under an atmosphere of dry, oxygen-free N_2 or Ar by means of standard Schlenk or glovebox techniques. N_2 and Ar were dried and deoxygenated by passing the gases through a column containing molecular sieves and activated CuO. Hexanes, toluene, tetrahydrofuran, and diethyl ether were purchased anhydrous from Aldrich, sparged with N_2 , and passed through columns containing activated alumina and Ridox catalyst. CDCl_3 , $\text{THF-}d_8$ and C_6D_6 were dried over activated 4 Å molecular sieves and freeze-pump-thaw degassed three times. Dichloromethane and acetonitrile were dried over CaH_2 and distilled prior to use. Pentane and benzene were dried over Na/benzophenone and distilled prior to use. ^1H , $^{31}\text{P}\{^1\text{H}\}$, and $^{13}\text{C}\{^1\text{H}\}$ NMR spectra were recorded on a Bruker AV-300 or a Bruker AV-400 spectrometer, operating at 300.1 and 400.0 MHz for ^1H spectra, respectively. All spectra were recorded at room temperature. ^1H NMR spectra were referenced to residual protons in the deuterated solvent: C_6D_6 (δ 7.16), CDCl_3 (δ 7.26). $^{31}\text{P}\{^1\text{H}\}$ NMR spectra were referenced to external $\text{P}(\text{OMe})_3$ (δ 141.0 with respect to 85% H_3PO_4 at δ 0.0). $^{13}\text{C}\{^1\text{H}\}$ NMR spectra are referenced to residual solvent: C_6D_6 (δ 128.0) or CDCl_3 (δ 77.23). Chemical shifts (δ)

listed are in ppm, and absolute values of the coupling constants are in Hz. Mass spectrometry (EI-MS), elemental analysis (C, H, N) and X-ray crystallography were all performed at the Department of Chemistry of the University of British Columbia.

2.4.2 Starting Materials and Reagents

Starting materials including trifluoromethanesulfonic anhydride, methyl iodide, 2,6-dimethylaniline, 2,6-diisopropylaniline, cyclopentanone, dichlorophenylphosphine and diisopropylamine were purchased from Aldrich. Dichlorophenylphosphine was distilled prior to use. 2,6-Dimethylaniline, 2,6-diisopropylaniline, and diisopropylamine were dried over CaH_2 and distilled prior to use. *n*-Butyllithium was purchased from Aldrich and the molarity was determined via direct titration with diphenylcarboxylic acid.¹⁸ Compounds calix[4]arene-toluene¹³ and 1,3-dimethoxycalix[4]arene¹³ were prepared according to the literature procedures.

Synthesis of *N*-cyclopentylidene-2,6-dimethylaniline (2.1). 2,6-Dimethylaniline (18.2 g, 0.15 mol, 18.4 ml), cyclopentanone (12.6 g, 0.15 mol, 13.3 ml), and *p*-tolylsulfonic acid (0.5 g, 2.91 mmol) in toluene (200 ml) were refluxed using an azeotropic distillation apparatus for 8 hours. The solution was concentrated and a dark-red oil was distilled under reduced pressure giving three distinct fractions. The first fraction is unreacted 2,6-dimethylaniline, followed by the colorless liquid of **2.1** (18.2 g, 97.5 mmol, 65%). The highest boiling fraction is the aldol condensation side product **A**.

¹H NMR (CDCl_3 , 300 MHz): δ = 7.01 (d, 2H, 6 Hz, *m*-Ar), 6.88 (t, 1H, 6 Hz, *p*-Ar), 2.59 (t, 2H, 6 Hz, CH_2), 2.04 (s, 6H, CH_3), 1.83 (m, 6H, CH_2).

EI-MS (m/z): 187 [M]⁺

Side product A

¹H NMR (CDCl₃, 300 MHz): δ = 7.02 (d, 2H, 6 Hz, *m*-Ar), 6.86 (t, 1H, 6 Hz, *p*-Ar), 2.93 (m, 2H), 2.51 (m, 2H), 2.39 (m, 2H), 2.04 (s, 6H, ArCH₃), 2.01 (m, 2H), 1.77 (m, 6H).

EI-MS (m/z): 253 [M]⁺

The procedure to prepare 2.3 is analogous to 2.1.

¹H NMR (CDCl₃, 300 MHz): δ = 7.10 (m, 3H, *m,p*-Ar), 2.82 (sept, 2H, 6 Hz, CH), 2.61 (t, 2H, 6 Hz, CH₂), 1.90 (m, 4H, CH₂), 1.78 (m, 2H, CH₂), 1.17 (d, 6H, 6 Hz, CH₃), 1.15 (d, 6H, 6 Hz, CH₃).

EI-MS (m/z): 243 [M]⁺

Synthesis of ^{CY5}[NPN]^{DMP}H₂ (2.2). In a round bottomed flask, lithium diisopropylamide was prepared by slow addition of 1.63 M *n*-butyllithium (8.72 ml, 14.2 mmol) to diisopropylamine (2.00 ml, 14.2 mmol) in 20 ml diethyl ether at -78 °C. The resulting mixture was stirred for 30 minutes while warming up to -50 °C. The solution was cooled to -78 °C again, and neat *N*-cyclopentylidene-2,6-dimethylaniline, **2.1** (2.66 g, 14.2 mmol), was added in dropwise. Thereafter the reaction mixture was warmed to -40 °C over 1 hr. Afterwards, the mixture was cooled again to -78°C and a solution of dichlorophenylphosphine (0.96 ml, 7.10 mmol) in 80 ml diethyl ether was added over 1 hr. The colorless solution gradually changed to pale yellow. Upon completion, the reaction vessel was warmed to room temperature and stirred overnight. The volatiles were then removed *in vacuo* and 20 ml toluene was added to the mixture, which was filtered through celite using a glass frit. Toluene was removed *in vacuo* giving a yellow oil

consisting of a mixture of isomers ($^{31}\text{P}\{^1\text{H}\}$ NMR signals at δ -5.6, -6.0, -8.5, -12.1, -32.1, and -36.7 in toluene). 10 ml pentane was added to the mixture, which resulted in a white precipitate. The suspension was cooled to -40 °C overnight, and the precipitate was collected on a glass frit and dried *in vacuo*. Yield: (1.62 g, 41%).

^1H NMR (C_6D_6 , 300 MHz): δ = 7.74 (m, 2H, *o*-PPh), 7.18 (m, 3H, *m*, *p*-PPh), 7.05 (d, 4H, 6 Hz, *m*-NAr), 6.94 (t, 2H, 6 Hz, *p*-NAr), 3.88 (t, 2H, 6 Hz, CH), 2.19 (s, 6H, ArCH₃), 2.09 (s, 6H, ArCH₃), 2.05 (m, 2H, CH₂), 1.68 (m, 6H, CH₂), 1.45 (m, 2H, CH₂), 1.30 (m, 2H, CH₂). $^{31}\text{P}\{^1\text{H}\}$ NMR (C_6D_6 , 161 MHz): δ = -9.4 (s).

$^{13}\text{C}\{^1\text{H}\}$ NMR (C_6D_6 , 101 MHz): δ = 181.2 (d, 9 Hz), 151.0, 135.7, 135.6 (d, 36 Hz), 129.3, 128.5, 128.3, 128.1, 127.8, 125.5 (d, 23 Hz), 122.9, 42.4 (d, 19 Hz), 32.6, 28.4 (d, 6 Hz), 23.6 (d, 5 Hz), 18.9, 18.3 (ArCH₃).

EI-MS (*m/z*): 480 [*M*]⁺.

Anal. Calcd. for C₃₂H₃₇N₂P: C, 79.97; H, 7.76; N, 5.83; Found: C, 80.06; H, 7.88; N, 5.70.

Synthesis of ^{CY5}[NPN]^{DIPP}H₂ (2.4). In a round bottomed flask, lithium diisopropylamide was prepared by slow addition of 1.6 M *n*-butyllithium (7.04 ml, 11.5 mmol) to diisopropylamine (1.62 ml, 11.5 mmol) in 20 ml diethyl ether at -78 °C. The resulting mixture was stirred for 30 minutes while warming up to -50 °C. The solution was cooled to -78 °C again, and neat *N*-cyclopentylidene-2,6-diisopropylaniline, **2.3** (2.81 g, 11.5 mmol), was added dropwise. Thereafter the reaction mixture was warmed to -40 °C over 1 hr. The mixture was cooled to -78 °C again, and a solution of dichlorophenylphosphine (0.78 ml, 5.75 mmol) in 80 ml diethyl ether was added over 1 hr. The colorless solution gradually changed to pale yellow. Upon completion, the reaction vessel was warmed to room temperature and stirred overnight. The

volatiles were then removed *in vacuo* and 20 ml toluene was added to the mixture, which was filtered through celite using a glass frit. Toluene was removed *in vacuo* giving a yellow oil, which consists a mixture of isomers ($^{31}\text{P}\{^1\text{H}\}$ NMR signals at δ -2.9, -3.8, -8.8, -28.5, and -37.2 in toluene). 10 ml pentane was added to the residue, which resulted in a white precipitate. The suspension was cooled to -40 °C overnight, and the precipitate was collected on a glass frit and dried *in vacuo*. Yield: (1.64g, 48%).

^1H NMR (C_6D_6 , 400 MHz): δ = 7.71 (dd, 2H, J_{HP} = 8 Hz, J_{HH} = 8 Hz, *o*-PPh), 7.19 – 7.09 (m, overlap with the solvent peak), 3.83 (t, 2H, 8 Hz, CH), 3.05 (sept, 4H, 4 Hz, CH), 2.10 (m, 2H, CH_2), 1.89 (m, 2H, CH_2), 1.70 (m, 4H, CH_2), 1.46 (m, 2H, CH_2), 1.35 (m, 2H, CH_2), 1.29 (d, 6H, 4 Hz, CH_3), 1.24 (d, 6H, 4 Hz, CH_3), 1.16 (d, 6H, 4 Hz, CH_3), 1.15 (d, 6H, 4 Hz, CH_3).

$^{31}\text{P}\{^1\text{H}\}$ NMR (C_6D_6 , 161 MHz): δ = - 8.8 (s).

$^{13}\text{C}\{^1\text{H}\}$ NMR (C_6D_6 , 75 MHz): δ = 181.3 (d, 8 Hz), 148.2, 136.2, 136.0, 135.8, 135.6, 135.4 (d, 26 Hz), 129.3, 128.0, 123.5 (d, 25 Hz), 123.2, 42.8 (d, 20 Hz), 33.0, 28.4, 28.2 (d, 6 Hz), 27.8, 24.6, 23.7 (d, 5 Hz), 23.4, 23.1, 22.9.

EI-MS (m/z): 592 $[\text{M}]^+$, 549 $[\text{M} - \text{CH}(\text{CH}_3)_2]^+$.

Anal. Calcd. for $\text{C}_{40}\text{H}_{53}\text{N}_2\text{P}$: C, 81.04; H, 9.01; N, 4.73; Found: C, 81.16; H, 8.86; N, 4.85.

Synthesis of 1,3-dimethoxy-2-monotriflatocalix[4]arene (2.5). Dichloromethane (10 ml) and pyridine (1 ml, 12.4 mmol) were added to 1,3-dimethylcalix[4]arene (677 mg, 1.00 mmol) in a 50ml round bottomed flask. The solution was cooled to 0°C. After trifluoromethanesulfonic anhydride (0.40 ml, 2.40 mmol) was added dropwise, the mixture was warmed to room temperature for 2 hr, and refluxed for six hours. The reaction progress was monitored via TLC and after the starting material was consumed, the mixture was cooled to room temperature and

poured into saturated aqueous solution NaHCO_3 . The aqueous layer was extracted with (3×10 ml) dichloromethane and the organic fractions were combined and dried with MgSO_4 . After filtration, the solution was concentrated *in vacuo* and the product was crystallized (620 mg, 77%)
 ^1H NMR (CDCl_3 , 300 MHz): $\delta = 7.19$ (0.08 - 1.35 (m, 36H, $-\text{C}(\text{CH}_3)_3$), 2.34 (s, 1H, OH), 3.2 - 3.73, 4.25 - 4.45 (m, 8H, CH_2), 3.65 - 3.97 (m, 6H, CH_3), 6.44 - 7.34 (m, 8H, Ar).
EI-MS (m/z): 808 $[\text{M}]^+$.

Synthesis of 1,3-ditriflatocalix[4]arene (2.6). Calix[4]arene·toluene (1.11 g, 1.50 mmol) was dissolved in 30 ml pyridine. The solution was cooled to 0 °C. Trifluoromethanesulfonic anhydride (0.60 ml, 3.60 mmol) was added and stirred for 5 hours at room temperature. The white precipitate which formed (pyridine salt) was filtered off, and the pale yellow filtrate was poured onto approximately 48 g ice. Immediately, a white precipitate was formed which was filtered and washed with cold water. The crude product was dried and subjected to column chromatography (silica gel, eluent chloroform) giving the pure product (1.25 g, 91%).

^1H NMR (CDCl_3 , 300 MHz): $\delta = 7.19$ (s, 4H), 6.80 (s, 4H), 4.24 (s, 2H), 4.19 (s, 2H), 4.12 (s, 2H), 3.57 (s, 2H), 3.52 (s, 2H), 1.35 (s, 18H), 0.92 (s, 18H).
EI-MS (m/z): 912 $[\text{M}]^+$.

Synthesis of 1,3-diactetylato-2,4-ditriflatocalix[4]arene (2.7). A mixture of **2.6** (0.86 g, 0.94 mmol), 6 ml acetic anhydride and 3 ml pyridine was refluxed for two hours. The reaction mixture was cooled to room temperature and poured into 5 ml ethyl acetate, and washed with saturated NaHCO_3 solution (3×5 ml). The organic layer was separated, and dried with MgSO_4 . The pure product was recrystallized from ethyl acetate. Yield (0.40, 43%).

^1H NMR (CDCl_3 , 300 MHz): [ppm] δ = 7.54 (s, 2H), 7.28 (s, 2H), 6.90 (s, 2H), 6.89 (s, 2H), 4.24 (s, 1H), 4.19 (s, 1H), 3.74 (s, 1H), 3.69 (s, 1H), 3.64 (s, 1H), 3.59 (s, 1H), 3.41(s, 1H), 3.36 (s, 1H), 2.06 (s, 3H), 1.65 (s, 3H), 1.39 (s, 9H), 1.38 (s, 9H), 1.10 (s, 18H).

EI-MS (m/z): 912 $[\text{M}]^+$.

2.5 References

- ¹ Pool, J. A.; Lobkovsky, E.; Chirik, P. J. *Nature* **2004**, 427, 527.
- ² a) Manriquez, J. M.; Sanner, R. D.; Marsh, R. E.; Bercaw, J. E. *J. Am. Chem. Soc.* **1974**, 96, 6229. b) Manriquez, J. M.; McAlister, D. R.; Sanner, R. D.; Bercaw, J. E. *J. Am. Chem. Soc.* **1978**, 100, 2716.
- ³ MacLachlan, E. A.; Fryzuk, M. D. *Organometallics* **2006**, 25, 1530.
- ⁴ Fryzuk, M. D.; Johnson, S. A.; Rettig, S. J. *J. Am. Chem. Soc.* **1998**, 120, 11024.
- ⁵ Fryzuk, M. D.; Mackay, B. A.; Johnson, S. A.; Patrick, B. O. *Angew. Chem. Int. Ed.* **2002**, 41, 2709.
- ⁶ Corkin, J. R.; Fryzuk, M. D. *unpublished results*.
- ⁷ a) MacLachlan, E. A.; Fryzuk, M. D. *Organometallics*, **2005**, 24, 1112. b) Ménard, G.; Fryzuk, M. D. *Organometallics* **2009**, 28, 5253.
- ⁸ MacLachlan, E. A.; Hess, F. M.; Patrick, B. O.; Fryzuk, M. D. *J. Am. Chem. Soc.* **2007**, 129, 10895.
- ⁹ Balmann, J.; Fryzuk, M. D. *unpublished results*.
- ¹⁰ Ménard, G. *Ligand Design and Synthesis for Early Metal Complexes*; Master thesis, University of British Columbia: Vancouver, 2007.
- ¹¹ Kawaguchi, H.; Matsuo, T. *Angew. Chem. Int. Ed.* **2002**, 41, 2792.
- ¹² Ménard, G. *Synthesis of Group 4 or 5 [NPN]^S or [OOO] complexes for the Activation of Dinitrogen*; Master thesis, University of British Columbia: Vancouver, 2007.
- ¹³ Arduini, A. and Casnati, A. in *Macrocyclic Synthesis: a practical approach* (Ed. Parker, D.); Oxford University Press: New York, 1996.

-
- ¹⁴ Zanotti-Gerosa, A.; Solari, E.; Giannini, L.; Floriani, C.; Chiesi-Villa, A.; Rizzoli, C. *J. Am. Chem. Soc.* **1998**, *120*, 437.
- ¹⁵ Guillemot, G.; Castellano, B.; Prange, T.; Solari, E.; Floriani, C. *Inorg. Chem.* **2007**, *46*, 5154.
- ¹⁶ Keim, W.; Killat, S.; Nobile, C. F.; Suranna, G. P.; Englet, U.; Wang, R.; Mecking, S.; Schroder, D. L. *J. Organomet. Chem.* **2002**, *662*, 150.
- ¹⁷ Ahman, J.; Buchwald, S. L. *Tetrahedron Letters*, **1997**, *38*, 6363.
- ¹⁸ Kofron, W. G.; Baclawski, L. M. *J. Org. Chem.* **1976**, *41*, 1879.

Chapter 3

Zirconium Complexes of the Cyclopentenyl-linked Diamidophosphine Ligands and Attempts to Activate Dinitrogen

3.1 Introduction

Since the serendipitous discovery of the first dinitrogen complex, $[\text{Ru}(\text{NH}_3)_5(\eta^1\text{-N}_2)]^{2+}$ in 1965,¹ many synthetic strategies have been developed to make dinitrogen complexes. Most late transition metal dinitrogen complexes are electronically saturated species prepared through ligand substitution reactions.² As shown in Figure 1a, $[\text{Mn}(\text{CO})(\text{dppe})_2(\text{N}_2)]^+$ weakly bonds N_2 in the end-on mode. In solution this compound is in equilibrium with the electron deficient $[\text{Mn}(\text{CO})(\text{dppe})_2]^+$, which is stabilized by two agostic interactions with the supporting dppe ligands.³ Some late transition metal dinitrogen complexes are formed from coordinatively unsaturated intermediates. For instance, Cl^- abstraction by Ag^+ in the piano-stool complex $\text{CpRu}(\text{dippe})\text{Cl}$ in the presence of N_2 generates the 18-electron dinitrogen compound $[\text{CpRu}(\text{dippe})\text{N}_2]^+$ (Figure 1b).⁴ The weakly coordinated N_2 unit is very easily released under reduced pressure,⁵ or displaced by other ligands.⁶

*A version of this chapter will be submitted for publication. Co-authors: Ting Zhu, Michael D. Fryzuk, Nathan Halcovitch.

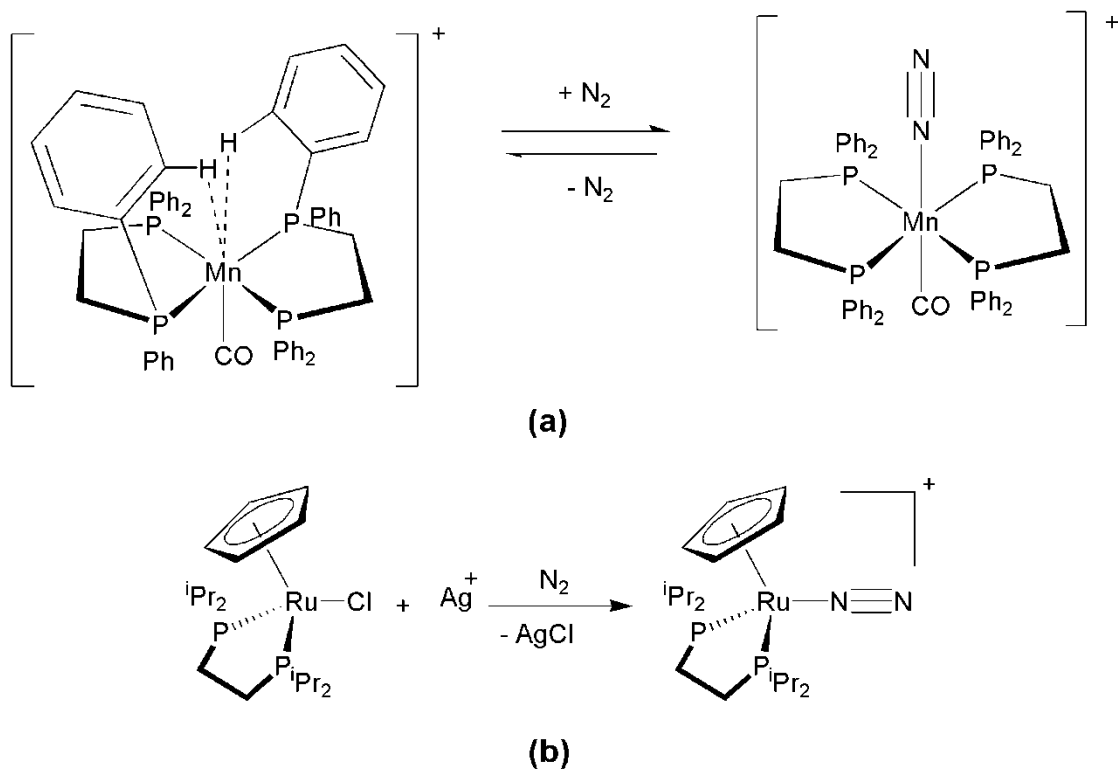


Figure 3.1. N_2 activated from late transition metal complexes.

Dinitrogen complexes of the early transition metals are usually synthesized by reducing a metal halide precursor complex with a strong alkali metal reagent in the presence of N_2 . In the Fryzuk lab, most of the dinitrogen species are generated using this methodology. Reduction of $[PNP]ZrCl_3$ with Na amalgam produces side-on bound ($[PNP]ZrCl)_2(\mu-\eta^2:\eta^2-N_2)$ (Scheme 1.1),⁷ while $[P_2N_2]ZrCl_2$,⁸ $[NPN]ZrCl_2$,⁹ and $[NPN]^*ZrCl_2$ ¹⁰ can be reduced by KC_8 to provide the corresponding side-on bound N_2 complexes (Figure 3.2).

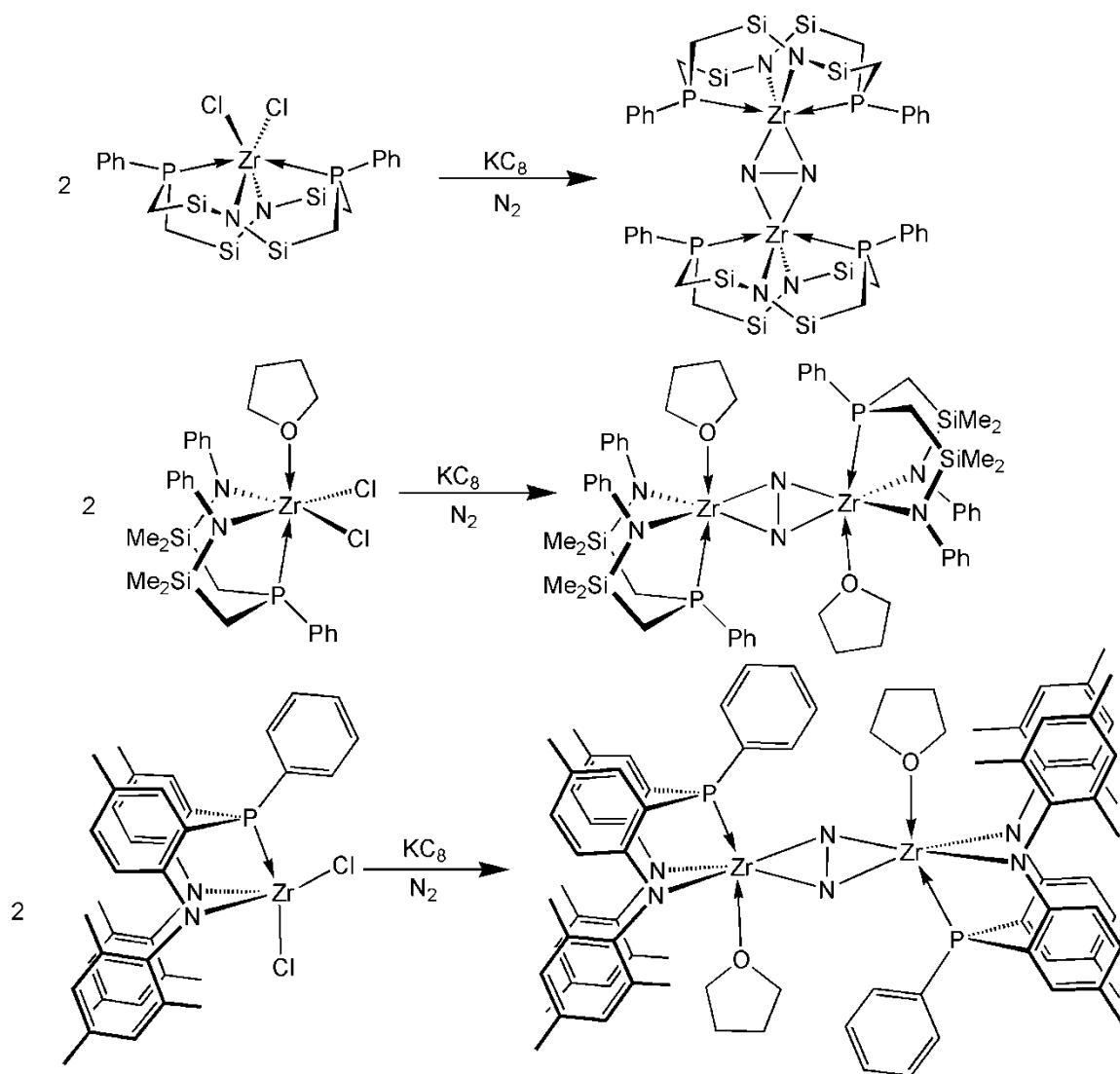


Figure 3.2. Activation of N_2 through reduction of metal halide (silyl methyl substituents of $[\text{P}_2\text{N}_2]$ omitted).

Early transition metal hydrides can also activate N_2 to produce dinitrogen-containing complexes. The side-on end-on dinitrogen complex, $([\text{NPN}]\text{Ta})_2(\mu\text{-H})_2(\mu\text{-}\eta^1\text{:}\eta^2\text{-N}_2)$, was produced by treating $([\text{NPN}]\text{Ta})_2(\mu\text{-H})_4$ under one atmosphere of N_2 (Figure 3.3a).¹¹ The end-on bound dinitrogen complex $[(\text{C}_5\text{Me}_4\text{H})_2\text{Ti}]_2(\mu\text{-}\eta^1\text{:}\eta^2\text{-N}_2)$ can also be generated via the titanium

hydride, $(C_5Me_4H)_2TiH$, which reacts with N_2 to produce the dinuclear dinitrogen complex and one equivalent of H_2 (Figure 3.3b).¹²

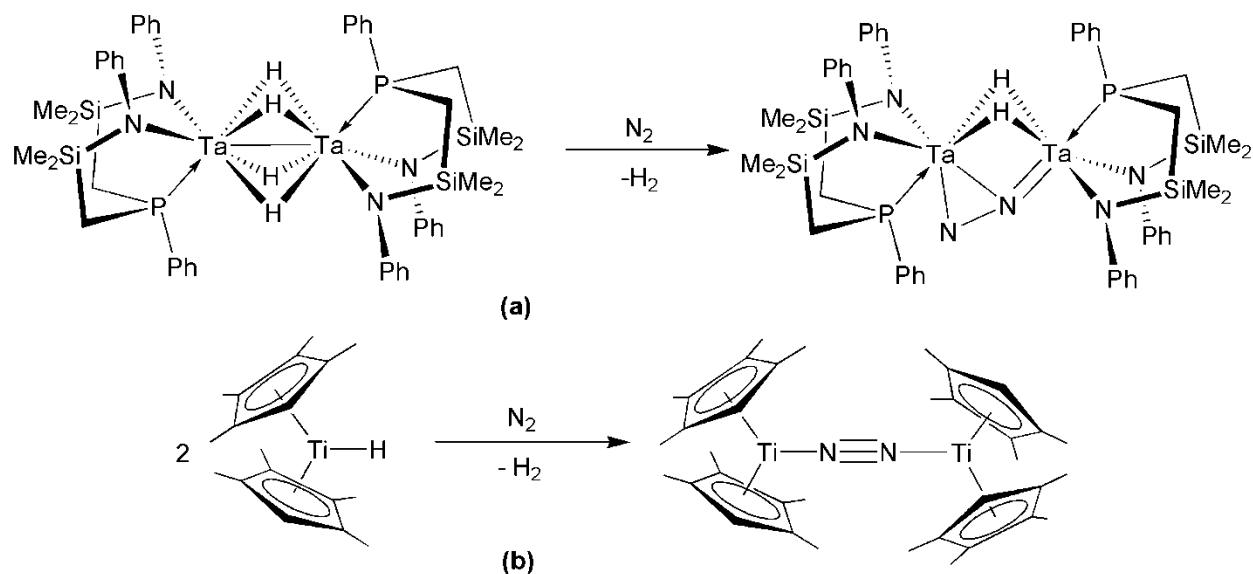


Figure 3.3. Activation of N_2 by early transition metal hydrides.

Some early transition metal complexes eliminate hydrocarbons to give coordinatively unsaturated intermediates that activate dinitrogen. The dinitrogen zirconium complex with end-on bound dinitrogen ligands was generated from the complex $Cp^*_2ZrH[CH_2C(CH_3)_3]$. The elimination of a molecule of CMe_4 acts as the driving force in this reaction (Figure 3.4),¹³ although the N_2 units are only weakly coordinated in this zirconium complex.

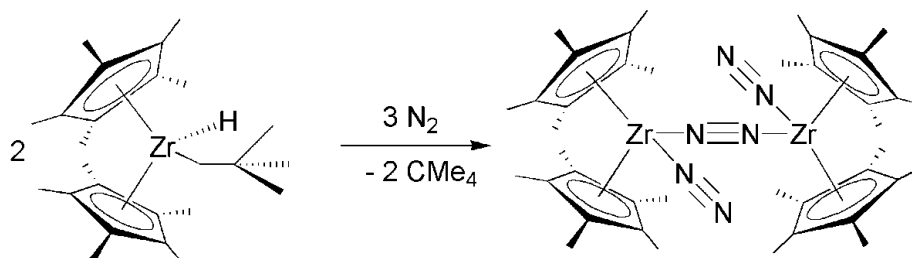


Figure 3.4. Activation of N_2 through elimination of hydrocarbon.

Strong activation of N_2 by low-valent metal complexes can also be achieved without using external reducing reagents. For example, complex $[\text{Ar}(\text{R})\text{N}]_3\text{Mo}\equiv\text{N}$ was generated from the reduced metal complex $[\text{Ar}(\text{R})\text{N}]_3\text{Mo}(\text{III})$ ($\text{Ar} = 3,5\text{-Me}_2\text{C}_6\text{H}_3$, $\text{R} = \text{C}(\text{CD}_3)_2\text{CH}_3$) and N_2 (Figure 3.5).¹⁴ The N-N triple bond was cleaved completely in this reaction.

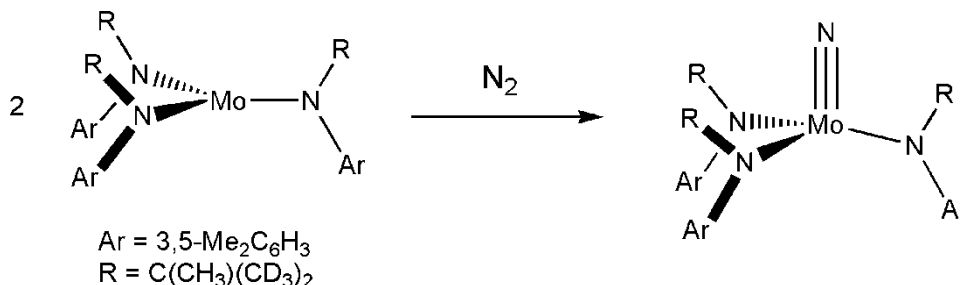
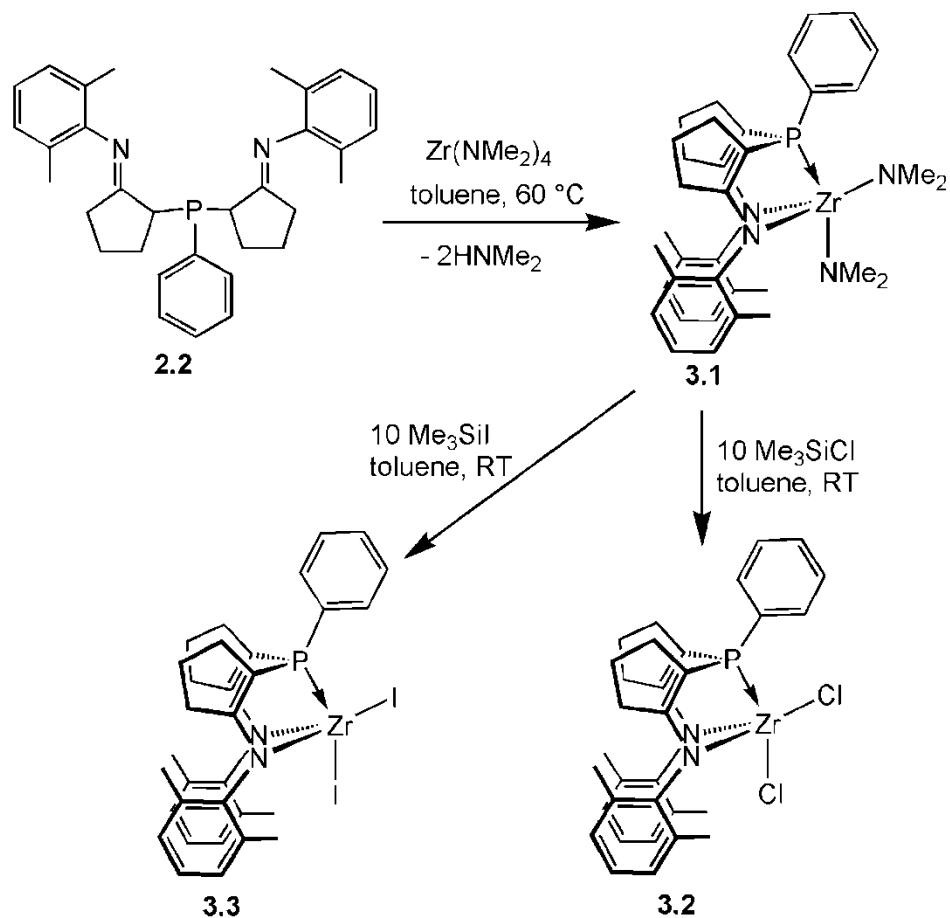


Figure 3.5. Activation of N_2 with low-valent metal complexes.

In this chapter, the synthesis and characterization of Zr complexes from the proligands $^{\text{CY5}}[\text{NPN}]^{\text{DMP}}\text{H}_2$ and $^{\text{CY5}}[\text{NPN}]^{\text{DIPP}}\text{H}_2$ are described. A dinuclear Zr- N_2 complex is obtained by the reduction of $^{\text{CY5}}[\text{NPN}]^{\text{DMP}}\text{ZrCl}_2$ in the presence of N_2 , and shows that the N_2 unit is coordinated side-on to the two Zr atoms as indicated by the single crystal X-ray analysis. The tentative reduction of $^{\text{CY5}}[\text{NPN}]^{\text{DIPP}}\text{ZrCl}_2$ by KC_8 is also discussed.

3.2 Results and Discussion

3.2.1 Synthesis of Zirconium Complexes of $^{CY5}[NPN]^{DMP}H_2$



Scheme 3.1

Diamidozirconium, dichlorozirconium and diiodozirconium complexes of $^{CY5}[NPN]^{DMP}$ are prepared as shown in scheme 3.1. $^{CY5}[NPN]^{DMP}Zr(NMe_2)_2$, **3.1** is generated by adding one equivalent of **2.2** to $Zr(NMe_2)_4$ in toluene, and heating for 12 hours at 60°C; upon workup, **3.1** is obtained as a yellow powder in high yield. Through protonolysis, the imine group in the proligand converts into an enamido moiety via rehybridization of the sp^3 carbon next to phosphorus to sp^2 . The $^{31}P\{^1H\}$ NMR spectrum of **3.1** in C_6D_6 shows a singlet at δ -38.9, in the $^1H\{^{31}P\}$ NMR spectrum, and there are two singlets for the $ArCH_3$ groups, indicating that the

aryl groups on the amido donor do not rotate freely. The two NMe₂ resonances at δ 2.90 and 2.24 correspond to two different amido methyl environments. Complex **3.1** appears to be a C_s symmetric complex in solution.

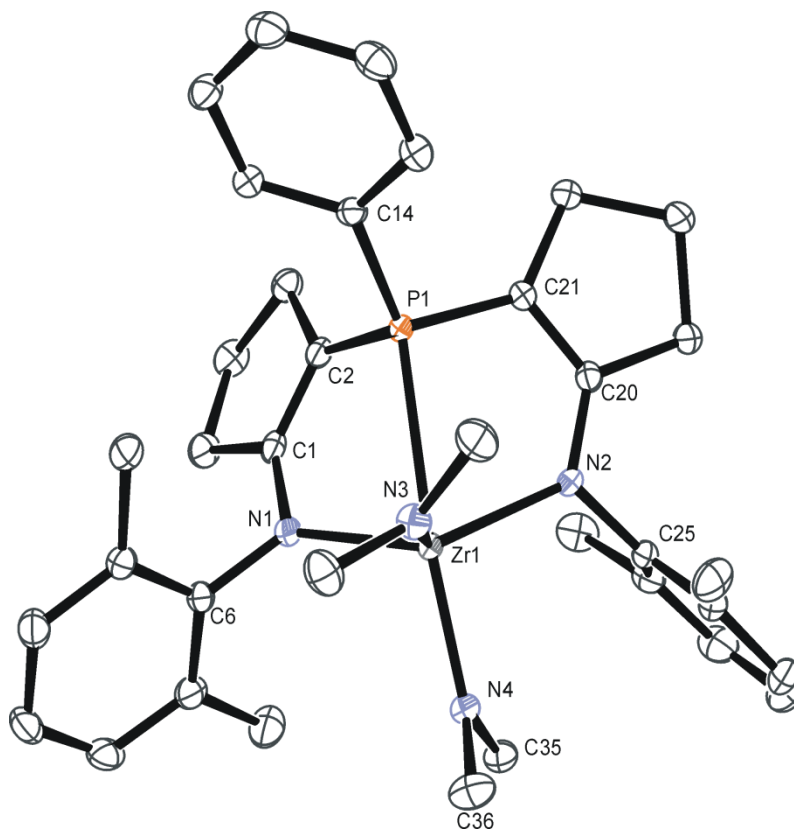


Figure 3.6. ORTEP drawing of the solid-state molecular structure of ^{CY5}[NPN]^{DMP}Zr(NMe₂)₂, **3.1** (ellipsoids at 50% probability level). All hydrogen atoms have been omitted for clarity. Selected bond length (Å) and angles (°): Zr1-N1 2.1727(10), Zr1-N2 2.1740(10), Zr1-P1 2.7756(3), Zr1-N3 2.0191(10), Zr1-N4 2.0670(10), C1-C2 1.3618(16), C20-C21 1.3570(16), N1-Zr1-N2 123.52(4), N3-Zr1-N4 104.88(4), N1-Zr1-P1 73.78(3), N2-Zr1-P1 72.59(3), N1-Zr1-N3 111.36(4), P1-Zr1-N3 89.90(3), P1-Zr1-N4 164.75(3), N1-Zr1-N4 103.49(4), N2-Zr1-N4 97.75(4), N2-Zr1-N3 112.54(4), C2-C1-N1 126.20(10), C21-C20-N2 125.67(10), C6-N1-Zr1 124.83(7), C25-N2-Zr1 118.89(7).

Similar to two previously reported diamidophosphine ligand systems in the Fryzuk group, $[\text{NPN}]^{\text{S}}\text{Zr}(\text{NMe}_2)_2$ ¹⁵ and $[\text{NPN}]^{\text{*}}\text{Zr}(\text{NMe}_2)_2$,¹⁶ in the solid state this complex is a distorted trigonal bipyramid with the N1, N2 and N3 donors at equatorial position, while P1 and N4 are apical. The N1-Zr1-P1 and N2-Zr1-P1 angles are 73.78(3) and 72.59(3)°, and these make the two amido donors extend out of the equatorial plane. The sum of the angles about N1 and N2 are 359.33 and 359.62°, respectively, indicating that the amide atoms are planar and sp^2 hybridized. The bond length for Zr-N, and Zr-P are within the values observed in Zr(IV) complexes.¹⁷

$^{\text{CY5}}[\text{NPN}]^{\text{DMP}}\text{ZrCl}_2$ can be obtained from **3.1** with excess Me_3SiCl in toluene and is isolated as an orange solid. The volatile by-product, $\text{Me}_3\text{SiNMe}_2$, is eliminated once the reaction mixture is left under vacuum. The $^{31}\text{P}\{^1\text{H}\}$ NMR spectrum of **3.2** in C_6D_6 shows a singlet at δ - 31.9. Similar to $^{\text{CY5}}[\text{NPN}]^{\text{DMP}}\text{Zr}(\text{NMe}_2)_2$, there are two singlets in $^1\text{H}\{^{31}\text{P}\}$ NMR spectrum for the *ortho*-methyl groups on the arylamide donors, which indicates hindered rotation about the N-Ar bond. Dissolution of **3.2** in THF results in sharp color change from orange to deep red, suggesting that THF may coordinate to **3.2**. This is supported by the $^{31}\text{P}\{^1\text{H}\}$ NMR spectrum in which a downfield shift to δ -21.4 is observed. Surprisingly, no change in the $^{31}\text{P}\{^1\text{H}\}$ NMR spectrum of **3.1** is observed when THF is added, which indicates that the bulkier dimethylamido donors prevent THF from coordination.

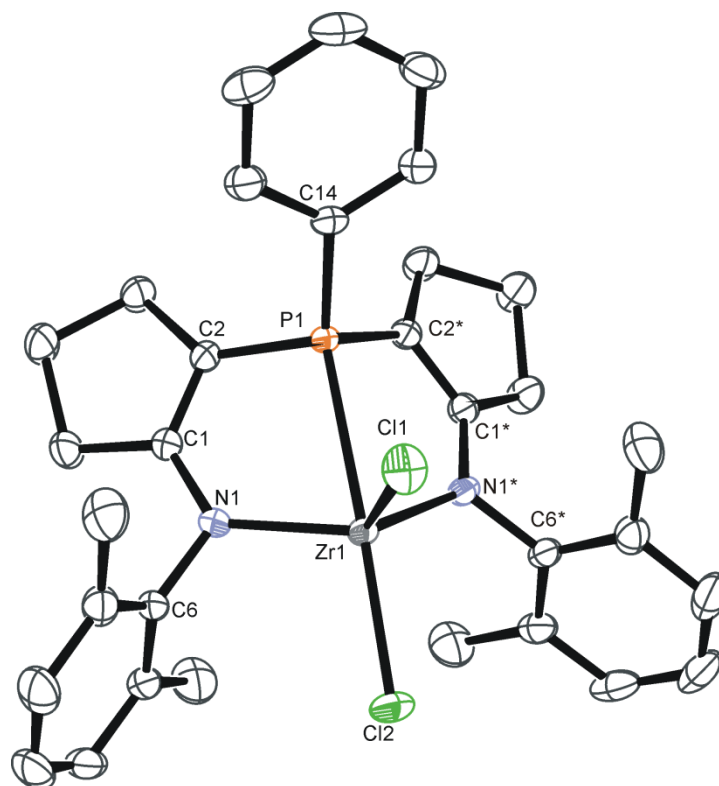


Figure 3.7. ORTEP drawing of the solid-state molecular structure of $\text{CY}^5[\text{NPN}]^{\text{DMP}}\text{ZrCl}_2$, **3.2** (ellipsoids at 50% probability level). All hydrogen atoms have been omitted for clarity. Selected bond length (Å) and angles (°): Zr1-N1 2.0844(11), Zr1-P1 2.7689(8), Zr1-Cl1 2.3887(10), Zr1-Cl2 2.4088(8), C1-C2 1.3512(16), N1-Zr1-N1* 120.12(6), Cl1-Zr1-Cl2 100.771(19), N1-Zr1-P1 73.22(3), N1-Zr1-Cl1 112.84(3), P1-Zr1-Cl1 86.401(16), P1-Zr1-Cl2 172.828(18), N1-Zr1-Cl2 103.63(3), C2-C1-N1 124.83(11), C6-N1-Zr1 116.55(7).

The ORTEP representation of the solid-state molecular structure of **3.2** is shown in Figure 3.7. The geometry around the metal centre is best described as a distorted trigonal bipyramid similar to the diamido complex. The N1-Zr1-P1 angle at 73.22(3)° deviates from 90° due to the strain imposed by the cyclopentene bridge. The C2-C1-N1 angle at 124.83(11)° is much larger than the corresponding bond angles in $[\text{NPN}]^*\text{ZrCl}_2$, which average 118°. ¹⁶ This

was expected in the five-membered cyclopentene linker as it enforces a wider angle around the metal centre compared to the arene ring bridged [NPN]*ZrCl₂.

^{CY5}[NPN]^{DMP}ZrI₂ **3.3** can be synthesized from ^{CY5}[NPN]^{DMP}Zr(NMe₂)₂ **3.1** and excess Me₃SiI. Upon addition of excess Me₃SiI to a toluene solution of **3.1**, an immediate colour change from yellow to slight red is observed. Pure orange powder is obtained following workup. The ³¹P{¹H} NMR spectrum in C₆D₆ shows a singlet at δ -30.1, slightly downfield compared to the dichloro species. The ¹H{³¹P} NMR is analogous to **3.2**, with two singlets for the *ortho*-methyl groups on the arylamido donors at δ 2.63 and 2.36, respectively. Proton NMR data suggests the complex is C_s symmetric in solution.

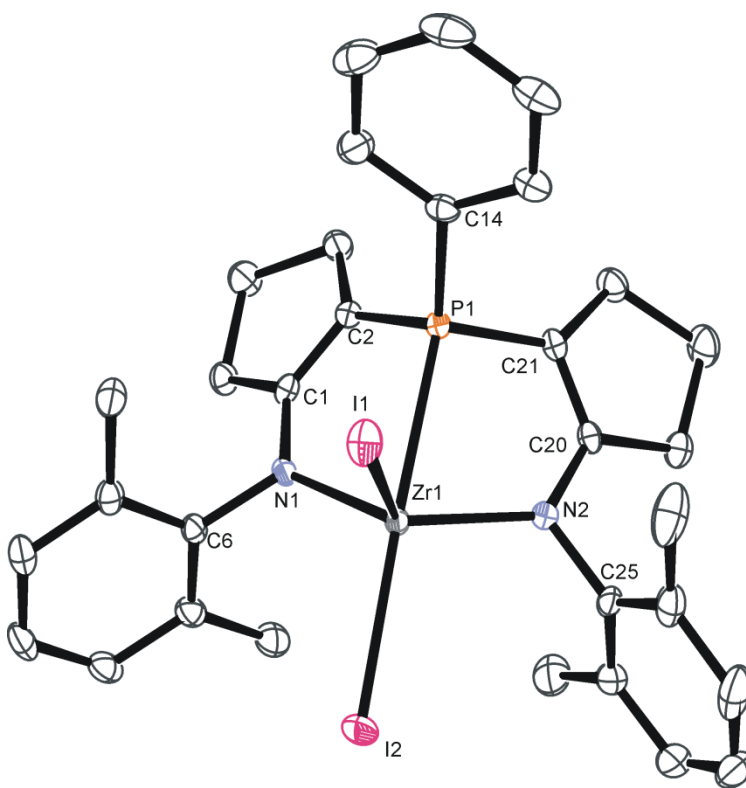
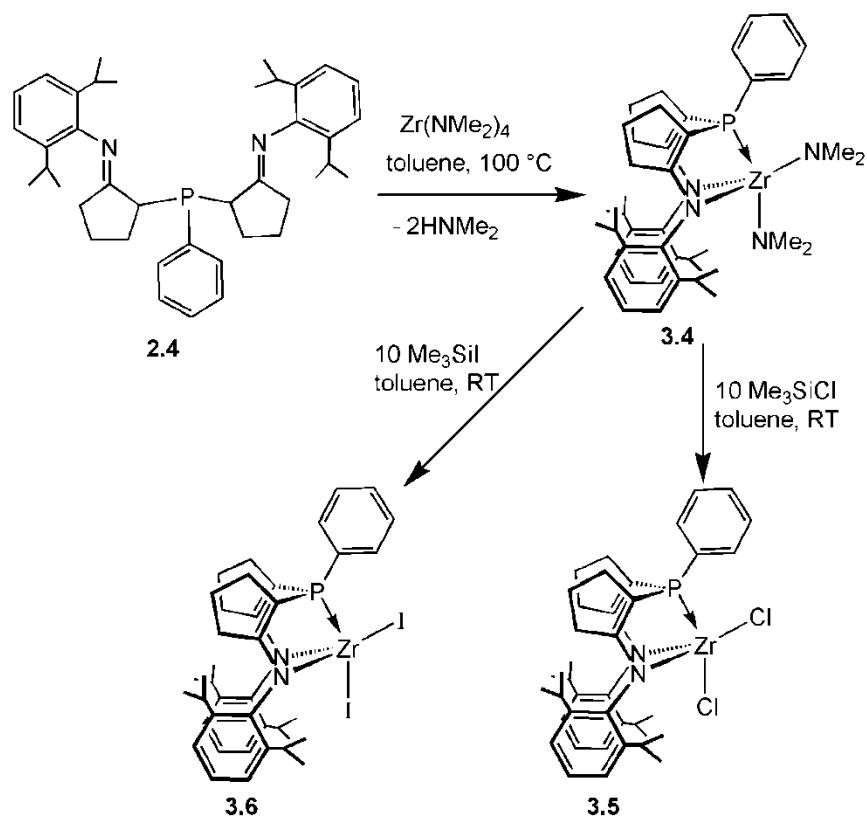


Figure 3.8. ORTEP drawing of the solid-state molecular structure of ^{CY5}[NPN]^{DMP}ZrI₂, **3.3** (ellipsoids at 50% probability level). All hydrogen atoms have been omitted for clarity. Selected bond length (Å) and angles (°): Zr1-N1 2.0837(19), Zr1-N2 2.0810(19), Zr1-P1 2.7536(8), Zr1-

I1 2.7859(17), Zr1-I2 2.7966(6), C1-C2 1.348(3), C20-C21 1.352(3), N1-Zr1-N2 120.44(8), I1-Zr1-I2 99.59(2), N1-Zr1-P1 72.94(5), N2-Zr1-P1 72.96(5), N1-Zr1-I1 109.59(6), P1-Zr1-I1 84.54(3), P1-Zr1-I2 175.773(16), N1-Zr1-I2 106.29(5), N2-Zr1-I2 104.31(5), N2-Zr1-I1 113.98(6), C6-N1-Zr1 117.04(14), C25-N2-Zr1 117.44(14), C2-C1-N1 124.6(2), C21-C20-N2 124.2(2)

As with **3.1** and **3.2**, the structure of **3.3** is a distorted trigonal bipyramid (Figure 3.8), with the two iodides *cis*-disposed. The Zr-I bond lengths average 2.79 Å, which agrees well with others reported in the literature.¹⁸

3.2.2 Synthesis of Zirconium Complexes of ^{CY5}[NPN]^{DIPP}H₂



Scheme 3.2

Similar to the Zr complexes incorporating $^{CY5}[NPN]^{DMP}$, $^{CY5}[NPN]^{DIPP}Zr(NMe_2)_2$, **3.4**, is synthesized in the same way as the diamido species **3.1** by adding one equivalent of **2.4** to $Zr(NMe_2)_4$ in toluene (Scheme 3.2). However, due to the bulkier *ortho*-diisopropylphenyl group on the two imine donors of the proligand, the protonolysis reaction with $Zr(NMe_2)_4$ requires heating for two weeks at 100°C in toluene to go to completion. Upon work up, complex **3.4** is obtained as a yellow solid, which is very soluble in both pentane and hexanes. The $^{31}P\{^1H\}$ NMR spectrum of **3.4** in C_6D_6 shows a singlet at δ -35.5, more downfield compared to the less bulkier analogue **3.1** at δ -38.9. The $^1H\{^{31}P\}$ NMR spectrum features four doublets that are assigned to the methyl groups on $Ar[CH(CH_3)_2]_2$, indicating the hindered rotation of the aryl group on the amido donor. Two inequivalent NMe_2 groups are assigned to two singlets at δ 2.71 and 2.51. The multiple peaks for four protons at δ 3.60 are attributed to the methine group on $Ar[CH(CH_3)_2]_2$. All the data combined suggest a C_s symmetric complex.

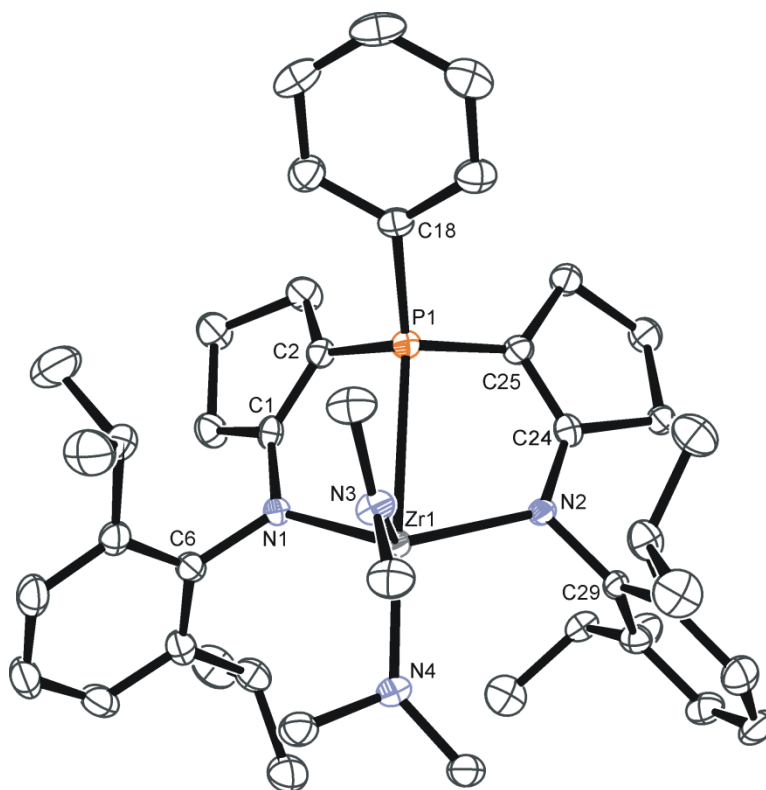


Figure 3.9. ORTEP drawing of the solid-state molecular structure of $^{\text{CY5}}[\text{NPN}]^{\text{DIPP}}\text{Zr}(\text{NMe}_2)_2$, **3.4** (ellipsoids at 50% probability level). All hydrogen atoms have been omitted for clarity. Selected bond length (Å) and angles (°): Zr1-N1 2.157(2), Zr1-N2 2.184(2), Zr1-P1 2.8643(8), Zr1-N3 2.057(2), Zr1-N4 2.042(2), C1-C2 1.358(4), C24-C25 1.352(4), N1-Zr1-N2 120.69(9), N3-Zr1-N4 93.94(9), N2-Zr1-P1 71.84(6), N1-Zr1-P1 72.26(6), N2-Zr1-N3 112.17(9), P1-Zr1-N3 90.22(7), P1-Zr1-N4 175.75(7), N2-Zr1-N4 105.67(9), N1-Zr1-N4 106.75(9), N1-Zr1-N3 113.53(9), C2-C1-N1 126.1(3), C6-N1-Zr1 119.71(18), C29-N2-Zr1 118.78(17).

The ORTEP representation of the solid-state molecular structure of **3.4** is shown in Figure 3.9. The geometry around Zr is a distorted trigonal bipyramid with the diamidophosphine ligand coordinated facially to the metal centre. Because of the strain created by the cyclopentene bridge, the N1-Zr1-P1 and N2-Zr1-P1 angles deviate greatly from 90°. Compared to its

analogue, **3.1**, the N3-Zr1-N4 angle of **3.4** at 93.94(9)° is much smaller than its analogue **3.1** at 104.88(4)°, while the P1-Zr1-N4 angle of **3.4** at 175.75(7)° is larger than 164.75(3)° observed in **3.1**. The Zr-P and Zr-N bond lengths are in agreement with reported complexes.¹⁷

As shown in Scheme 3.2, ^{CY5}[NPN]^{DIPP}ZrCl₂, **3.5**, can be isolated as an orange powder in high yield from the reaction of **3.4** with excess Me₃SiCl in toluene. A singlet at δ -32.3 is observed in the ³¹P{¹H} NMR spectrum. Similar to the ¹H {³¹P} NMR spectrum of complex **3.4**, there are four doublets for the methyl groups on Ar[CH(CH₃)₂]₂. A remarkable feature is that there are two methine signals at δ 3.68 and 3.44, respectively, due to the different electronic environments of the *ortho*-isopropyl groups as a result of hindered rotation of the aryl groups; this is not observed for ^{CY5}[NPN]^{DIPP}Zr(NMe₂)₂, **3.4**, which could be due to the overlap of the methine signals.

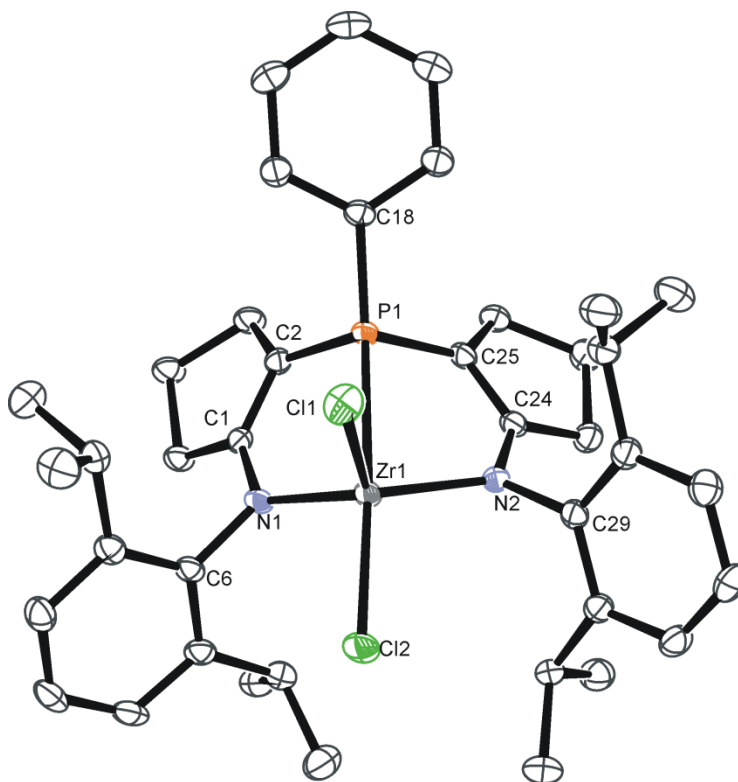


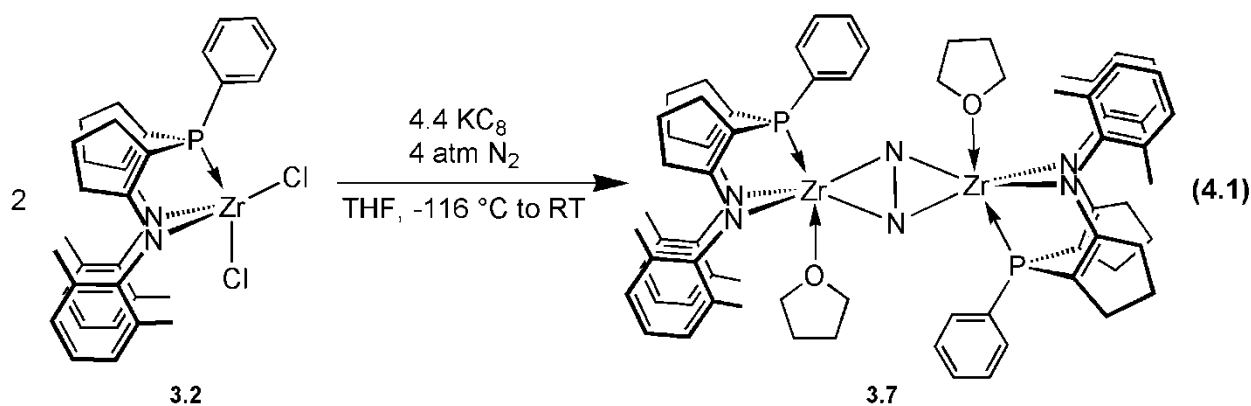
Figure 3.10. ORTEP drawing of the solid-state molecular structure of $^{\text{CY5}}[\text{NPN}]^{\text{DIPP}}\text{ZrCl}_2$, **3.5** (ellipsoids at 50% probability level). All hydrogen atoms have been omitted for clarity. Selected bond length (Å) and angles (°): Zr1-N1 2.0987(18), Zr1-N2 2.0775(18), Zr1-P1 2.7770(6), Zr1-Cl1 2.3845(6), Zr1-Cl2 2.3989(6), C1-C2 1.357(3), C24-C25 1.354(3), N1-Zr1-N2 118.46(7), Cl1-Zr1-Cl2 97.61(2), N1-Zr1-P1 73.90(5), N2-Zr1-P1 74.33(5), N1-Zr1-Cl1 116.09(5), P1-Zr1-Cl1 87.602(19), P1-Zr1-Cl2 173.53(2), N1-Zr1-Cl2 100.25(5), N2-Zr1-Cl2 106.80(5), N2-Zr1-Cl1 113.64(5), C6-N1-Zr1 119.86(13), C29-N2-Zr1 117.10(13), C2-C1-N1 125.00(19), C25-C24-N2 124.34(19).

The ORTEP representation of the solid-state molecular structure of **3.5** is shown in Figure 3.10. The structure of **3.5** resembles that of **3.2** with minor differences in bond lengths and angles. The geometry around the Zr is a distorted trigonal bipyramid, with two chlorides in

cis position. The C6-N1-Zr1 and C29-N2-Zr1 angles open wider than those in **3.2**, most likely due to the bulky Ar[CH(CH₃)₂]₂ group on the amido donors.

^{CY5}[NPN]^{DIPP}ZrI₂, **3.6**, is prepared from **3.4** and excess Me₃SiI, and is isolated as a yellow powder. Compared to similar reactions, it is hard to force the reaction to completion even when a large excess of Me₃SiI is used. Upon workup, the product is always mixed with ^{CY5}[NPN]^{DIPP}Zr(NMe₂)₂ and ^{CY5}[NPN]^{DIPP}Zr(NMe₂)I. Due to the low solubility of **3.6** in pentane, the mono, or bi-substituted amido Zr complexes can be washed away easily to get the pure diiodo Zr complex **3.6**. The ³¹P{¹H} spectrum of **3.6** in C₆D₆ shows a singlet at δ 3.4, more downfield compared to **3.3** at δ -30.1. The ¹H{³¹P} NMR spectrum closely resembles that of **3.5**, and suggests a C_s symmetric trigonal-bipyramidal structure for **3.6**.

3.2.3 Synthesis of Zirconium Dinitrogen Complexes



As mentioned earlier, most dinitrogen species discovered in Fryzuk group were generated from reduction of a metal halide complex by strong alkali metal reducing agents, such as KC₈ or Na/Hg amalgam. The reduction conditions involve vacuum transfer of water- and oxygen-free solvent, usually THF, diethyl ether, or toluene to an intimate mixture of the metal halide and reducing agent at -197 °C. The mixture is pressurized with 1 atmosphere of N₂ and slowly

warmed slowly to room temperature in an EtOH/dry ice/liquid nitrogen bath, which generates approximately 4 atmospheres at room temperature. During the whole process, the solution is stirred vigorously to increase the concentration of the N₂ in the solution.

Several attempts were made to obtain a dinitrogen complex by reduction of ^{CY5}[NPN]^{DMP}ZrCl₂ with 2.2 equivalents of KC₈ in THF under 4 atmospheres of N₂. In each case, a deep green solution was obtained, typically indicative of a dinitrogen complex. The ³¹P{¹H} NMR spectrum showed the formation of multiple products, and featured no signal for the starting material ^{CY5}[NPN]^{DMP}ZrCl₂. The observation of a deep green coloured solution is characteristic of the formation of an N₂ complex; however, attempts to isolate a single product were unsuccessful. When treating the concentrated deep green THF solution with pentane, a blue colored solid quickly precipitated out. This blue solid was insoluble in all solvents tested, and could be a result of decomposition. However, some black crystals suitable for X-ray diffraction were obtained from the THF solution of the original reaction mixture in an NMR tube. Through single crystal X-ray analysis, it was shown that a dinitrogen complex with N₂ bound in a side-on mode was generated.

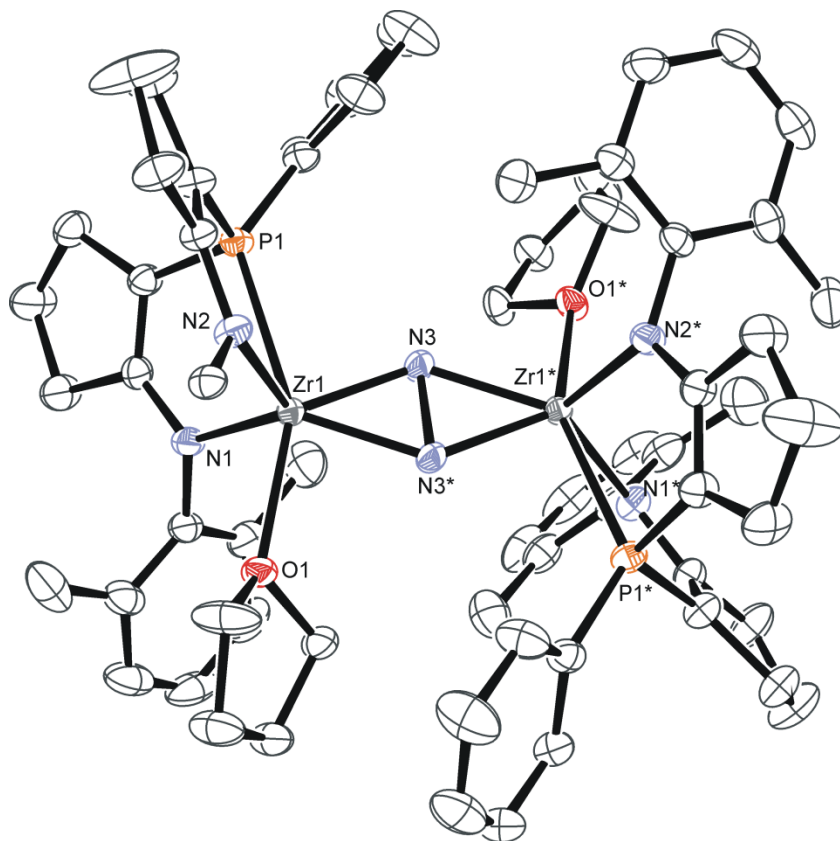


Figure 3.11. ORTEP drawing of the solid-state molecular structure of $\{\text{CY}^5[\text{NPN}]^{\text{DMP}}\text{Zr}(\text{THF})\}_2(\mu\text{-}\eta^2\text{:}\eta^2\text{-N}_2)$, **3.7** (ellipsoids at 50% probability level). All hydrogen atoms have been omitted for clarity. Carbons of the 2,6-dimethylphenyl substituent (except C_{ipso}) on N2 donor are omitted for clarity, Selected bond length (Å) and angles (°): Zr1-P1 2.7136(9), Zr1-N1 2.237(3), Zr1-N2 2.189(3), Zr1-O1 2.348(2), Zr1-N3 2.017(3), Zr1-N3* 2.073(3), N3-N3* 1.508(5), P1-Zr1-N1 74.35(7), P1-Zr1-N2 74.61(7), N3-Zr1-N3* 43.25(14), Zr1-N3-Zr1* 136.75(14), O1-Zr1-P1 152.32(6), P1-Zr1-N3 82.54(8).

The ORTEP representation of the solid-state molecular structure of **3.7** is shown in Figure 3.11. The side view of the arrangement of P, N, and O donors about Zr is illustrated in Figure 3.12. Compound **3.7** displays a side-on bound N_2 unit to two zirconium centres with

almost no distortion. The dihedral angle of the two ZrN_2 planes is 179.5° . Similar to that reported for $\{[\text{NPN}]^*\text{Zr}(\text{THF})\}_2(\mu\text{-}\eta^2\text{:}\eta^2\text{-N}_2)$ with an N-N bond at $1.503(6) \text{ \AA}$,⁷ the N-N bond in **3.7** is $1.508(5) \text{ \AA}$, corresponding to the reduction of N_2 to N_2^{4-} . One THF molecule is coordinated to each Zr centre, and overall, **3.7** displays C_2 symmetry in the solid state. A two-fold rotation axis bisects the N-N bond, while perpendicular to the plane of Zr_2N_2 core. The Zr-N bond lengths of the N_2 core are slightly different from each other: Zr1-N3 is $2.017(3) \text{ \AA}$, while Zr1-N3* is $2.073(3) \text{ \AA}$. The Zr1-N1 and Zr1-N2 bonds are $2.237(3) \text{ \AA}$ and $2.189(3) \text{ \AA}$, respectively. Compared to the Zr- N_{amido} bond length at about 2.1 \AA in the zirconium complexes **3.1** - **3.6**, these bond lengths are quite elongated. The Zr1-P1 bond is $2.7136(9) \text{ \AA}$, and the Zr1-O1 bond is $2.348(2) \text{ \AA}$, which are typical. As observed in other $\text{CY}^5[\text{NPN}]^{\text{DMP}}\text{Zr}$ complexes, the P1-Zr1-N1 and P1-Zr1-N2 angles are at $74.35(7)^\circ$ and $74.61(7)^\circ$.

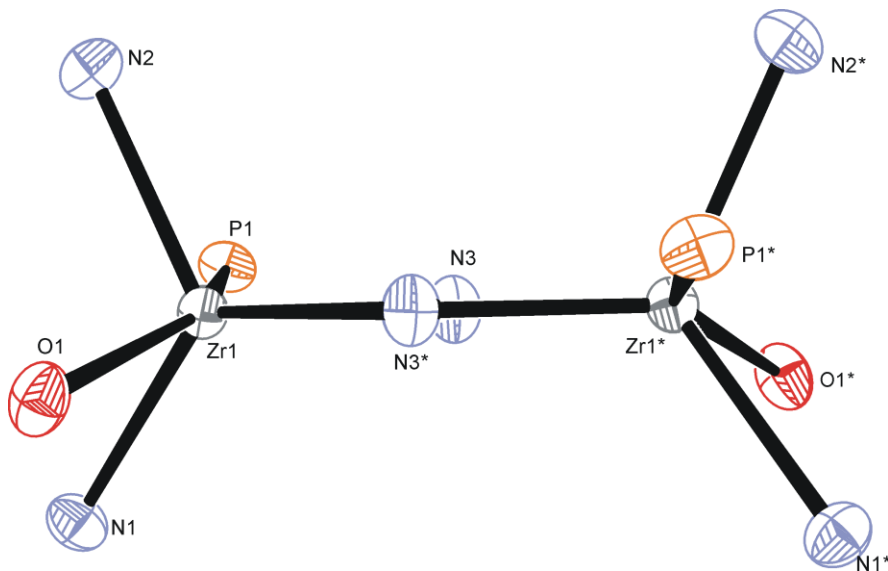


Figure 3.12. The side view of the stereochemistry around Zr in **3.7**.

The $^{31}\text{P}\{^1\text{H}\}$ NMR spectrum of the black crystals analyzed by X-ray diffraction shows a singlet at $\delta -25.2$ in $\text{THF-}d_8$, indicating that both of the phosphines in the dinuclear complex are

equivalent. Despite many efforts, the acquisition of a good quality ^1H NMR spectrum was unsuccessful. The N_2 complex, **3.7**, is extremely unstable; upon isolation from a THF solution, the black powder decomposes to an unidentified blue residue within minutes in the glovebox. It is known that dissociation of THF can lead to the decomposition of the N_2 complex $\{[\text{NPN}]\text{Zr}(\text{THF})\}_2(\mu\text{-}\eta^2\text{:}\eta^2\text{-N}_2)$.⁷ The decomposition of **3.7** was also observed in THF over the course of a few days, changing from green coloured solution to brown. Due to this fact and the presence of impurities, other spectroscopic and analytical data could not be obtained.

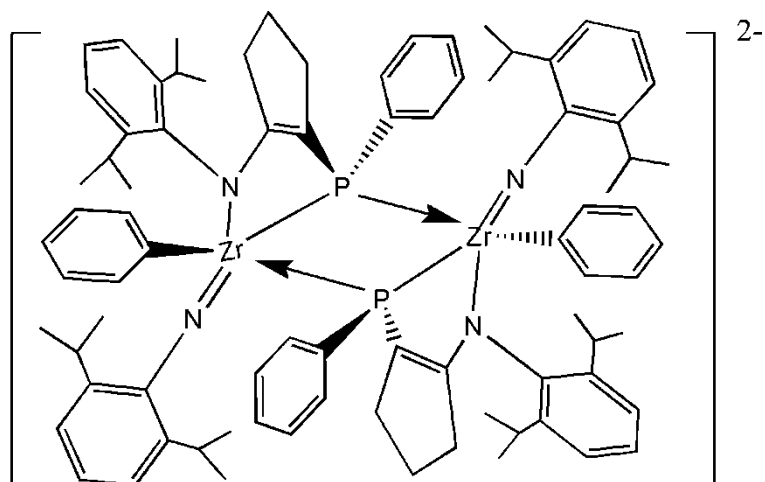
In an attempt to improve the yield of the N_2 complex and reduce the formation of by-products, a wide range of different reaction conditions were attempted. For example, several attempts were made to change the concentration of the reactants in THF. The resulting reaction mixtures were generally a dark green/brown color. Four peaks were consistently seen in the $^{31}\text{P}\{^1\text{H}\}$ NMR spectrum at δ -25.0, -31.9, -32.7, and -44.4; the peak at δ -25.0 is assumed to correspond to the N_2 complex. Compared to the $[\text{NPN}]\text{ZrCl}_2$ system, where the concentration of zirconium dichloride is 100mg/ml, a very concentrated solution of **3.2** was not beneficial for the formation of N_2 complex; through several attempts, it was found that 40 mg/ml gave the optimal result in which the number of by-products were minimized.

Changing the solvent from THF to diethyl ether also reduced the number of by-products. Only three peaks appeared in the $^{31}\text{P}\{^1\text{H}\}$ NMR spectrum at δ -25.0, -32.9, and -32.6. The color of the reaction mixture was bright green, slightly different from that in THF. The peak at δ -25.0 is possibly attributed to the desired N_2 complex.

Diiodide metal complexes have been shown to improve the yield of the corresponding dinitrogen complexes compared to dichloro metal complexes in these reduction reactions.¹⁹ For this reason, the reaction of $^{\text{CY5}}[\text{NPN}]^{\text{DMP}}\text{ZrI}_2$ with 2.2 equivalents of KC_8 in THF was performed

under the same conditions used for the dichloro metal complex. After workup, the solution was brown. $^{31}\text{P}\{^1\text{H}\}$ NMR analysis of the crude reaction mixture clearly showed the formation of two products at δ -30.9 and -46.2, with minor impurities. No peak showed up around δ -25.0, where the N_2 complex signal is assumed to appear. The reduction of $^{\text{CY5}}[\text{NPN}]^{\text{DMP}}\text{ZrCl}_2$ was also performed with reducing reagent sodium naphthalenide, and the result was a mixture of several species without any peaks observed at δ -25.0 in the $^{31}\text{P}\{^1\text{H}\}$ NMR spectrum.

Attempts were also made to prepare a zirconium-dinitrogen compound from $^{\text{CY5}}[\text{NPN}]^{\text{DIPP}}\text{ZrCl}_2$ and KC_8 in diethyl ether. After warming to room temperature overnight, the solution was brown in colour. $^{31}\text{P}\{^1\text{H}\}$ NMR spectrum of the crude reaction mixture in diethyl ether showed the presence of two doublets at δ 89.1, 76.4 and one singlet at δ -27.1. The coupling constants for the two doublets are 52 Hz and 48 Hz, respectively. A black colored solid was obtained after workup in diethyl ether. Attempts to purify the reaction mixture by washing the solid with pentane were unsuccessful. However, some orange crystals suitable for X-ray analysis were obtained by vapour diffusion of pentane into a concentrated THF solution of the reaction mixture. The solid-state molecular structure of these crystals **3.8** is shown in Figure 3.13. This dimeric complex is formally a dianionic complex.²⁰ It is generated via ligand cleavage during reduction by KC_8 . The $^{31}\text{P}\{^1\text{H}\}$ NMR signal of this single product corresponds to the singlet at δ -27.1 in the $^{31}\text{P}\{^1\text{H}\}$ NMR spectrum of reaction mixture.



3.8

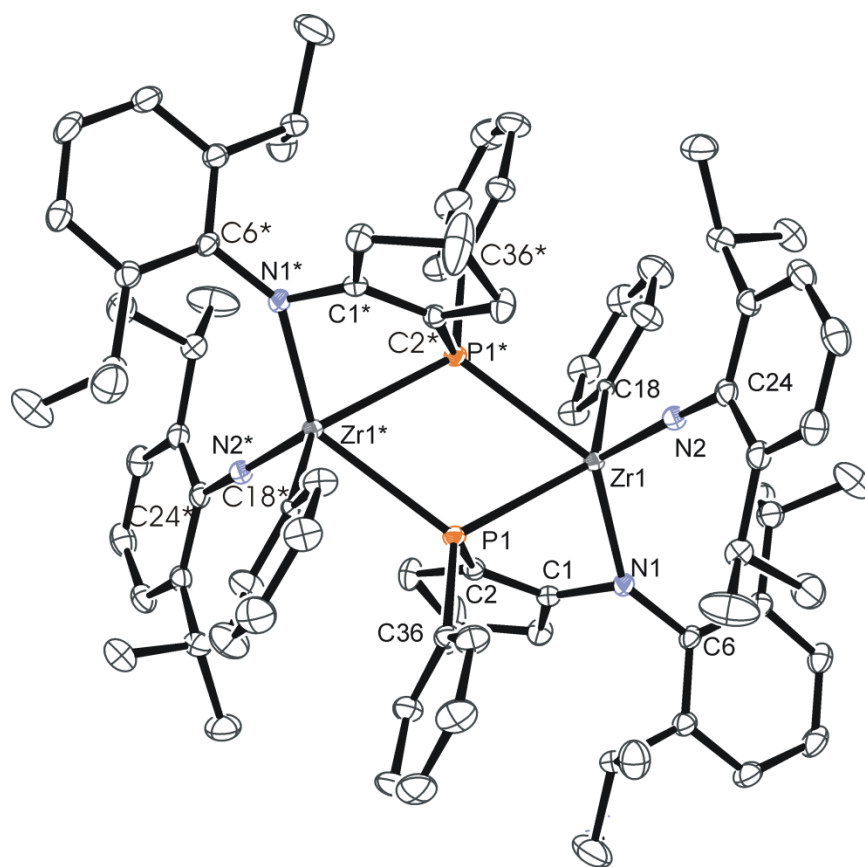


Figure 3.13. ORTEP drawing of the solid-state molecular structure of **3.8** (ellipsoids at 50% probability level). All hydrogen atoms have been omitted for clarity. Selected bond length (Å) and angles (°): C1-C2 1.382(3), C1-N1 1.379(2), Zr1-N1 2.1532(16), Zr1-N2 1.8762(18), Zr1-P1

2.6651(5), Zr1-P1* 2.7873(5), Zr1-C18 2.3411(17), P1-C36 1.829 (2), C2-P1 1.824(2), C24-N2 1.381(3), N1-C6 1.432(2), Zr1-N1-C6 143.40(13), Zr1-N1-C1 94.86(11), C6-N1-C1 117.95(16), N1-C1-C2 124.60(18), N1-C1-C5 123.66(17), C2-C1-C5 111.42(17), P1-Zr1-P1* 65.670(17), Zr1-P1-Zr* 114.330(17), P1-Zr1-N1 83.14(5).

3.3 Conclusions

In this chapter, zirconium complexes of the proligands $^{CY5}[NPN]^{DMP}H_2$ and $^{CY5}[NPN]^{DIPP}H_2$ can be prepared by protonolysis and metathesis reactions in high yield. Zirconium bis(dimethylamido) complexes of these ligands are prepared from the two proligands and $Zr(NMe_2)_4$. The reaction of proligand $^{CY5}[NPN]^{DIPP}H_2$ with $Zr(NMe_2)_4$ needs a higher temperature and a longer reaction time due to the bulkiness of the two *ortho*-isopropyl groups on the amidoaryl substituent. Reactions of $^{CY5}[NPN]^{DMP}Zr(NMe_2)_2$ and $^{CY5}[NPN]^{DIPP}Zr(NMe_2)_2$ with excess Me_3SiCl generate the corresponding dichloride complexes. The diiodide complexes can also be prepared in high yield from the corresponding diamido Zr derivatives and excess Me_3SiI . Both the zirconium diamide complexes and dichloride complexes, as well as $^{CY5}[NPN]^{DMP}ZrI_2$, have been characterized in the solid state by single-crystal X-ray diffraction.

The attempted reduction reactions of $^{CY5}[NPN]^{DMP}ZrCl_2$ by KC_8 to form a dinitrogen complex generally led to a mixture of products. However, the formation of the zirconium dinitrogen complex, $\{^{CY5}[NPN]^{DMP}Zr(THF)\}_2(\mu-\eta^2:\eta^2-N_2)$, is confirmed in the solid state. It shows that the N_2 moiety is coordinated side-on to two Zr atoms, with the N-N bond length of 1.509(5) Å, corresponding to reduction to N_2^{4-} .

Diethyl ether was also tried in the reduction of $^{CY5}[NPN]^{DMP}ZrCl_2$ with KC_8 in the presence of N_2 . Although the reduction in diethyl ether reduced the number of generated by-products, the yield of the dinitrogen complex did not improve. Changing the zirconium halide to $^{CY5}[NPN]^{DMP}ZrI_2$ or using other reducing reagents like sodium naphthalenide was also tried, in an attempt to generate the anticipated dinitrogen complex. However, both these routes led to unidentifiable products.

The reduction of $^{CY5}[NPN]^{DIPP}ZrCl_2$ using 2.2 equivalents of KC_8 in diethyl ether led to a mixture of products. A single product identified by single crystal X-ray diffraction proves the formation of a dimeric zirconium species due to the cleavage of the ligand. No definitive evidence was found for the formation of a dinitrogen complex. In light of the evidence from the reduction of both dichlorozirconium complexes **3.2** and **3.4**, it seems that the cyclopentene ring linker is not robust enough to sustain such harsh reduction conditions.

The complexity of products that can result by the use of strong reducing agents in the preparation of dinitrogen complexes has been illustrated previously in other systems.²¹ During the preparation of dark blue $([P_2N_2]Zr)_2(\mu-\eta^2:\eta^2-N_2)$ (Figure 3.2), a small amount of a yellow crystalline byproduct was observed as shown in Figure 3.14. This byproduct does not contain dinitrogen; instead, a phosphorus-phenyl group on one $[P_2N_2]Zr$ unit is bound to the zirconium center of another $[P_2N_2]Zr$ fragment. Because dinitrogen is not a particularly good ligand, highly reduced complexes can undergo other competing reactions rather than activate N_2 . This may be one reason for the formation of multiple by-products in the reduction of **3.2** and **3.4**.

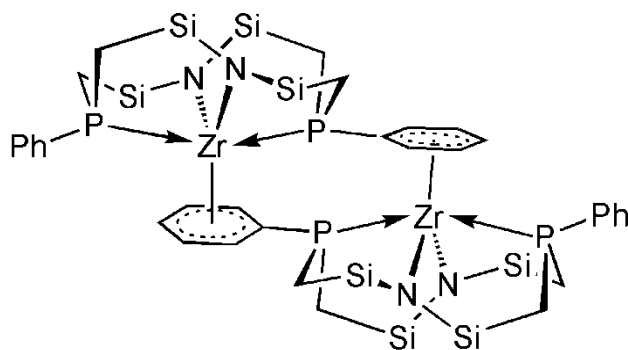


Figure 3.14. The minor byproduct observed in the preparation of $([P_2N_2]Zr)_2(\mu-\eta^2:\eta^2-N_2)$ (silyl methyl substituents of $[P_2N_2]$ omitted).

3.4 Experimental

3.4.1 General Experimental

General experimental conditions are given in chapter two.

3.4.2 Starting Materials and Reagents

KC_8 was prepared according to literature procedure;²² sodium naphthalenide was prepared and titrated according to a literature procedure.²³ Me_3SiCl and Me_3SiI were purchased from Aldrich and used without further purification. $Zn(NMe_2)_4$ was purchased from Strem and used without further purification.

Synthesis of $^{CY5}[NPN]^{DMP}Zr(NMe_2)_2$ (3.1)

$Zr(NMe_2)_4$ (1.463 g, 3.05 mmol) and **2.2** (0.815 g, 3.05 mmol) were mixed together, and dissolved in toluene (20 ml). The reaction mixture was then transferred to a 100-ml Kontes-sealed reaction vessel (bomb), and stirred in oil bath at 60°C for 12 h. The resulted yellow solution was taken to dryness to obtain a yellow residue. Upon addition of pentane (10 ml), a

light yellow precipitate formed, and was collected on a frit and dried (1.71 g, 2.60 mmol, 85%). Yellow single crystals of **3.1** suitable for X-ray diffraction were grown by slow evaporation of a pentane solution of the compound.

^1H NMR (C_6D_6 , 400 MHz): δ = 7.58 (dd, 2H, J_{HP} = 8 Hz, J_{HH} = 8 Hz, *o*-PPh), 7.25 (t, 2H, 8 Hz, *m*-PPh), 7.11 (t, 1H, 8 Hz, *p*-PPh), 7.05 (d, 2H, 8 Hz, *m*-NAr), 7.03 (d, 2H, 8 Hz, *m*-NAr), 6.92 (t, 2H, 8 Hz, *p*-NAr), 2.90 (s, 6H, $\text{N}(\text{CH}_3)_2$), 2.74 (m, 2H), 2.53 (m, 2H), 2.34 (s, 6H, ArCH_3), 2.33 (s, 6H, ArCH_3), 2.24 (s, 6H, $\text{N}(\text{CH}_3)_2$), 2.08 (m, 2H), 1.90 (m, 6H).

$^{31}\text{P}\{^1\text{H}\}$ NMR (C_6D_6 , 162 MHz): δ = -38.9 (s).

$^{13}\text{C}\{^1\text{H}\}$ NMR (C_6D_6 , 101 MHz): δ = 173.1 (d, 37 Hz), 148.9, 135.7, 134.7, 133.9 (d, 32 Hz), 131.2 (d, 12 Hz), 128.7, 128.6, 128.1, 127.8, 124.3, 93.5 (d, 32 Hz), 42.8, 42.2, 34.2 (d, 11 Hz), 31.0 (d, 3 Hz), 24.3 (d, 6 Hz), 19.5, 19.4.

EI-MS (m/z): 656 $[\text{M}]^+$, 612 $[\text{M} - \text{NMe}_2]^+$.

Anal. Calcd. for $\text{C}_{36}\text{H}_{47}\text{N}_4\text{PZr}$: C, 65.71; H, 7.20; N, 8.51; Found: C, 65.36; H, 7.30; N, 8.24.

Synthesis of $^{\text{CY5}}[\text{NPN}]^{\text{DMP}}\text{ZrCl}_2$ (**3.2**)

To a stirred yellow toluene solution (30 ml) of **3.1** (1.53 g, 2.33 mmol) was added trimethylsilane chloride (2.53 g, 23.3 mmol) dropwise. The solution was stirred for overnight. An orange precipitate gradually formed. The reaction mixture was taken to dryness to get an orange powder that was collected on a frit, washed with pentane (3×5 ml), and dried (1.42 g, 2.22 mmol, 95%). X-ray quality orange crystals of **3.2** were grown by slow evaporation of a benzene solution of the compound.

^1H NMR (C_6D_6 , 400 MHz): δ = 7.58 (dd, 2H, J_{HP} = 8 Hz, J_{HH} = 8 Hz, *o*-PPh), 7.16 (t, 2H, 8 Hz, *m*-PPh), 7.06 (t, 1H, 8 Hz, *p*-PPh), 6.96 (m, 6H), 2.64 (m, 2H), 2.48 (s, 6H, ArCH_3), 2.50 (m,

2H), 2.43 (s, 6H, ArCH₃), 1.91 (m, 2H), 1.78 (m, 2H), 1.69 (m, 4H).

³¹P{¹H} NMR (C₆D₆, 162 MHz): δ = -31.9 (s)

¹³C{¹H} NMR (C₆D₆, 101 MHz): δ = 172.4 (d, 51 Hz), 143.5, 135.8 (d, 35 Hz), 130.7 (d, 15 Hz), 129.7, 129.4, 129.2, 129.1, 128.7, 128.4, 127.4, 103.6 (d, 53 Hz), 32.5 (d, 18 Hz), 30.6 (d, 5 Hz), 24.0 (d, 9 Hz), 19.7, 19.0.

EI-MS (m/z): 640 [M]⁺, 532 [M-PPh]⁺.

Anal. Calcd. for C₃₂H₃₅Cl₂N₂PZr•0.73 toluene: C, 62.93; H, 5.82; N, 3.96; Found: C, 62.58; H, 5.79; N, 3.88.

Synthesis of ^{CY5}[NPN]^{DMP}ZrI₂ (**3.3**)

To a stirred yellow toluene solution (5 ml) of **3.1** (0.276 g, 0.421 mmol) was added trimethylsilane iodide (0.842 g, 4.21 mmol) dropwise. The solution was stirred for overnight. An orange precipitate gradually formed. The reaction mixture was taken to dryness to give a deep orange powder that was collected on a frit, washed with pentane (3 × 1 ml), and dried (0.318 g, 0.387 mmol, 92%). X-ray quality crystals of **3.3** were grown by slow diffusion of pentane into a benzene solution of the compound.

¹H NMR (C₆D₆, 400 MHz): δ = 7.49 (dd, 2H, J_{HP} = 8 Hz, J_{HH} = 8 Hz, *o*-PPh), 7.18 (t, 2H, 8 Hz, *m*-PPh), 7.07 (t, 1H, 8 Hz, *p*-PPh), 7.05 (t, 2H, 8 Hz, *p*-NAr), 6.98 (m, 4H, *m*-NAr), 2.63 (s, 6H, ArCH₃), 2.58 (m, 2H), 2.39 (m, 2H), 2.36 (s, 6H), 1.92 (m, 2H), 1.74 (m, 6H).

³¹P{¹H} NMR (C₆D₆, 162 MHz): δ = -30.1 (s)

¹³C{¹H} NMR (C₆D₆, 101 MHz): δ = 172.8 (d, 36 Hz), 142.8, 136.2 (d, 30 Hz), 130.6 (d, 10 Hz), 129.8, 129.7, 129.2, 129.1, 129.0, 128.0, 127.8, 105.7 (d, 38 Hz), 32.9 (d, 12 Hz), 31.1 (d, 3 Hz), 24.30 (d, 6 Hz), 21.1, 20.8.

EI-MS (m/z): 822 [M]⁺, 695 [M - I]⁺.

Anal. Calcd. for C₃₂H₃₅I₂N₂PZr: C, 46.66; H, 4.28; N, 3.40; Found: C, 46.64; H, 4.58; N, 3.27.

Synthesis of ^{CY5}[NPN]^{DIPP}Zr(NMe₂)₂ (**3.4**)

Zr(NMe₂)₄ (0.186 g, 0.699 mmol) and **2.4** (0.414 g, 0.699 mmol) were mixed together, and dissolved in toluene (10 ml). The reaction mixture was then transferred to a 100-ml Kontes-sealed reaction vessel (bomb), and stirred in oil bath at 100°C for ten days. The resulted yellow solution was taken to dryness to obtain a yellow residue. Upon addition of pentane (5 ml), a light yellow precipitate formed, and was collected on a frit and dried (0.435 g, 0.566 mmol, 81%). Yellow single crystals of **3.4** suitable for X-ray diffraction were grown by slow evaporation of a pentane solution of the compound.

¹H NMR (C₆D₆, 400 MHz): δ = 7.58 (dd, 2H, J_{HP} = 8 Hz, J_{HH} = 8 Hz, *o*-PPh), 7.28 (t, 2H, 8 Hz, *m*-PPh), 7.18 (t, 2H, 8 Hz, *p*-NAr), 7.16 (t, 2H, 8 Hz, *p*-PPh), 7.10 (m, 4H, *m*-NAr), 3.60 (sept, 4H, 4 Hz, CH), 2.71 (s, 6H, N(CH₃)₂), 2.70 (m, 2H), 2.51 (s, 6H, N(CH₃)₂), 2.49 (m, 2H), 2.17 (m, 4H, CH₂), 1.88 (m, 2H, CH₂), 1.76 (m, 2H, CH₂), 1.32 (d, 6H, 4 Hz, CCH₃), 1.30 (d, 6H, 4 Hz, CCH₃), 1.21 (d, 6H, 4 Hz, CCH₃), 1.10 (d, 6H, 4 Hz, CCH₃).

³¹P{¹H} NMR (C₆D₆, 162 MHz): δ = -35.5 (s).

¹³C{¹H} NMR (C₆D₆, 101 MHz): δ = 173.9 (d, 33 Hz), 146.3, 144.9, 134.2, 131.4 (d, 13), 128.6 (d, 9 Hz), 128.1, 127.8, 125.3, 123.8, 123.4, 90.6 (d, 35), 42.3, 40.5, 34.8 (d, 9 Hz), 31.3 (d, 3 Hz), 27.9, 27.7, 25.7, 25.2, 24.6 (d, 5 Hz), 23.7.

EI-MS (m/z): 768 [M]⁺, 725[M- CH(CH₃)₂]⁺.

Anal. Calcd. for C₄₄H₆₃N₄PZr: C, 68.62; H, 8.24; N, 7.27; Found: C, 68.37; H, 7.86; N, 6.94.

Synthesis of ^{CY5}[NPN]^{DIPP}ZrCl₂ (3.5)

To a stirred yellow toluene solution (10 ml) of **3.4** (0.601g, 0.782 mmol) was added trimethylsilane chloride (0.845 g, 7.82 mmol) dropwise. The solution was stirred for overnight. An orange precipitate gradually formed. The reaction mixture was taken to dryness to get an orange powder that was collected on a frit, washed with pentane (3 × 2 ml), and dried (0.563 g, 0.751 mmol, 96%). X-ray quality orange crystals of **3.5** were grown by slow evaporation of a benzene solution of the compound.

¹H NMR (C₆D₆, 300 MHz): δ = 7.63 (dd, 2H, J_{HP} = 6 Hz, J_{HH} = 6 Hz, *o*-PPh), 7.19 – 7.14 (m, overlap with the solvent peak), 7.08 (m, 3H), 3.68 (sept, 2H, 6 Hz, CH), 3.44 (sept, 2H, 6 Hz, CH), 2.60 (m, 2H), 2.49 (m, 2H), 2.14 (m, 2H), 1.78 (m, 4H), 1.64 (m, 2H), 1.53 (d, 6H, 6 Hz, CH₃), 1.42 (d, 6H, 6 Hz, CH₃), 1.19 (d, 6H, 6 Hz, CH₃), 1.09 (d, 6H, 6 Hz, CH₃).

³¹P{¹H} NMR (C₆D₆, 121 MHz): δ = -32.3 (s)

¹³C{¹H} NMR (C₆D₆, 101 MHz): δ = 172.3 (d, 48 Hz), 146.3, 145.0, 141.9, 131.2 (d, 16 Hz), 129.9, 128.9 (d, 13 Hz), 128.0, 127.7, 124.9, 124.4, 102.4 (d, 50 Hz), 34.1 (d, 17 Hz), 31.0 (d, 4 Hz), 29.0, 28.5, 25.7, 25.6, 24.4, 24.3 (d, 8 Hz), 24.0.

EI-MS (m/z): 752 [M]⁺

Anal. Calcd. for C₄₀H₅₁Cl₂N₂PZr: C, 63.81; H, 6.83; N, 3.72; Found: C, 63.54; H, 6.63; N, 3.72.

Synthesis of ^{CY5}[NPN]^{DIPP}ZrI₂ (3.6)

To a stirred yellow toluene solution (10 ml) of **3.4** (0.500 g, 0.651 mmol) was added trimethylsilane iodide (2.60 g, 13.0 mmol) dropwise. The solution was stirred for overnight. A yellow precipitate gradually formed. The reaction mixture was taken to dryness to get yellow color residue that was washed with pentane (3 × 2 ml), and dried (0.255 g, 0.273 mmol, 42%).

^1H NMR (C_6D_6 , 400 MHz): δ = 7.45 (dd, 2H, J_{HP} = 8 Hz, J_{HH} = 8 Hz, *o*-PPh), 7.17 (m, overlap with the solvent peak), 7.12 – 7.02 (m, 7H), 3.60 (bs, 2H, CH), 3.50 (bs, 2H, CH), 2.40 (m, 6H), 2.08 (m, 2H), 1.74 (m, 2H), 1.56 (m, 2H), 1.59 (d, 6H, 8 Hz, CH_3), 1.30 (d, 6H, 8 Hz, CH_3), 1.25 (d, 6H, 8 Hz, CH_3), 1.08 (d, 6H, 8 Hz, CH_3).

$^{31}\text{P}\{^1\text{H}\}$ NMR (C_6D_6 , 162 MHz): δ = 3.4 (s)

EI-MS (m/z): 934 $[\text{M}]^+$, 807 $[\text{M} - \text{I}]^+$.

Anal. Calcd. for $\text{C}_{40}\text{H}_{51}\text{I}_2\text{N}_2\text{PZr}$: C, 51.34; H, 5.49; N, 2.99; Found: C, 51.56; H, 5.69; N, 3.00.

General Procedure for the Reduction Reactions

The general procedure is given for the reduction of $^{\text{CY5}}[\text{NPN}]^{\text{DMP}}\text{ZrCl}_2$ (**3.2**) with 2.2 equivalent of KC_8 in THF. All the other reductions introduced in this Chapter use the similar reaction procedure unless described specifically.

Compound $^{\text{CY5}}[\text{NPN}]^{\text{DMP}}\text{ZrCl}_2$ (**3.2**) (0.296 g, 0.463 mmol) and KC_8 (0.137 g, 1.02 mmol) were added to a 200 ml thick-walled Kontes-sealed reaction vessel (bomb) and shaken to mix thoroughly. THF (10 ml) was vacuum-transferred to the solid mixture at -196°C . The flask was filled with N_2 at -196°C , sealed, and warmed slowly to room temperature in a liquid- N_2 /dry ice/EtOH slurry behind a blast shield. After the mixture gradually melted in one hour, it was stirred vigorously. The solution was stirred overnight. The next day, the bomb was depressurized by first cooling to -196°C , opening the seal to N_2 and allowing the bomb to warm to room temperature. The green solution was filtered through Celite to remove all the residual graphite and salt. The filtrate was concentrated to about 3 ml and pentane (5 ml) was added.

Some blue color solid quickly precipitated out. Crystals of **3.7** suitable for X-ray analysis were grown in an NMR tube by slow evaporation of THF solution.

Compound 3.7

$^{31}\text{P}\{^1\text{H}\}$ NMR (d_8 -THF, 162 MHz): $\delta = -25.2$ (s)

3.5 References

- ¹ Allen, A. D.; Senoff, C. V. *Chem. Commun.* **1965**, 621.
- ² Fryzuk, M. D.; Johnson, S. A. *Coord. Chem. Rev.* **2000**, 200, 379.
- ³ King, W. A.; Scott, B. L.; Eckert, J.; Kubas, G. J. *Inorg. Chem.* **1999**, 38, 1069.
- ⁴ de los Rios, I.; Tenoria, M. J.; Padilla, J.; Puerta, M. C.; Valerga, P. *Organometallics* **1996**, 15, 4565.
- ⁵ Manriquez, J. M.; Bercaw, J. E. *J. Am. Chem. Soc.* **1974**, 96, 6229.
- ⁶ Hidai, M.; Tominari, K.; Uchida, Y. *J. Am. Chem. Soc.* **1972**, 94, 110.
- ⁷ Fryzuk, M. D.; Haddad, T. S.; Rettig, S. J. *J. Am. Chem. Soc.* **1990**, 112, 8185.
- ⁸ Morello, L.; Ferreira, M. J.; Patrick, B. O.; Fryzuk, M. D. *Inorg. Chem.* **2008**, 47, 1319.
- ⁹ Morello, L.; Yu, P.; Carmichael, C. D.; Patrick, B. O.; Fryzuk, M. D. *J. Am. Chem. Soc.* **2005**, 127, 12796.
- ¹⁰ MacLachlan, E. A.; Hess, F. M.; Patrick, B. O.; Fryzuk, M. D. *J. Am. Chem. Soc.* **2007**, 129, 10895.
- ¹¹ Ballmann, J.; Munhá, R. F.; Fryzuk, M. D. *Chem. Comm.* **2010**, 46, 1013.
- ¹² de Wolf, J. M.; Blaauw, R.; Meetsma, A.; Teuben, J. H.; Gyepes, R.; Varga, V.; Mach. K.; Veldma, N.; Spek, A. L. *Organometallics* **1996**, 15, 4977.
- ¹³ Pool, J. A.; Lobkovsky, E.; Chirik, P. J. *Organometallics* **2003**, 22, 2797.
- ¹⁴ Laplaza, C. E.; Cummins, C. C. *Science* **1995**, 268, 861.
- ¹⁵ Menard, G.; Fryzuk, M. D. *Organometallics* **2009**, 28, 5253.
- ¹⁶ MacLachlan, E. A.; Fryzuk, M. D. *Organometallics* **2005**, 24, 1112.
- ¹⁷ a) Skinner, M. E. G.; Li, Y.; Mountford, P. *Inorg. Chem.* **2002**, 41, 1110. b) Chien, P-S; Liang, L-C, *Inorg. Chem.* **2005**, 44, 5147.

¹⁸ King, W. A.; Di Bella, S.; Gulino, A.; Lanza, G.; Fragala, I. L.; Stern, C. L.; Marks, I. J. *J. Am. Chem. Soc.* **1999**, *121*, 355.

¹⁹ Fryzuk, M. D.; Corkin, J. R.; Patrick, B. O. *Can. J. Chem.* **2003**, *81*, 1376.

²⁰ The contrary cation could not be identified because the collected X-ray data is not good enough. cryst. sys. = monoclinic, space group = P 21/c, a = 13.7517(4) Å, b = 18.2284(6) Å, c = 17.4805(6) Å, $\alpha = 90^\circ$, $\beta = 111.3290(10)^\circ$, $\gamma = 90^\circ$, V = 4066.7(6) Å³, final R indices [I > 2sigma(I)]: R1 = 0.0433, wR2 = 0.1317, R indices (all data): R1 = 0.0561, wR2 = 0.1399.

²¹ Fryzuk, M. D.; Kozak, C. M.; Mehrkhodavandi, P.; Morello, L.; Patrick, B. O.; Rettig, S. J. *J. Am. Chem. Soc.* **2002**, *124*, 516.

²² Bergbreiter, D. E.; Killough, J. M. *J. Am. Chem. Soc.* **1978**, *100*, 2126.

²³ Adam, W.; Arce, J. *J. Org. Chem.* **1972**, *37*, 507.

Chapter 4

Thesis Summary and Future Work

4.1 Thesis Summary

In this thesis, two new diiminophosphine proligands were synthesized. These two proligands, $^{CY5}[NPN]^{DMP}H_2$ (DMP = 2, 6-Me₂C₆H₃) and $^{CY5}[NPN]^{DIPP}H_2$ (DIPP = 2, 6-ⁱPr₂C₆H₃), featuring a five-membered cyclopentyl linker, were investigated to determine their effect on zirconium to activate N₂. The two-step synthetic strategy for these proligands is simple and straightforward. Zirconium complexes bearing these two ligands, $^{CY5}[NPN]^{DMP}$ and $^{CY5}[NPN]^{DIPP}$, were synthesized. Through the comparison of the solid-state structures between the corresponding zirconium complexes, $[NPN]^*ZrCl_2$ and $^{CY5}[NPN]^{DMP}ZrCl_2$, it is shown that this cyclopentenyl linked diamidophosphine ligand, $^{CY5}[NPN]^{DMP}$, can expose the zirconium metal centre more than $[NPN]^*$.¹ Reduction of the $^{CY5}[NPN]^{DMP}ZrCl_2$ complex using KC₈ in THF under 4 atmospheres of N₂ can produce a side-on bound dinitrogen complex, $\{^{CY5}[NPN]^{DMP}Zr(THF)\}_2(\mu-\eta^2:\eta^2-N_2)$, which is confirmed by single crystal X-ray diffraction. Similar to the reported $\{[NPN]^*Zr(THF)\}_2(\mu-\eta^2:\eta^2-N_2)$,² the triple N-N bond is reduced to a single bond. The N₂-unit is bound to two zirconium centres without any significant distortion. Due to the large number of side products observed in the reaction and the facile decomposition of the N₂ complex, it is impossible to obtain pure dinitrogen complex necessary to do further reactivity test.

The reduction of $^{CY5}[NPN]^{DIPP}ZrCl_2$ was performed with 2.2 equivalents of KC₈ in diethyl ether, which led to a mixture of products. One minor product could be partially identified by single crystal X-ray diffraction. It was confirmed to be a dimeric zirconium species formed

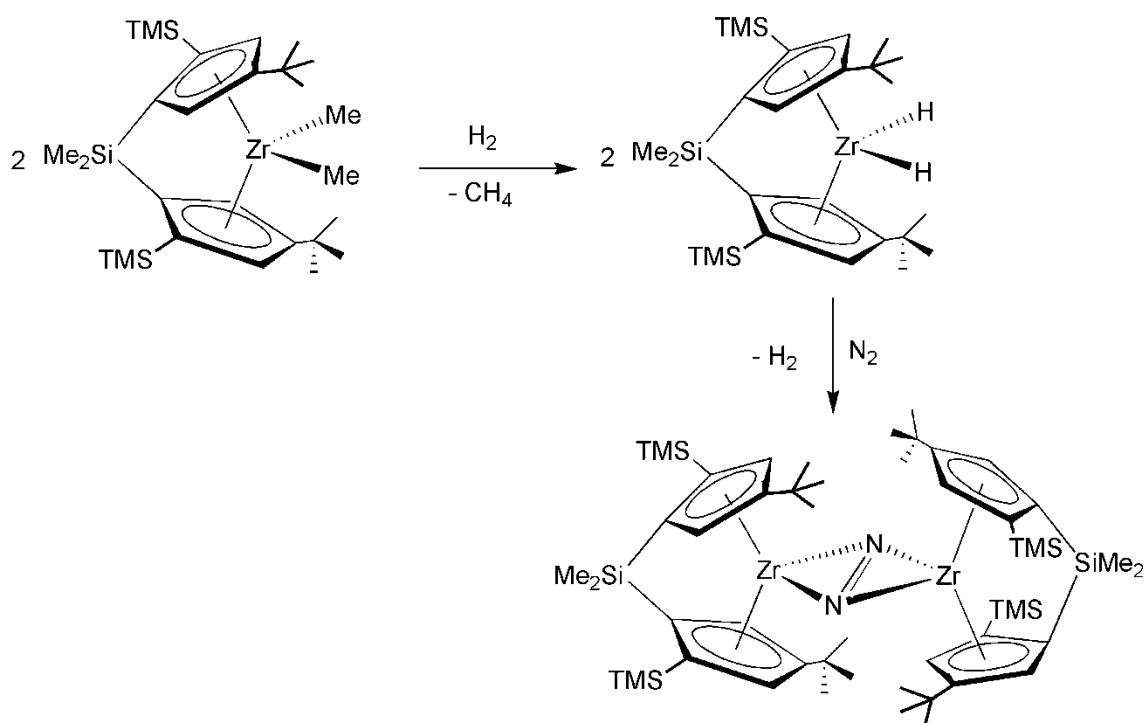
from the cleavage of the ligand. Combining the evidence from the reduction of both the dichloro Zr complexes, it seems that the cyclopentene ring linker is not robust enough to sustain such harsh reduction conditions.

The synthesis of a diamidodioxo ligand based on the scaffold of the macrocycle compound calix[4]arene was attempted. Modification of the phenol-donors to amine donors was generally unsuccessful due to the bulkiness created by the four *t*-butyl groups on the aryl rings.

4.2 Future Work

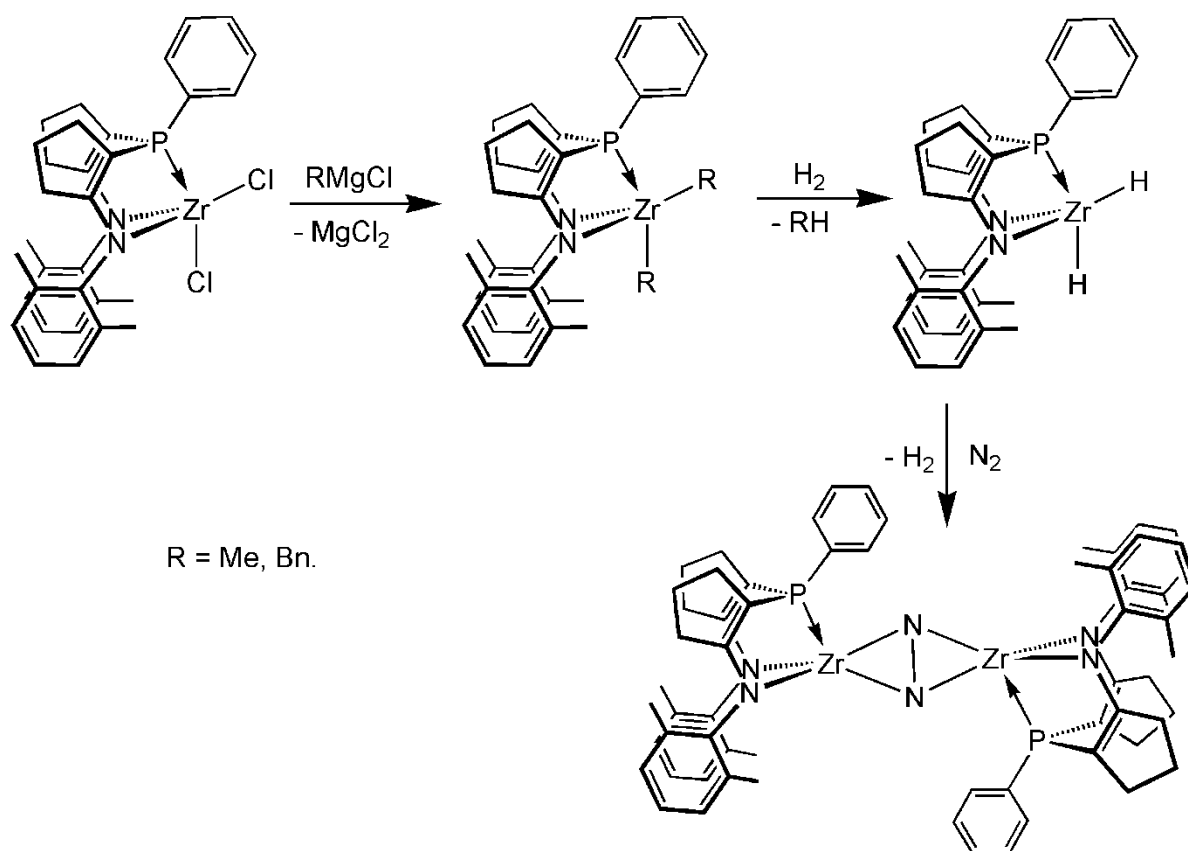
A new reaction for the activation of N₂ emerged in the late 1990s when an early transition-metal alkyl complex reacted with H₂ gas, followed by N₂ gas.³ The synthesis of N₂ complexes by the hydrogenolysis of early transition-metal alkyl complexes is attractive because H₂ is the only reagent used besides N₂. There are many examples of early transition metal complexes that activate N₂ by an alkali metal reagent, such as potassium graphite (KC₈) or sodium amalgam. The use of strong reductants is one of the major barriers to the development of industrially applicable homogeneous catalysis for N₂ fixation.

An *ansa*-zirconocene dinitrogen complex, [*rac*-(Bp)Zr]₂(μ-η²:η²-N₂) (*rac*-Bp = [Me₂Si(-2-SiMe₃-4-*t*Bu-η⁵-C₅H₂)₂]²⁻) was prepared by hydrogenolysis of an alkylzirconium complex. When a solution of (*rac*-Bp)ZrMe₂ was exposed to H₂ gas, (*rac*-Bp)ZrH₂ was formed. Exposure of the dihydride to N₂ gas yielded [*rac*-(Bp)Zr]₂(μ-η²:η²-N₂) with loss of H₂ (Scheme 4.1).⁴ The advantage to use H₂ as the reductant in the synthesis of N₂ complexes is the compatibility of H₂ with a range of reagents that functionalize coordinated N₂.



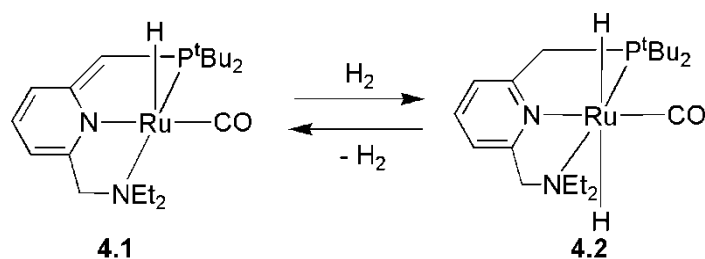
Scheme 4.1

Further efforts using these two ancillary ligands ($^{CY5}[NPN]^{DMP}$ and $^{CY5}[NPN]^{DIPP}$) will concentrate on synthesizing Zr hydride complexes to determine if a Zr- N_2 complex could be generated through the elimination of H_2 . The synthetic strategy for the ligand $^{CY5}[NPN]^{DMP}$ is proposed as shown in Scheme 4.2. Zr alkyl complexes, $^{CY5}[NPN]^{DMP}ZrR_2$ ($R = Me, Bn$), would be generated from $^{CY5}[NPN]^{DMP}ZrR_2$ and $RMgCl$. Upon exposure to H_2 , a Zr-dihydride species could be obtained, which will be used to test its reactivity towards N_2 .



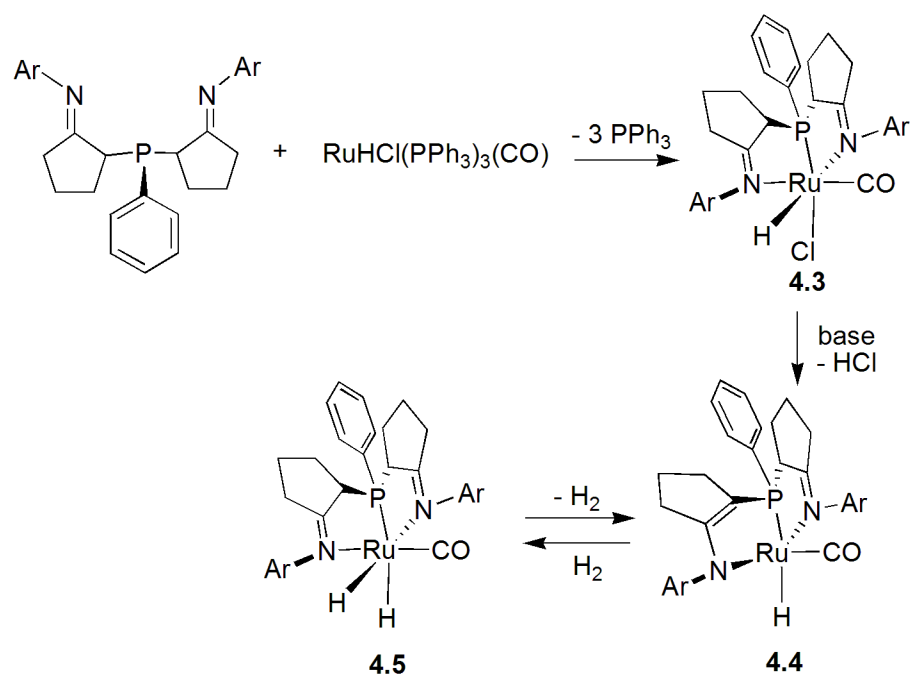
Scheme 4.2

In recent years, the Milstein group reported one PNN-type ruthenium pincer complex **4.1** (Scheme 4.1) which could catalytically facilitate the dehydrogenative coupling of primary alcohols to give esters,⁵ the dehydrogenation of secondary alcohols to give ketones,⁶ the hydrogenation of esters to give alcohols,⁷ and the coupling of alcohols with amines to form amides with the liberation of H₂.⁸ This catalyst features a “dearomatizable” aminomethyl phosphinomethyl pyridine pincer ligand (Scheme 4.3),⁷ and is remarkable for its versatile functions useful in forming fine chemicals. All the reactions are based on metal-ligand cooperation during the reversible deprotonation of a pyridinyl methylene group in which dearomatization/aromatization are key catalytic steps.



Scheme 4.3

Based on the notable feature that enamine and imine equilibrium can happen in the cyclopentane linked diiminophosphine proligands, its ruthenium chemistry similar to the PNN-type ligand system in dehydrogenation and hydrogenation could be the focus of further study. One possible strategy to synthesize the ruthenium metal catalyst **4.4** is proposed in Scheme 4.4. Addition of the diiminophosphine proligand to $\text{RuHCl}(\text{PPh}_3)_3(\text{CO})$ would lead to metal complex **4.3**, which could generate compound **4.4** upon deprotonation by one equivalent of base. Metal-ligand cooperation during the reversible deprotonation of one imine group of the ligand as shown between compounds **4.4** and **4.5** would be the key step to promote the whole catalytic cycle.



Scheme 4.4

4.3 References

- ¹ MacLachlan, E. A.; Fryzuk, M. D. *Organometallics*, **2005**, *24*, 1112.
- ² MacLachlan, E. A.; Hess, F. M.; Patrick, B. O.; Fryzuk, M. D. *J. Am. Chem. Soc.* **2007**, *129*, 10895.
- ³ Ballmann, J.; Munhá, R. F.; Fryzuk, M. D. *Chem. Comm.* **2010**, *46*, 1013.
- ⁴ Chirik, P. J.; Henling, L. M.; Bercaw, J. E. *Organometallics* **2001**, *20*, 534.
- ⁵ Zhang, J.; Leitus, G.; Ben-David, Y.; Milstein, D. *J. Am. Chem. Soc.* **2005**, *127*, 10840.
- ⁶ a) Zhang, J.; Gandelman, M.; Shimon, L. J. W.; Milstein, D. *Dalton Trans.* **2007**, 107. b) Gunanathan, C.; Shimon, L. J. W.; Milstein, D. *J. Am. Chem. Soc.* **2009**, *131*, 3146.
- ⁷ Zhang, J.; Leitus, G.; Ben-David, Y.; Milstein, D. *Angew. Chem. Int. Ed.* **2006**, *45*, 1113.
- ⁸ Gunannathan, Y.; Ben-David, Y.; Milstein, D. *Science* **2007**, *317*, 790.

Appendix

X-ray Crystal Structure Data and Analysis

A.1 X-ray Crystal Structure Data

Table A.1. Crystal Data and Structure Refinement for **2.5** and ^{CY5}[NPN]^{DMP}Zr(NMe₂)₂ (**3.1**).

compound	2.5	3.1
formula	C ₄₇ H ₅₉ F ₃ O ₆ S	C ₃₆ H ₄₇ N ₄ PZr
FW	809.00	657.97
T, K	173	173
cryst. sys.	triclinic	triclinic
space group	P-1	P-1
a, Å	12.404(3)	11.5299(4)
b, Å	14.603(3)	11.7212(4)
c, Å	15.070(4)	12.9070(5)
α, °	61.255(10)	89.473(2)
β, °	69.429(11)	88.110(2)
γ, °	72.545(11)	72.927(2)
V, Å ³	2211.9(9)	1666.53(10)
Z	2	2
ρ _{calc} , g/cm ³	1.215	1.311
abs. coeff., mm ⁻¹	0.132	0.408
F(000)	864	692
cryst. size, mm	0.32 x 0.11 x 0.07	0.60 x 0.50 x 0.44
radiation	Mo	Mo
θ range, °	1.72 – 22.48	1.82 – 28.02
total no. of reflns	23666	43830
no. of unique reflns	5719	7969
completeness to	θ = 22.48°, 98.9%	θ = 28.02°, 98.7%
max and min. trans.	0.9908 and 0.8833	0.8408 and 0.7918
gof	1.013	1.062
final R indices [I > 2σ(I)]	R1 = 0.0472, wR2 = 0.0995	R1 = 0.0209, wR2 = 0.0543
R indices (all data)	R1 = 0.0943, wR2 = 0.1179	R1 = 0.0229, wR2 = 0.0553
largest diff. peak and hole, e/Å ³	0.535 and -0.260	0.363 and -0.297

Table A.2. Crystal Data and Structure Refinement for $^{CY5}[NPN]^{DMP}ZrCl_2$ (**3.2**) and $^{CY5}[NPN]^{DMP}ZrI_2$ (**3.3**).

compound	3.2	3.3
formula	$C_{32}H_{35}Cl_2N_2PZr$	$C_{32}H_{35}I_2N_2PZr$
FW	640.74	823.61
T, K	173	173
cryst. sys.	orthorhombic	monoclinic
space group	Pcmn	P_21/c
a, Å	12.976(4)	19.192(5)
b, Å	14.267(5)	7.563(5)
c, Å	19.098(7)	22.219(5)
α , °	90	90.000(5)
β , °	90	91.090(5)
γ , °	90	90.000(5)
V, Å ³	3536(2)	3224(2)
Z	8	4
ρ_{calc} , g/cm ³	1.350	1.697
abs. coeff., mm ⁻¹	0.536	2.328
F(000)	1488	1608
cryst. size, mm	0.40 x 0.40 x 0.35	0.35 x 0.24 x 0.20
radiation	Mo	Mo
θ range, °	1.90 – 27.89	1.83 – 25.07
total no. of reflns	46631	37845
no. of unique reflns	4392	5702
completeness to	$\theta = 27.89^\circ$, 100.0%	$\theta = 25.07^\circ$, 99.9%
max and min. trans.	0.8346 and 0.8142	0.7452 and 0.6152
gof	1.053	1.127
final R indices [$I > 2\sigma(I)$]	R1 = 0.0216, wR2 = 0.0590	R1 = 0.0193, wR2 = 0.0486
R indices (all data)	R1 = 0.0260, wR2 = 0.0610	R1 = 0.0214, wR2 = 0.0499
largest diff. peak and hole, e/Å ³	0.339 and -0.306	0.979 and -0.348

Table A.3. Crystal Data and Structure Refinement for $^{CY5}[NPN]^{DIPP}Zr(NMe_2)_2$ (**3.4**) and $^{CY5}[NPN]^{DIPP}ZrCl_2$ (**3.5**).

compound	3.4	3.5
formula	$C_{44}H_{63}N_4PZr$	$C_{40}H_{51}Cl_2N_2PZr$
FW	770.20	752.95
T, K	173	173
cryst. sys.	triclinic	monoclinic
space group	$P_{\bar{1}}$	$P 2_1/c$
a, Å	10.9990(4)	16.5347(14)
b, Å	17.8520(6)	19.8606(16)
c, Å	21.4760(9)	12.7659(10)
α , °	99.108(2)	90
β , °	99.135(2)	91.719(4)
γ , °	90.293(2)	90
V, Å ³	4108.9(3)	4190.3(6)
Z	2	5
ρ_{calc} , g/cm ³	1.245	1.317
abs. coeff., mm ⁻¹	0.341	0.462
F(000)	1640	1744
cryst. size, mm	0.30 x 0.20 x 0.08	0.20 x 0.10 x 0.04
radiation	Mo	Mo
θ range, °	0.97 – 25.03	1.23 – 27.46
total no. of reflns	52990	101430
no. of unique reflns	14397	9540
completeness to	$\theta = 25.03^\circ$, 99.1%	$\theta = 27.46^\circ$, 99.3%
max and min. trans.	0.9732 and 0.9046	0.9818 and 0.9133
gof	0.982	1.105
final R indices [$I > 2\sigma(I)$]	$R1 = 0.0407$, $wR2 = 0.0809$	$R1 = 0.0364$, $wR2 = 0.0874$
R indices (all data)	$R1 = 0.0742$, $wR2 = 0.0882$	$R1 = 0.0510$, $wR2 = 0.0977$
largest diff. peak and hole, e/Å ³	0.508 and -0.512	1.519 and -0.322

Table A.4. Crystal Data and Structure Refinement for $\{\text{}^{\text{CY5}}[\text{NPN}]^{\text{DMP}}\text{Zr}(\text{THF})\}_2(\mu\text{-}\eta^2\text{:}\eta^2\text{-N}_2)$ (**3.7**)*.

compound	3.7
formula	$\text{C}_{72}\text{H}_{86}\text{N}_6\text{O}_2\text{P}_2\text{Zr}_2$
FW	1311.89
T, K	173
cryst. sys.	monoclinic
space group	C 2/c
a, Å	25.1464(7)
b, Å	17.1479(5)
c, Å	18.2636(5)
α , °	90
β , °	107.6160 (10)
γ , °	90
V, Å ³	7506.1(4)
Z	8
ρ_{calc} , g/cm ³	1.225
abs. coeff., mm ⁻¹	0.368
F(000)	2904
cryst. size, mm	0.40 x 0.30 x 0.20
radiation	Mo
θ range, °	1.70 – 27.91
total no. of reflns	33430
no. of unique reflns	8934
completeness to	$\theta = 27.91^\circ$, 99.7%
max and min. trans.	0.9300 and 0.8667
gof	1.179
final R indices [I > 2sigma(I)]	R1 = 0.0512, wR2 = 0.1736
R indices (all data)	R1 = 0.0705, wR2 = 0.1950
largest diff. peak and hole, e/Å ³	3.032 and -1.018

*Residual electron density consistent with disordered solvent was evident, however, no reasonable model could be established. Instead, the program SQUEEZE was used to generate a data set that corrects for the scattering contribution from this disordered solvent.

A.2 X-ray Crystal Structure Analysis

Selected crystals were coated in oil, mounted on a glass fiber, and placed under an N₂ stream. Measurements for compounds were made on a Bruker X8 Apex II diffractometer or a Bruker X8 Apex DUO diffractometer, both with graphite-monochromated Mo K α radiation ($\lambda = 0.71073$ Å). The data were collected at a temperature of 173 ± 1 K. Data were collected and integrated using the Bruker SAINT software package.¹ Data were corrected for absorption effects using the multi-scan technique (SADABS)² and for Lorentz and polarization effects. Neutral atom scattering factors were taken from Cromer and Waber.³ Anomalous dispersion effects were included in F_{calc} ;⁴ the values for $\Delta f''$ and $\Delta f'''$ were those of Creagh and McAuley.⁵ The values for the mass attenuation coefficients are those of Creagh and Hubbell.⁶ All refinements were performed using the SHELXTL crystallographic software package of Bruker-AXS. The structure was solved by direct methods. All non-hydrogen atoms were refined anisotropically using SHELXL-97. Except where noted, hydrogen atoms were included in fixed positions. Structures were solved and refined using the WinGX software package version 1.70.01.

A.3 References

¹ SAINT. Version 6.02. Bruker AXS Inc., Madison, Wisconsin, USA. (1999).

² SADABS. Bruker Nonius area detector scaling and absorption correction - V2.05, Bruker AXS Inc., Madison, Wisconsin, USA.

³ Cromer, D. T.; Waber, J. T. *International Tables for X-ray Crystallography, Vol. IV*; The Kynoch Press: Birmingham, England, 1974, Table 2.2 A.

⁴ Ibers, J. A.; Hamilton, W. C. *Acta Crystallogr.* **1964**, *17*, 781.

⁵ Creagh, D. C.; McAuley, W.J. *International Tables for Crystallography, Vol C*; Wilson, A. J. C., ed., Kluwer Academic Publishers: Boston, 1992, Table 4.2.6.8, pp. 219-222.

⁶ Creagh, D. C.; Hubbell, J.H. *International Tables for Crystallography, Vol C*; Wilson, A.J.C, ed., Kluwer Academic Publishers: Boston, 1992, Table 4.2.4.3, pp. 200-206.